Fundamentals of reduced basis method for problems governed by parametrized PDEs and applications

Gianluigi Rozza*
SISSA, International School for Advanced Studies, *mathLab*
Via Bonomea 265, 34136 Trieste, Italy
gianluigi.rozza@sissa.it

Abstract

In this chapter we consider Reduced Basis (*RB*) approximations of parametrized Partial Differential Equations (*PDEs*). The the idea behind *RB* is to decouple the generation and projection stages (Offline/Online computational procedures) of the approximation process in order to solve parametrized *PDEs* in a fast, inexpensive and reliable way. The *RB* method, especially applied to 3D problems, allows great computational savings with respect to the classical Galerkin Finite Element (FE) Method. The standard *FE* method is typically ill suited to (i) iterative contexts like optimization, sensitivity analysis and many-queries in general, and (ii) real time evaluation. We consider for simplicity coercive *PDE*s. We discuss all the steps to set up a *RB* approximation, either from an analytical and a numerical point of view. Then we present an application of the *RB* method to a steady thermal conductivity problem in heat transfer with emphasis on geometrical and physical parameters.

1 Introduction

Any design problem can be summarized in the following statement: *Given a physical process and given a set of suitable* parameters*, the physical behaviour depends on finding the optimal values of these parameters in order to obtain a desirable behaviour of the process.*

In this chapter the attention is focused on the designer point of view, but it is also important to recall that there are many other applications of interest, such as *real time* evaluation of the performances of a system or *sensitivity analysis* with respect to certain parameters.

The *physical process* may belong to any field of engineering interest, such as, heat and mass transfer, elasticity, acoustics, fluid dynamics, electromagnetism, etc., or even in a broader sense to any quantitative disciplines (e.g., finance, biology, ecology and medicine) and their interdisciplinary combinations.

The physical process is analysed in order to find the best mathematical *model* able

*This work has been developed thanks to the contribution of the SISSA NOFYSAS excellence grant and INdAM-GNCS. Mr Alberto Trezzini is kindly acknowledged for the preparation of the schemes and for the numerical results. G. Rozza ackwnowledges the long lasting collaboration with Prof. A.T. Patera (MIT) and his group on the subject. This Chapter is based on the lectures given by the author in summer 2013 at CISM, International Centre for Mechanical Sciences in Udine, Italy. Thanks to Prof. G. Maier (Politecnico di Milano) for insights and remarks.

to describe the behaviour of the *system*. As *model* we refer to a system of equations and/or other mathematical relationships able to "catch" the main properties of the process and to predict its evolution in time and/or space. In this stage the engineer introduces all the simplifications that the observation and a subsequent qualitative analysis suggest to take into account.
The analytical model is then constituted by conservation laws and constitutive equations. In this work the attention will be focused on models whose conservation laws are those of *continuum mechanics* which appears as balance of suitable quantities (e.g., mass, energy, linear momentum, angular momentum, etc. . .).
The constitutive relationships come from experimental evidence and depends upon the essential features of the process itself. The result of the combination of these conservation laws and constitutive equations is often an equation or a system of *Partial Differential Equations* PDEs. This means that in the equations the unknowns will appear along with partial derivatives with respect to multiple variables (temporal or spatial). To solve differential equation it is also necessary, in order to obtain the closure of the problem, specify a suitable set of boundary/initial conditions.
Therefore the parameters in the process can be:

- physical, within this category we have:
  - coefficient of constitutive equation for the particular physical process addressed;
  - non-dimensional numbers;[1]
  - imposed boundary conditions;
- and geometrical.

The desired behaviour could be a particular performance of the system, such as an average temperature in a thermal block, a maximum displacement of a loaded beam, a level of vorticity in a flow-field and so on, depending on the particular process addressed.
Finally, the optimal configuration of these parameters can be found through an iterative optimization process in which a suitable *cost functional*, that depends upon the particular desired performance, has to be minimized.
To wit, the designer is interested to evaluate iteratively the *input-output* relationship to estimate the cost functional.
The solution of *PDEs* by classical discretization methods like finite element, spectral method or finite volume, typically involves thousands (in some cases millions) of degrees of freedom (DOFs) to obtain a "good" solution; therefore a single evaluation of the input-output relationship is very expensive and at last, in most cases, not suitable in a *many-query* context on which the design strategy is based on.
In this context it is necessary to rely on suitable *Reduced Order Modelling* ROM techniques that reduce the computational cost and time. The *Reduced Basis* (RB) method is one of the possible options and this memoir focuses on this method that, as it will be shown, is able to reduce the computational cost of *orders of magnitude*. Moreover the *RB* method is a *certified* and *reliable* method because in addition to an efficient output calculation is able to provide *rigorous a-posteriori error estimators* on the *"truth" solution*[2].
An important remark is constituted by the fact that all the procedure is built upon a *reference domain* on which a *suitable discretization* is constructed. Then there is no need to re-discretize the domain at each iteration, re-building a mesh,

[1] It is always necessary to write the *PDEs* in a non-dimensional version in order to highlight the actual physical dependence on these parameters.
[2] The discussion on our assumption of "truth" solution will be given in section1.2.

or deforming the domain itself in the case of a *parameter-dependent geometry*.

1.1 Overview on reduced basis method

As already said the *RB* method is a *reduced order method* that is able to reduce the complexity of a system without loss of information or accuracy of the results thanks to the *rigorous error bound* provided and by the properties of the *Galerkin* projection (Patera and Rozza, 2007; Rozza et al., 2008).
This method does not replace an existing discretization method but "works in collaboration with it" and upon it.
In this work the discretization method adopted for the applications is the *finite element method* (FE): this choice does not constitute a limitation because the *RB* method is built upon the *user-defined* assumption of *"truth"* solution. The choice of the correct method able to describe the physical process is demanded to the user and it will not be considered here.
The basic idea is to start with *FE* basis of dimension $\mathcal{N}$ and then construct a *RB* basis whose dimension N is much smaller than the former, so that $N << \mathcal{N}$.
The power of the *RB* method resides in the splitting of the computational procedures into two parts:

1. an Offline phase,
2. an Online phase,

where the former is $\mathcal{N}$ dependent and computed once, whereas the latter is N dependent and allows a *fast*, *inexpensive* and *reliable* input-output evaluation.
The role played by this decomposition is immediately clear taking in consideration for example an optimization process. The optimal configuration can be found thanks to an iterative process, in which a *PDEs* state solution is needed at every step of iteration. In this context the *RB* advantage is that the evaluation of the solution for every step is orders of magnitude smaller; furthermore the real time evaluation of the *PDEs* solution is feasible, unlike as in the *FE* case.
The splitting procedure is possible if the weak formulation of the *PDEs* can be expressed in an *affine parameter decomposition*. This is one of the *key-point* of the procedure: all the parametric dependences of the *PDEs* are actually separated by the non-parametric part, in order to allow computing the latter just in a *reference domain*, whereas the former can be computed several times with a very inexpensive computational burden (Rozza, 2009b).
A graphical sketch of this idea is shown in Figure 1. The *RB* method is depicted in the upper figure , whereas the *FE* classical method is depicted in the lower one. In the *RB* sketch it appears that the *Offline* computational burden that is proportional to $\mathrm{K}\mathcal{N}$, where $\mathcal{N}$ is the number of degrees of freedom for the *FE* problem and K is a positive constant that depends upon many ingredients that will be in depth discussed in section 3. It is worth to recall that in the *RB* methodology the so-called *Offline* part is very expensive but in a *real time* or in a *many-query context* the most important part is played by the *online* evaluation of the *input-output relationship* which is very inexpensive in the *RB* methodology.
In addition, by dealing with parametrized equations it is clear that in many cases it is possible to restrict the attention on a tipically *smooth* and rather *low-dimensional parametrically induced manifold* of the functional space, which is a set of fields engendered as the input varies over the parameter domain (Patera and Rozza, 2007; Rozza et al., 2008). In Section 1.2 a more involved discussion over these concepts will be given, which are the key points the reduced basis method has been built upon.

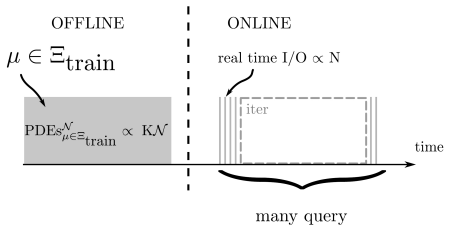

(a) *RB* method

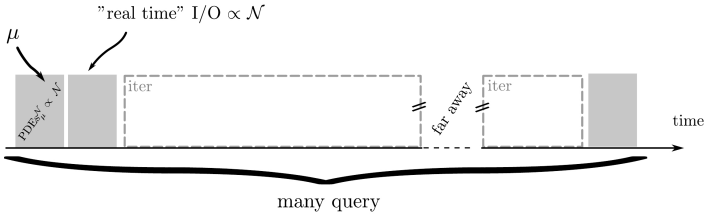

(b) *FE* method

Figure 1: *RB* computational saving

After the motivations and scopes of the *RB* method, a brief historical perspective will be recalled in this section, then in section 2 we will recall some mathematical generalities and we will provide the abstract formulation for coercive problems.
In section 3 the steps for the generation of the *RB* approximation spaces for the solution of parametrized *PDEs* will be explained. Later, in section 4, the *affine geometry preconditions* will be presented focused on the 3D case, necessary to allow a fully decoupling between *Offline* and *Online* procedures.
In section 5 the *RB* approximation for a parametrized 3D thermal block will be addressed, followed by some conclusions and perspectives.

1.2 RB scope and historical perspective

In the past few years, thanks to the increased computational performances it has been possible to use numerical simulation in the very first steps of design in several fields.
Unfortunately despite this hardware improvement, the greater part of engineering problem involves the solution of partial differential equations, furthermore in a *design context* the number of solutions for various configurations of attempt can become *very large* and eventually excessive. Therefore it is necessary to develop techniques that are able to reduce the complexity of the system without a loss of information or accuracy of the results. The *RB* method is a promising approach to respond to this need, moreover this method is not only *rapid* and *efficient*, but also provides a reliable solution of partial differential equations thanks to a certified *a-posteriori error bound*.
This method provides a useful tool for engineers, in fact thanks to the very low cost of the input-output relationship evaluation, the design procedure can be enriched with highly accurate numerical simulation since the very first steps.

The *real-time* and *many-query contexts* represent not only computational challenges but also computational opportunities.

It is possible to identify two key opportunities that can be gainfully exploited with *RB* method (Rozza et al., 2008):

- **Opportunity I**
  In the parametric setting, the attention is restricted to a typically *smooth* and rather *low-dimensional parametrically induced manifold*: the set of fields engendered as the input varies over the parameter domain; in the case of single parameter, the parametrically induced manifold is a one-dimensional filament within the infinite dimensional space which characterizes general solutions to the PDEs. Clearly, generic approximation spaces are *unnecessarily rich* and hence *unnecessarily expensive* within the parametric framework.
- **Opportunity II**
  In the *real-time* or *many-query contexts*, in which the premium is on marginal cost (or equivalently asymptotic average cost) per *input-output* evaluation, we can accept greatly increased pre-processing or *Offline* cost, not admitted for a single or few evaluations, in exchange for greatly decreased *Online* (or deployed) cost for each new/additional input-output evaluation (Rozza et al., 2008). Clearly, resources allocation typical for *single-query* investigations will be far from optimal for many-query and real-time exercises. We shall review the development of RB methods in terms of these two opportunities.

Opportunity I: A reduced basis discretization is, in brief, a Galerkin projection on an N-dimensional approximation space that focuses on the parametrically induced manifold identified in Opportunity I.

Initial work (about in 1980s) grew out of two related streams of inquiry: from the need for more effective, and perhaps also more interactive, many-query design evaluation (Fox and Miura, 1971) considering linear structural examples; and from the need of more efficient parameter continuation methods (Almroth et al., 1978; Noor and Peters, 1980; Noor, 1978, 1982) considering nonlinear structural analysis problems.

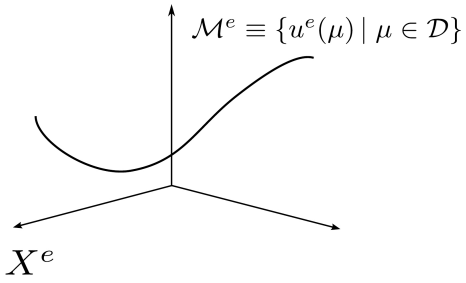

(a) X^e space

Figure 2: Parametrically induced manifold

Some modal analysis techniques proposed in the same years (Nagy, 1979) deals with geometrically nonlinear behaviour and are closely related to RB notions.
At the very first moment the reduced basis method arises from the study of nonlinear elasticity problems. The development of the *RB* method has been mainly due to the engineering needs to obtain a very efficient tool in the design context.
The following decade saw further expansion into different applications and classes of equations (Ito and Ravindran, 1998) dealing also with the control of PDEs and (Peterson, 1989) applications of reduced order methods to fluid dynamics and incompressible Navier-Stokes equations. However, in these early methods, the approximation spaces tended to be rather local and typically rather low dimensional in parameter (often say a single parameter). In part, this was due to the nature of the applications taken in account (parametric continuation), but it was also due to the *absence* of *a-posteriori error estimators* and *effective sampling procedures*. In fact the absence of this kind of techniques did not allow a *certified* an *accurate*

prediction of the error between the *"truth" solution*[3] and the solution obtained by the reduced order model; the lack of a rigorous error certification is unacceptable for example in a safe engineering context, in which the reliability is an imperative. Much current effort is thus devoted to development of (i) a posteriori error estimation procedures, in particular rigorous error bounds for outputs of interest (Prud'homme et al., 2002a) and (ii) effective sampling strategies, in particular for higher dimensional parameter domains (Bui-Thanh et al., 2008; Nguyen et al., 2005; Rozza, 2009a).
The *a-posteriori error bounds* are of course mandatory for *rigorous certification* of any particular reduced basis (*Online*) output evaluation. However, the error estimators can also play an important role in efficient and effective (greedy) sampling procedures: the inexpensive error bounds permit us, first, to explore much larger subsets of the parameter domain in search of most representative or best *snapshots*, and, second, to determine when the basis functions are enough to control the error within a certified bound.
The most used sampling methods are (i) the *Greedy sampling procedure* and (ii) the *POD* (Proper Orthogonal Decomposition): these two procedures differ under some aspects that will be discussed in section 3.3. It is worth to anticipate that the *Greedy* procedure is optimized for higher dimensions of the parameter space, while the *POD* procedure is better suited for one dimensional (typically time) domain (Atwell and King, 1999; Kunisch and Volkwein, 2003; Ravindran, 2002; Willcox and Peraire, 2002).

Opportunity II: Early work on the reduced basis method took into consideration the Opportunity II, but without being able to fully decouple the underlying standard (*FE*) discretization.
More precisely, often the *Galerkin stiffness equations* for the reduced basis system were generated by direct appeal to the high dimensional *FE* representation: essentially, pre and post multiplying the FE stiffness system by rectangular basis matrices; as a result the computational saving offered by the model reduction was not fully exploited Noor (1978); Porsching (1985); Porsching and Lee (1987). The complete decoupling between the reduced order model and the standard discretization model is one of the crucial point on which much of the current work has been devoted at that time.
In this work we will denote with $\mathcal{N}$ the computational complexity of the standard discretization and with N the *RB* complexity. This opportunity has been exploited thanks to an *Offline/Online procedure* that is possible in a context of an *affine parameter dependence* of the operators constituting the *PDEs*; this important concept will be recalled in section 2.2.
One of the benefits related to this procedure is shown in Figure 3; it is clear that in a many-query context, such as an optimization design process, or in a real-time closed loop control the split allows a much more faster sub-iteration (*I/O* evaluation), that could not be possible in the classical *FE* discretization. In fact in the FE case (Figure 3b) a subiteration involves a cost proportional to $\mathcal{N}$, whereas RB involves a cost proportional only to N.
The Offline-Online idea is quite self-apparent and it has been treated quite often (Ito and Ravindran, 1998; Jabbar and Azeman, 2004; Peterson, 1989), nonetheless the idea/application of *a-posteriori error bound* is more involved and recent

[3] "Truth" here means the assumption of faithfulness achieved with the standard discretization method, see section 2.3 for further explanation on the hypothesis and on the consequences of this choice

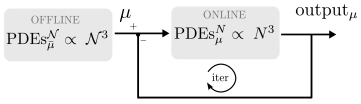

(a) RB procedure

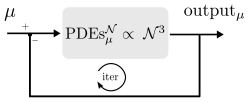

(b) FE procedure

Figure 3: Offline/Online splitting

(Huynh et al., 2007; Prud'homme et al., 2002a,b).
Actually even in the case of a *non-affine parameter dependence* the development of the procedure is yet possible, although more complex procedures, that have been estabilished in the few last years (M. et al., 2004; Grepl et al., 2007), are needed in order to turn the non-affine form into an approximated affine problem.

1.3 Problems addressed

This chapter will deal with *linear output functional* and *affinely parametrized linear coercive* PDEs: these problems are relevant to many important applications in various field of engineering interest.
Although we focuse on these problems, the reduced basis method is much more general and is able to treat nonaffine problems (Grepl et al., 2007) and parabolic equations (Atwell and King, 1999).
Furthermore, the *RB* method may be used for nonlinear equations such as the incompressible (quadratically non-linear) *Navier-Stokes* equations, finally even the hyperbolic equations are subject of study, there are proofs which demonstrate that RB approximation and a posteriori error estimation can be applied, although up to now there are still many issues related to *smoothness* and *stability* (Haasdonk and Ohlberger, 2008; Patera and Ronquist, 2007).
The application chosen in this work deals with thermal conduction in continuum mechanics and it proves to be a convenient expository vehicle for the methodology exploitation.

2 Parametrized Elliptic PDEs

In the first part of this section, we will briefly introduce some generalities about *parametric* bilinear form, *parametric* linear functional, coercivity and continuity constants. In particular the abstract formulation for coercive problem will be reported.

2.1 Parametric operators

In this section, definitions and properties about *parametric bilinear* and *bilinear forms* will be introduced.

The theory presented here is available with further details and explanations in Patera and Rozza (2007) for the coercive case, in Rozza and Veroy (2006) for the non coercive case.
The basic concept of functional analysis concerning Cartesian product, functional norms, bilinear forms and dual spaces are given as known (Quarteroni and Valli, 1997; Yosida, 1971).

Linear and bilinear parametric forms. We first introduce a closed bounded parameter domain $\mathcal{D} \subset \mathbb{R}^P$ with a typical parameter vector, or $P-$tuple, in $\mathcal{D}$ shall be denoted $\boldsymbol{\mu} = (\mu_1, \ldots, \mu_P)$. We assume that $\mathcal{D}$ is suitably regular.
It is now necessary to introduce some definition that resembles the classical definition for non-parametric linear operators.

Definition 2.1. Let Z be an inner product space over $\mathbb{R}$, $b : Z \times Z \times \mathcal{D} \to \mathbb{R}$ is a *parametric bilinear form* if, for all $\boldsymbol{\mu} \in \mathcal{D}$, $b(\cdot, \cdot; \boldsymbol{\mu}) : Z \times Z \to \mathbb{R}$ is a bilinear form, i.e. for any $\alpha \in \mathbb{R}$ and for any $w, v, z \in Z$:

$$b(\alpha w + v, z; \boldsymbol{\mu}) = \alpha b(w, z; \boldsymbol{\mu}) + b(v, z; \boldsymbol{\mu}) \quad \forall\, \boldsymbol{\mu} \in \mathcal{D}$$

and for any $\beta \in \mathbb{R}$ and for any $w, v, z \in Z$:

$$b(w, \beta v + z; \boldsymbol{\mu}) = \beta b(w, v; \boldsymbol{\mu}) + b(w, z; \boldsymbol{\mu}) \quad \forall\, \boldsymbol{\mu} \in \mathcal{D}.$$

Definition 2.2. A parametric bilinear form $b : Z \times Z \times \mathcal{D} \to \mathbb{R}$is *symmetric* if, for any $v, w \in Z$:

$$b(w, v; \boldsymbol{\mu}) = b(v, w; \boldsymbol{\mu}) \quad \forall\, \boldsymbol{\mu} \in \mathcal{D} \tag{1}$$

A parametric bilinear form $b : Z \times Z \times \mathcal{D} \to \mathbb{R}$ is *skew-symmetric* if, for any $v, w \in Z$:

$$b(w, v; \boldsymbol{\mu}) = -b(v, w; \boldsymbol{\mu}) \quad \forall\, \boldsymbol{\mu} \in \mathcal{D} \tag{2}$$

Starting from the Definition 2.2 it is possible to define the symmetric and the skew-symmetric part of the bilinear form as it follows:

Definition 2.3. Given a parametric bilinear form, we define:

- the symmetric part of b as:

$$b_S(w, v; \boldsymbol{\mu}) = \frac{1}{2}\left(b(w, v; \boldsymbol{\mu}) + b(v, w; \boldsymbol{\mu})\right) \tag{3}$$

- the skew-symmetric part of b as:

$$b_{SS}(w, v; \boldsymbol{\mu}) = \frac{1}{2}\left(b(w, v; \boldsymbol{\mu}) - b(v, w; \boldsymbol{\mu})\right). \tag{4}$$

For the coercive case it is necessary to introduce the definition of the coercivity of the parametric bilinear form.

Coercivity.

Definition 2.4. We say that a parametric bilinear form $b : Z \times Z \times \mathcal{D} \to \mathbb{R}$ is *coercive* over Z if:

$$\alpha(\boldsymbol{\mu}) = \inf_{w \in Z} \frac{b(w, w; \boldsymbol{\mu})}{||w||_Z^2} \tag{5}$$

is *positive* for all $\boldsymbol{\mu} \in \mathcal{D}$.

We can define $(0 <)\ \alpha_0 = \min_{\boldsymbol{\mu} \in \mathcal{D}} \alpha(\boldsymbol{\mu})$.

Continuity. Now it is possible to define the *continuity* of the parametric bilinear form in very similar way. We say that:

Definition 2.5. A parametric bilinear form $b : Z \times Z \times \mathcal{D} \to \mathbb{R}$ is *continuous* over Z if:

$$\gamma(\boldsymbol{\mu}) = \sup_{w \in Z} \sup_{v \in Z} \frac{b(\, w,\, v\,; \boldsymbol{\mu})}{||w||_Z ||v||_Z} \tag{6}$$

is *finite* for all $\boldsymbol{\mu} \in \mathcal{D}$.

It is useful to define $\gamma_0 = \max_{\boldsymbol{\mu} \in \mathcal{D}} \gamma(\boldsymbol{\mu})$.

Linear parametric form. Similarly as already done with the parametric bilinear form, we recall:

Definition 2.6. Let Z be an inner product space over $\mathbb{R}$. $g : Z \times \mathcal{D} \to \mathbb{R}$ is a *parametric linear form* if, for all $\boldsymbol{\mu} \in \mathcal{D}$, and for any $w \in Z$, $g(\,\cdot\,; \boldsymbol{\mu}) : Z \times \mathcal{D} \to \mathbb{R}$ is a linear form. That is, for all $\alpha \in \mathbb{R}$, and for any $w, v \in Z$:

$$g(\, \alpha w + v\,; \boldsymbol{\mu}) = \alpha g(\, w\,; \boldsymbol{\mu}) + g(\, v\,; \boldsymbol{\mu}) \quad \forall\, \boldsymbol{\mu} \in \mathcal{D} \tag{7}$$

Continuity. In order to ensure the well posedness of the problem, the continuity of the parametric linear form is needed. We say that:

Definition 2.7. A parametric linear form g is *continuous* if, for all $\boldsymbol{\mu} \in \mathcal{D}$, $g(\,\cdot\,; \boldsymbol{\mu}) \in Z'$.

Z' denotes the *dual space*, that we recall is the space of all linear bounded functionals over Z. Note that the dual norm of a parametric linear form g, $||g(\,\cdot\,; \boldsymbol{\mu})||_{Z'}$, will of course be a (finite) function of $\boldsymbol{\mu}$ over $\mathcal{D}$.

Coercivity eigenproblem. We recall here an additional problem which will be useful in order to evaluate a rigouros error bound as it will be seen in the section 3.5 (Patera and Rozza, 2007; Quarteroni et al., 2000).
It is necessary to introduce an eigenproblem because in the subsequent analysis it will be useful to recognize that $\alpha(\boldsymbol{\mu})$ (and $\beta(\boldsymbol{\mu})$ in the non-coercive case) can be seen as the minimum eigenvalue of a *generalized eigenproblem*.

It is possible to rewrite (5) replacing the form b with his symmetric part, denoted with b_s:

$$\alpha(\boldsymbol{\mu}) = \inf_{w \in Z} \frac{b_s(\, w,\, w\,; \boldsymbol{\mu})}{||w||_Z^2} \tag{8}$$

it follows that $\alpha(\boldsymbol{\mu})$ can be expressed as a minimun eigenvalue.
It is useful to introduce the coercivity symmetric (generalized) eigenproblem associated with the parametric bilinear form $b : Z \times Z \times \mathcal{D} \to \mathbb{R}$.
Given $\boldsymbol{\mu} \in \mathcal{D}$, find the couple $(\chi,\, \lambda)_i(\boldsymbol{\mu}) \in Z \times \mathbb{R}$, $i = 1, \ldots, \dim(Z)$, such that:

$$b_S(\chi_i,\, v;\, \boldsymbol{\mu}) = \nu_i(\chi_i(\boldsymbol{\mu}), v)_Z \tag{9}$$

and

$$||\chi_i(\boldsymbol{\mu})|| = 1 \tag{10}$$

of course it will be possible to sort the $\dim(Z)$ eigenvalues in ascending order such that: $\lambda_1(\boldsymbol{\mu}) < \ldots < \lambda_{\dim(Z)}(\boldsymbol{\mu})$.
It simply descends from (9) and (8) that if b is coercive, then $\alpha(\boldsymbol{\mu}) = \lambda_1(\boldsymbol{\mu}) > 0$.

2.2 Affine parametric dependence

The *affine parametric dependence* of the bilinear form and of the linear functional is one of the most important ingredient in the offline/online decomposition and of course in the real-time input/output evaluation.
The idea is rather simple: split all the parametric dependent component by those parametrically independent. In addition we recall also the parametric coercivity definition.

Affine parametric bilinear forms. With regard to the bilinear parametric forms the affine dependence states that:

Definition 2.8. A parametric bilinear form $b : Z \times Z \times \mathcal{D} \to \mathbb{R}$ is *affine* in the parameter $\boldsymbol{\mu}$ if, for all $v, w \in Z$:

$$b(w, v; \boldsymbol{\mu}) = \sum_{q=1}^{Q_b} \theta_b^q(\boldsymbol{\mu})\, b^q(w, v) \quad \forall\, \boldsymbol{\mu} \in \mathcal{D} \tag{11}$$

for some finite, preferably small, Q_b.

Here the $\theta_b^q(\boldsymbol{\mu}) : \mathcal{D} \to \mathbb{R}$ are (tipically very smooth) parameter- dependent functions, and $b^q(w, v) : Z \times Z \to \mathbb{R}$ are parameter-independent bilinear forms.

Parametric coercivity. In the scope of an affine dependence it is useful also to consider the parametric coercivity of the bilinear form.

Definition 2.9. We say that an affine parametric (coercive) form $b : Z \times Z \times \mathcal{D} \to \mathbb{R}$ (definition 2.8) is *parametrically coercive* if, $c \equiv b_s$ (the symmetric part of b) admits an *affine development*:

$$c(w, v; \boldsymbol{\mu}) = \sum_{q=1}^{Q_c} \theta_c^q(\boldsymbol{\mu})\, c^q(w, v) \quad \forall\, \boldsymbol{\mu} \in \mathcal{D} \tag{12}$$

that satisfies two conditions:

$$\theta_c^q(\boldsymbol{\mu}) > 0 \quad \forall\, w, v \in Z,\ \forall\, \boldsymbol{\mu} \in \mathcal{D},\ 1 \le q \le Q_b \tag{13}$$

and

$$c^q(v, v) > 0 \quad \forall\, v \in Z,\ 1 \le q \le Q_b. \tag{14}$$

Note that we suppose that each $c^q(w, v)$ is symmetric.

Affine parametric linear form. Similarly as done for the bilinear form it is worth to introduce the affine dependence for a linear bounded functional.

Definition 2.10. We shall say that the parametric linear form $g : Z \times \mathcal{D} \to \mathbb{R}$ is affine in the parameter if, for any $v \in Z$:

$$g(v; \boldsymbol{\mu}) = \sum_{q=1}^{Q_g} \theta_g^q(\boldsymbol{\mu})\, g^q(v) \quad \forall\, \boldsymbol{\mu} \in \mathcal{D} \tag{15}$$

for some finite Q_g.

Once again, here the $\theta_g^q : Z \times \mathcal{D} \to \mathbb{R}$ are smooth parameter-dependent functions and the $g^q(v) : Z \to \mathbb{R}$ are parameter-independent bounded linear forms.
The affine representations (11) and (15) are not unique, though in general will exist minimum Q_b (in the former case) and Q_g (in the latter) terms of expansion able to describe the forms with an affine development.
Tipically the number of terms Q mainly depends on the complexity of the parameter-dependent geometry. This concept will be treated in the section 4.3 where the decomposition in the 2D and in the more involved 3D case will be considered.

2.3 Abstract formulation of a coercive parametrized problem

In this section, an abstract problem for *coercive* elliptic partial differential equations with affine parameter dependence will be introduced. First the exact formulation (in weak form) of the problem will be presented, then a finite element discretization will be introduced in order to build the *"truth"* space on which the reduced basis will be built upon.
As mentioned in the introduction, the interest resides in the evaluation of the *solution field* and the *output* that depends on the state equation which is solution of a *PDE*.

Exact formulation. Let $\Omega \in \mathbb{R}^d$, $d = 1, 2, 3$ be a suitable physical domain with Lipschitz continuous boundary $\partial\Omega$. Let $\mathcal{D} \subset \mathbb{R}^P$ be the parameter domain.
Moreover let Γ, be a boundary measurable segments of $\partial\Omega$, over which we shall ultimately impose *Dirichlet boundary condition* on the components of the field variable. We next introduce a suitable scalar space Y_i^e, $1 \leq i \leq d$:

$$Y_i^e \equiv \left\{ v \in H^1(\Omega) \mid v \mid_{\Gamma_i^D} = 0 \right\} \tag{16}$$

in general $H_0^1(\Omega) \subset Y^e \subset H^1(\Omega)$. Clearly if $\Gamma = \partial\Omega$, then $X^e \equiv H_0^1$.
We then construct the space in which our *vector-valued* field variable shall reside as a Cartesian product:

$$X^e = Y_1^e \times Y_2^e \times \ldots \times Y_1^d$$

We equip X^e with an inner product $(v, w)_{X^e}$, $\forall\, v, w \in X^e$ and induced norm $||w||_{X^e} = \sqrt{(w, w)_{X^e}}$, $\forall\, w \in X^e$; any inner product which induces a norm equivalent to the $\left(H^1\right)^d$ is admissible.

Problem statement. It is now possible to state the problem in the "exact" space: let $a : Z \times Z \times \mathcal{D} \to \mathbb{R}$ be a *continuous coercive parametric bilinear* form, let $f : Z \times \mathcal{D} \to \mathbb{R}$ and l be a *parametric linear functional bounded over* X^e.
Given $\boldsymbol{\mu} \in \mathcal{D} \subset \mathbb{R}^P$, find $u(\boldsymbol{\mu}) \in X^e$ such that

$$a\left(u^e(\boldsymbol{\mu}, v; \boldsymbol{\mu})\right) = f\left(v; \boldsymbol{\mu}\right) \quad \forall\, v \in X^e \tag{17}$$

and evaluate

$$s^e(\boldsymbol{\mu}) = l(u^e(\boldsymbol{\mu}); \boldsymbol{\mu}). \tag{18}$$

Here $s^e(\boldsymbol{\mu})$ is the output of interest, $s^e(\boldsymbol{\mu}) : \mathcal{D} \to \mathbb{R}$ is the input-output relationship and l is the linear *"output"* functional that links the input to the output through the field variable.
It follows from our hypothesis on a, f and l that the problem has a unique solution thanks to the *Lax-Milgram theorem* (Quarteroni et al., 2000; Quarteroni and Valli,

1997).
Recalling the affine development of the bilinear form and of the linear functional (section 2.2), it is possible to write the operators in the following form; for any $\boldsymbol{\mu} \in \mathcal{D}$:

$$a(w, v; \boldsymbol{\mu}) = \sum_{q=1}^{Q_a} \theta_a^q(\boldsymbol{\mu})\, a^q(w, v) \quad \forall\, v, w \in X^e \tag{19}$$

$$f(v; \boldsymbol{\mu}) = \sum_{q=1}^{Q_f} \theta_f^q(\boldsymbol{\mu})\, f^q(v) \quad \forall\, v \in X^e \tag{20}$$

$$l(v; \boldsymbol{\mu}) = \sum_{q=1}^{Q_l} \theta_l^q(\boldsymbol{\mu})\, l^q(v) \quad \forall\, v \in X^e \tag{21}$$

for finite and *preferebly* small Q_a, Q_f, Q_l. We implicitly assume that the θ_a^q for $1 \le q \le Q_a$, θ_f^q for $1 \le q \le Q_f$ and θ_l^q for $1 \le q \le Q_l$ are simple algebraic expressions that can be readily evaluated in $\mathcal{O}(1)$ operations.

Compliant problem. In this section the problems considered will be *"compliant"*, i.e. :

1. $l(\,\cdot\,; \boldsymbol{\mu}) = f(\,\cdot\,; \boldsymbol{\mu})$
2. $a(w; v; \boldsymbol{\mu}) = a(v, w; \boldsymbol{\mu}) \quad \forall\, w, v \in X^e$

that is the *output* functional and the *load/source* functional are the same and the bilinear form is symmetric (e.g. "compliancy" in linear elasticity). Considering these two hypotheses the problem (17)-(18) can be rewritten as it follows.
Given $\boldsymbol{\mu} \in \mathcal{D} \subset \mathbb{R}^P$, find $u(\boldsymbol{\mu}) \in X^e$ such that

$$a\left(u^e(\boldsymbol{\mu}, v; \boldsymbol{\mu})\right) = f\left(v; \boldsymbol{\mu}\right) \quad \forall\, v \in X^e \tag{22}$$

and evaluate

$$s^e(\boldsymbol{\mu}) = f(u^e(\boldsymbol{\mu}); \boldsymbol{\mu}). \tag{23}$$

Truth approximation. We focus the attention on the *"truth" approximation*. The reduced basis approximation will be built upon and the error will be measured relatives to this assumption of truth.
The role played by this assumption is very important; during the basis assembling and the error measuring the *RB* will completely "forget" the error between the *exact* solution and the *truth-assumption*. Then it is necessary to take some caution in order to ensure that this error remains suitably small for any given $\boldsymbol{\mu} \in \mathcal{D}$.
For analytical purposes, we assume that the *"truth"* takes the place of the *exact* statement. *Standard finite element FE* approximation (Quarteroni, 2013) may be chosen to represent the truth and to measure the error in order to build the *RB* basis and evaluate the error bounds for a given new set of parameter input $\boldsymbol{\mu}$.

Galerkin projection. We introduce a family of conforming approximation spaces $X^{\mathcal{N}} \subset X^e$ of dimension $\dim(X^{\mathcal{N}}) = \mathcal{N} < \infty$.
We then associate to our space a set of basis functions $\phi_k^{\mathcal{N}} \subset X^{\mathcal{N}}$, $1 \le k \le \mathcal{N}$, by construction, any member of $X^{\mathcal{N}}$ can be represented by a unique linear combination of the basis functions $\phi_k^{\mathcal{N}} \subset X^{\mathcal{N}}$.
Finally, we associate the inner products and induced norms $X^{\mathcal{N}}$ is equipped, denoted by $(v, w)_{X^{\mathcal{N}}}$, $\forall\, v, w \in X^{\mathcal{N}}$, and induced norm $||w||_{X^{\mathcal{N}}} = \sqrt{(w, w)_{X^{\mathcal{N}}}}$, $\forall\, w \in X^{\mathcal{N}}$.
This inner product, along with those related to the exact space, is explained below.

Inner product and induced norms. We now define the inner product and the norm over the space $X^{\mathcal{N}}$ and X^e and the *energy norm* given by the coercive bilinear form a.
For $w, v \in X^e$, we define respectively the *energy inner product* and the *energy norm* as:

$$\begin{aligned} ((w,v))_{\boldsymbol{\mu}} &= a\,(w,v;\boldsymbol{\mu})\,, \\ |||w|||_{\boldsymbol{\mu}} &= \sqrt{(w,w)_{\boldsymbol{\mu}}}, \end{aligned} \tag{24}$$

moreover, for a given $\bar{\boldsymbol{\mu}} \in \mathcal{D}$, we define for $w, v \in X^e$ the X^e-inner product and the X^e-norm as:

$$\begin{aligned} (w,v)_{X^e} &= ((w,v))_{\bar{\boldsymbol{\mu}}} + \tau\,(w,v)_{L^2(\Omega)}\,, \\ ||w||_{X^e} &= \sqrt{(w,w)_{X^e}}, \end{aligned} \tag{25}$$

where τ is a negative real parameter and$(w,v)_{L^2(\Omega)} = \displaystyle\int_\Omega w\,v\;d\Omega$.
Remark 1: We note that in order to define our X^e-norm we have chosen a fixed valued of the parameter $\overline{\boldsymbol{\mu}}$.
Remark 2: since $X^{\mathcal{N}} \subset X^e$, the inner products and the norms defined above are the same for the space $X^{\mathcal{N}}$.
The choice of $\bar{\boldsymbol{\mu}}$ and τ will affect the quality and efficiency of our reduced basis a posteriori error estimators, but this will not affect directly our reduced basis output predictions (Rozza et al., 2008).

Truth problem statement. Now we can state the problem in the truth space taking the *Galerkin projection* of the problem (22)-(23); given $\boldsymbol{\mu} \in \mathcal{D} \subset \mathbb{R}^P$, find $u(\boldsymbol{\mu}) \in X^{\mathcal{N}}$ such that

$$a\left(u^{\mathcal{N}}(\boldsymbol{\mu}), v; \boldsymbol{\mu}\right) = f\,(v;\boldsymbol{\mu}) \quad \forall\, v \in X^{\mathcal{N}} \tag{26}$$

and evaluate

$$s^{\mathcal{N}}(\boldsymbol{\mu}) = f(u^{\mathcal{N}}(\boldsymbol{\mu});\boldsymbol{\mu}). \tag{27}$$

Coercivity and continuity. We can define precisely the *exact* and the finite element *approximated coercivity constants* respectively, as:

$$\alpha^e(\boldsymbol{\mu}) = \inf_{w \in X^e} \frac{b(\,w,\,w\,;\boldsymbol{\mu})}{||w||^2_{X^e}}, \tag{28}$$

$$\alpha^{\mathcal{N}}(\boldsymbol{\mu}) = \inf_{w \in X^{\mathcal{N}}} \frac{b(\,w,\,w\,;\boldsymbol{\mu})}{||w||^2_{X^e}}. \tag{29}$$

From the coercivity hypothesis, we have that $\alpha^e(\boldsymbol{\mu}) > \alpha_0$, $\forall\, \boldsymbol{\mu} \in \mathcal{D}$; furthermore from our hypothesis on $X^{\mathcal{N}}$, that is a conforming space, we have that $\alpha^{\mathcal{N}}(\boldsymbol{\mu}) > \alpha^e(\boldsymbol{\mu})$, $\forall\, \boldsymbol{\mu} \in \mathcal{D}$. Than even after the approximation the problem remains coercive.
In the same way, the continuity constants are defined as

$$\gamma^e(\boldsymbol{\mu}) = \sup_{w \in X^e} \sup_{v \in X^e} \frac{b(\,w,\,v\,;\boldsymbol{\mu})}{||w||_{X^e}||v||_{X^e}}, \tag{30}$$

$$\gamma^{\mathcal{N}}(\boldsymbol{\mu}) = \sup_{w \in X^{\mathcal{N}}} \sup_{v \in X^{\mathcal{N}}} \frac{b(\,w,\,v\,;\boldsymbol{\mu})}{||w||_{X^{\mathcal{N}}}||v||_{X^{\mathcal{N}}}}, \tag{31}$$

once again from our hypothesis it follows $\gamma^e(\boldsymbol{\mu}) < \infty$ and $\gamma^{\mathcal{N}}(\boldsymbol{\mu}) \leq \gamma^e(\boldsymbol{\mu})$, $\forall\, \boldsymbol{\mu} \in \mathcal{D}$.

Well-posedness. The Galerkin approximation on $X^{\mathcal{N}}$ must satisfy the same conditions that the exact formulation satisfies over X^e. For the particular class of problems of interest in this section (elliptic coercive PDEs) the Galerkin formulation in fact *directly inherits* and even *improves upon* all the good properties of the exact formulation:

1. The dual norm of f over $X^{\mathcal{N}}(\subset X^e)$ is bounded by the dual norm of f over X^e;
2. symmetry is preserved;
3. a is coercive over $X^{\mathcal{N}}$ with:

$$\alpha^{\mathcal{N}}(\boldsymbol{\mu}) \geq \alpha^e(\boldsymbol{\mu}) \quad \forall\, \boldsymbol{\mu} \in \mathcal{D} \tag{32}$$

4. a is continuos over $X^{\mathcal{N}}$ with:

$$\gamma^{\mathcal{N}}(\boldsymbol{\mu}) \leq \gamma^e(\boldsymbol{\mu}) \quad \forall\, \boldsymbol{\mu} \in \mathcal{D} \tag{33}$$

5. the *affine expansions* for f and a are still valid for w, v restricted to $X^{\mathcal{N}}$;
6. a still satisfies the two conditions for parametric coercivity (section 2.2);

thus, for any $\mathcal{N}$ and associated $X^{\mathcal{N}}$, the Galerkin approximation preserves the *parametrically coercivity* and *affine compliancy* property.

3 RB method for parametrized elliptic coercive PDEs

In this section we will introduce the relevant steps for the generation of the rapidly convergent global RB approximation spaces for the approximation of the solution of parametrized *coercive* elliptic partial differential equations with affine parameter dependence will be explained.
Subsequently it will be possible to introduce the reduced basis approximation methodology, the sampling strategies and the construction of the reduced spaces. Then an *a-posteriori error bound* necessary to achieve an efficient *RB* sampling it will be introduced.

3.1 The RB heuristic idea

As described in section 1.2, the *RB* approach derives from the two *opportunities*. In particular regarding the *Opportunity I*, although $u^{\mathcal{N}}(\boldsymbol{\mu})$ is a member of the space $X^{\mathcal{N}}$ of typically very high dimension $\mathcal{N}$, in fact $u^{\mathcal{N}}(\boldsymbol{\mu})$ resides on a *low-dimensional parametrically induced*

manifold $\mathcal{M} \equiv \{u^{\mathcal{N}}(\boldsymbol{\mu}) \mid \boldsymbol{\mu} \in \mathcal{D}\}$.

In Figure 4 a graphical heuristic idea of the finite dimensional (*truth*) manifold $X^{\mathcal{N}}$ with the parametrically induced manifold $\mathcal{M}^{\mathcal{N}}$ (filament) is shown. The same idea in the exact infinite dimensional space is depicted in Figure 2.
It is thus wasteful to express the solution $u(\boldsymbol{\mu})$ as an arbitrary member of the unnecessarily rich space $X^{\mathcal{N}}$; rather, presuming that $\mathcal{M}$ is sufficiently smooth, we should represent $u(\boldsymbol{\mu})$ in terms of elements of an *ad-hoc* manifold much more lower dimensional (Patera and Rozza, 2007; Rozza et al., 2008).
The *RB* recipe is very simple (see Figure 5 for a graphical interpretation). The basic idea is to *efficiently* chose and compute N solutions or *"snapshots"* $\xi_1^{\mathcal{N}}, \xi_2^{\mathcal{N}}, \ldots, \xi_N^{\mathcal{N}} \in X^{\mathcal{N}}$ and then, for any arbitrary new $\boldsymbol{\mu}^* \in \mathcal{D}$, compute the solution $u_N^{\mathcal{N}}(\boldsymbol{\mu}^*)$ associated to this parameter thanks to an *appropriate combination* of the previously computed snapshots $\xi_k^{\mathcal{N}}$, $k = 1, \ldots, N$.
Note that "$u_N^{\mathcal{N}}(\boldsymbol{\mu})$" is not redundant; it means that this is the solution in the truth

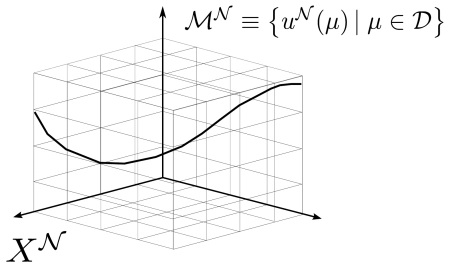

(a)

Figure 4: Parametrically induced manifold on $X^{\mathcal{N}}$

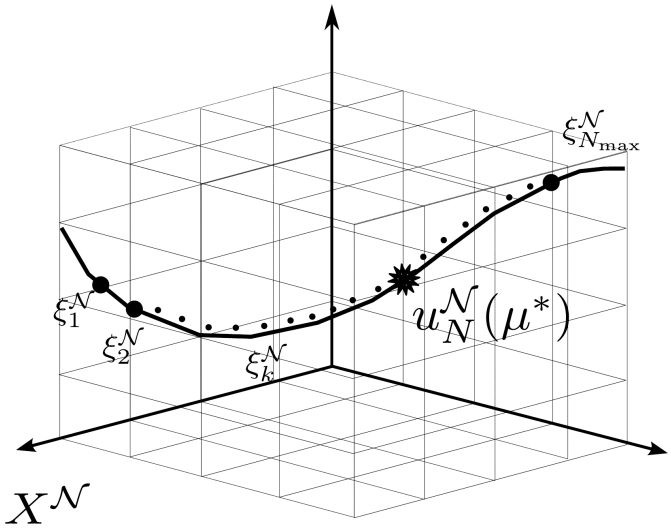

(a)

Figure 5: Approximation of $u^{\mathcal{N}}_N(\boldsymbol{\mu}^*)$

space $X^{\mathcal{N}}$ computed along the reduced manifold $\mathcal{M}^{\mathcal{N}}$, selecting N snapshots.
In the most part this work, if not specified, when dealing with *RB* solution we will always simply write $u_N(\boldsymbol{\mu})$ meaning the reduced solution in the truth space.
Now also the *Opportunity II* (section 1.2) can be understood; starting from the *RB* idea it is evident that are needed *at least* N solutions of the problem on the $\mathcal{N}$-dimensional *truth space*.
The *RB* approach is thus clearly *ill-suited* to the *single-query* or *few-query* situation; however, in the *real-time* and *many-query context* this *Offline* investment is readily acceptable in exchange for future asymptotic or Online computational burden reduction.

3.2 RB spaces and bases

In this section the *RB* problem formulation in the *coercive* case is discussed.
We begin introducing the spaces and basis that allow us to build the reduced basis problem, subsequently the *creation* of the *RB* system, the *Offline/Online* procedure and the *a-posteriori* error bound will be introduced.
There are different possible choices for the selection of the reduced basis spaces (Hermite, Lagrange, etc ...) that will lead ultimately to different reduced order model (Rozza et al., 2008; Patera and Rozza, 2007; Porsching, 1985; Ito and Ravin-

dran, 2001). In the following the *Lagrange hierarchical spaces* used in this work will be discussed.

Lagrange hierarchical spaces. We introduce a set of linearly independent functions:

$$\xi^n \in X, \quad 1 \leq n \leq N_{\max} \tag{34}$$

where $N_{\max}$ is the maximum dimension of the *RB* space, in terms of which we define the *RB* approximation spaces:

$$X_N = \text{span}\,\{\xi^n,\, 1 \leq n \leq N\} \quad 1 \leq N \leq N_{\max} \tag{35}$$

where we assume, in order to build a "reduced basis" that the ξ^n are somehow related to the manifold $\mathcal{M}$.
By construction we obtain

$$X_N \subset X, \quad \dim(X_N) = N, \quad 1 \leq N \leq N_{\max} \tag{36}$$

moreover, as the same property holds recursively for any nested subset of X_N, we can say that the space X is *hierarchical*.

Definition 3.1. Given a space X, given $N_{\max}$ subsets of this space $X_n \subset X$, $1 \leq n \leq N_{\max}$, we say that X is a *hierarchical (or nested)* space if:

$$X_1 \subset X_2 \subset \ldots \subset X_{N_{\max}-1} \subset X_{N_{\max}}. \tag{37}$$

The hierarchical property (37), as we shall see, is important in ensuring (memory) efficiency for the resulting reduced basis approximation.
To introduce the Lagrange (hierarchical) *RB* recipe, we first define a master set of parameter points $\boldsymbol{\mu}^n \in \mathcal{D}$, $1 \leq n \leq N_{\max}$, we then define, for given $N \in \{1, \ldots, N_{\max}\}$, the Lagrange parameter samples

$$S_N = \left\{\boldsymbol{\mu}^1, \ldots, \boldsymbol{\mu}^N\right\}, \tag{38}$$

that we choose *nested* in order to build a hierarchical space, that is:

$$S_1 = \left\{\boldsymbol{\mu}^1\right\} \subset S_2 = \left\{\boldsymbol{\mu}^1, \boldsymbol{\mu}^2\right\} \subset \ldots \subset S_{N_{\max}}. \tag{39}$$

The associated *Lagrange RB* spaces are defined as:

$$W_N^{\mathcal{N}} = \text{span}\left\{u^{\mathcal{N}}(\boldsymbol{\mu}^n)\right\}, \quad 1 \leq n \leq N. \tag{40}$$

We observe that, by construction, these Lagrange spaces are hierarchical; in fact the samples S_N are nested thanks to the choice (39), then accordingly:

$$W_1^{\mathcal{N}} = \text{span}\left\{u^{\mathcal{N}}(\boldsymbol{\mu}^1)\right\} \subset W_2^{\mathcal{N}} = \text{span}\left\{u^{\mathcal{N}}(\boldsymbol{\mu}^2),\, u^{\mathcal{N}}(\boldsymbol{\mu}^1)\right\} \subset \ldots \subset W_{N_{\max}}^{\mathcal{N}} \tag{41}$$

The $u^{\mathcal{N}}(\boldsymbol{\mu}^n)$, $1 \leq n \leq N_{\max}$ are the so-called *"snaphots"* related to the low dimensional manifold $\mathcal{M}^{\mathcal{N}}$. As already mentioned in section 3.1, we would expect to well approximate any member of the manifold thanks to a good combination of the available snapshots.
In theory, in order to build the *RB* approximation spaces, it would be necessary to choose a set of parameter samples that induces a set of linearly independent snapshots; the *greedy* sampling, that will be introduced in section 3.3, induces linear dependent functions as N increases. In fact, if the snapshot chosen W_N contains much of the $\mathcal{D}$ induced manifold $\mathcal{M}$, then it will be clear that the new $\boldsymbol{\mu}^{N+1} \in \mathcal{D}$ will perforce be a combination of this functions.
We therefore pursue a Gram-Schmidt orthogonalization in the $(\,\cdot\,,\,\cdot\,)_X$ inner product to recover an orthonormal well-conditioned set of basis functions in order to guarantee a good algebraic stability without ill-conditioning (Patera and Rozza, 2007).

Orthogonal *RB* bases. To achieve the orthogonalization, we apply the already mentioned Gram-Schmidt standard orthogonalization (Meyer, 2000). Given the basis functions $\xi^n,\ 1 \le n \le N_{\max}$ (34), that in the Lagrange space choice are the $u(\boldsymbol{\mu}_n),\ 1 \le n \le N_{\max}$ (40), we obtain the set of basis function $\zeta^n,\ 1 \le n \le N_{\max}$ as:

$$\begin{aligned}
&\zeta^1 = \xi^1/||\xi^1||_X;\\
&\texttt{for } n = 2 : N_{\max}\\
&\quad z^n = \xi^n - \sum_{m=1}^{n-1}, (\xi^n, \zeta^m)_X\ \zeta^m;\\
&\quad \zeta^n = z^n/||z^n||_X;\\
&\texttt{end}
\end{aligned} \tag{42}$$

As a result of this process we obtain the orthogonality condition:

$$(\zeta^m, \zeta^n)_X = \delta_{mn} \quad 1 \le m, n \le N_{\max} \tag{43}$$

where δ_{mn} is the Kronecker-delta symbol.
Finally we can express our reduced basis spaces X_N as:

$$X_N = \text{span}\,\{\zeta^n,\ 1 \le n \le N\} \quad 1 \le N \le N_{\max}. \tag{44}$$

Now any function $w_N \in X_N$ can be expressed as a linear combination of the reduced base X_N as:

$$w_N = \sum_{n=1}^{N} w_{N_n}\,\zeta^n \quad 1 \le N \le N_{\max} \tag{45}$$

for a unique combination of (RB) coefficients $w_{N_n} \in \mathbb{R},\ 1 \le n \le N_{\max}$.

Algebraic representation of *RB* bases. We now reconsider the orthogonalization process in order to introduce some concepts that will be necessary to build our *RB* problem starting from the *FE* original frame.
If we express our snapshots ξ^n in terms of *FE* functions $\phi_i,\ 1 \le i \le \mathcal{N}$:

$$\xi^n = \sum_{i=1}^{\mathcal{N}} \xi_i^n\,\phi_i, \quad 1 \le n \le N_{\max}, \tag{46}$$

similarly we may express our *RB* orthogonalized functions ζ^n as

$$\zeta^n = \sum_{i=1}^{\mathcal{N}} \zeta_i^n\,\phi_i, \quad 1 \le n \le N_{\max}. \tag{47}$$

Now, in the two cases above, we sort the *FE* coefficients in an array

$$\underline{\xi}^n \equiv \left\{\ \xi_1^n\ \xi_2^n\ \dots\ \xi_{\mathcal{N}}^n\ \right\}^T \quad 1 \le n \le, N_{\max} \tag{48}$$

$$\underline{\zeta}^n \equiv \left\{\ \zeta_1^n\ \zeta_2^n\ \dots\ \zeta_{\mathcal{N}}^n\ \right\}^T \quad 1 \le n \le N_{\max}. \tag{49}$$

We then introduce the algebraic representation $\underline{\underline{\mathbb{X}}}^{\mathcal{N}} \in \mathbb{R}^{\mathcal{N}\times\mathcal{N}}$ of the inner product $(\cdot,\cdot)_X$:

$$\underline{\underline{\mathbb{X}}}^{\mathcal{N}}_{ij} = \left(\phi^i, \phi^j\right)_{X^{\mathcal{N}}} \quad 1 \le i, j \le \mathcal{N}. \tag{50}$$

The orthogonalization process can be now formulated as:

$$
\begin{aligned}
&\underline{\zeta}^1 = \underline{\xi}^1 / \sqrt{\underline{\xi}^{1\,T} \underline{\underline{\mathbb{X}}}\, \underline{\xi}^1};\\
&\texttt{for } n = 2 : N_{\max}\\
&\qquad \underline{z}^n = \underline{\xi}^n - \sum_{m=1}^{n-1} \left(\underline{\xi}^n \underline{\underline{\mathbb{X}}}\, \underline{\zeta}^m\right)\, \underline{\zeta}^m;\\
&\qquad \underline{\zeta}^n = \underline{z}^n / \sqrt{\underline{z}^{n\,T} \underline{\underline{\mathbb{X}}}\, \underline{z}^n};\\
&\texttt{end}
\end{aligned}
\tag{51}
$$

Finally it is useful to introduce the *"basis"* matrices $\underline{\underline{Z}} \in \mathbb{R}^{\mathcal{N} \times N}$, $1 \leq N \leq N_{\max}$:

$$
Z_{N_j\, n} = \zeta_j^n \quad 1 \leq j \leq \mathcal{N},\ 1 \leq n \leq N. \tag{52}
$$

This matrices is built in such a way that the n$^{\text{th}}$-column of the matrix is formed by the vector of *FE* coefficients $\zeta_{N_j}^n,\ 1 \leq j \leq \mathcal{N}$ associated to the n$^{\text{th}}$ *RB* function.

Galerkin projection. The projection strategy used in order to obtain the *RB* approximation is given by a Galerkin projection, which is arguably the best approach. We remark that the *RB* weak formulation has formally the same appearance as the *"exact"* weak formulation (see equations (17)-(18), section 2.3); in this case we properly replace the *FE* truth functional space with the *RB* approximation space; in the next Section we will show how to obtain the latter from the former by means of an algebraic procedure.
The problem states: given $\boldsymbol{\mu} \in \mathcal{D}$, find $u_N \left(\equiv u_N^{\mathcal{N}}\right) \in X_N \left(X_N^{\mathcal{N}}\right)$ such that

$$
a(u_N(\boldsymbol{\mu}), v; \boldsymbol{\mu}) = f(v; \boldsymbol{\mu}) \quad \forall\, v \in X_N \tag{53}
$$

we evaluate

$$
s_N(\boldsymbol{\mu}) = f(u_N(\boldsymbol{\mu})). \tag{54}
$$

From coercivity and continuity hypothesis on a and f, our conforming reduced basis $X_N^{\mathcal{N}} \subset X^{\mathcal{N}}$, and from our assumption of linear independence of snapshots, the problem (53)-(54) admits an unique solution (Quarteroni and Valli, 1997; Quarteroni, 2013). Thanks to the Galerkin projection, the optimality results subsequently discussed holds (Rozza et al., 2008; Patera and Rozza, 2007).

Proposition 3.2. *For any $\boldsymbol{\mu} \in \mathcal{D}$ and $u_N(\boldsymbol{\mu})$ and $s_N(\boldsymbol{\mu})$ satisfying (53)-(54):*

$$
|||u^{\mathcal{N}} - u_N^{\mathcal{N}}|||_{\boldsymbol{\mu}} = \inf_{w_N \in X_N^{\mathcal{N}}} |||u^{\mathcal{N}} - w_N|||_{\boldsymbol{\mu}} \tag{55}
$$

$$
||u^{\mathcal{N}} - u_N^{\mathcal{N}}||_X \leq \sqrt{\frac{\gamma^e(\boldsymbol{\mu})}{\alpha^e(\boldsymbol{\mu})}} \inf_{w_N \in X_N^{\mathcal{N}}} ||u^{\mathcal{N}} - w_N||_X \tag{56}
$$

as regard the output optimality results, in the compliant case *we obtain:*

$$
\begin{aligned}
s_N - s_N^{\mathcal{N}} &= |||u^{\mathcal{N}} - u_N^{\mathcal{N}}|||_{\boldsymbol{\mu}}^2\\
&= \inf_{w_N \in X_N^{\mathcal{N}}} |||u^{\mathcal{N}} - w_N|||_{\boldsymbol{\mu}}^2
\end{aligned}
\tag{57}
$$

and furthermore

$$
0 \leq s_N - s_N^{\mathcal{N}} \leq \gamma^e(\boldsymbol{\mu}) \inf_{w_N \in X_N^{\mathcal{N}}} ||u^{\mathcal{N}} - w_N||_X^2, \tag{58}
$$

where $\gamma^e(\boldsymbol{\mu})$ and $\alpha^e(\boldsymbol{\mu})$ are the continuity and coercivity constants, respectively (defined in (6) and (5)) in the exact space. It will be shown that these optimality results will be used even after, replacing the exact constants with those evaluated with the reduced space approximation.
It is also necessary to remark from (57) that, in the *compliant case*, the error on the output is the *square* of the error of the field variable: we have the so-called *"square effect"*, this is crucial for the input/output accuracy and efficiency of the method.
Last but not least, $s_N(\boldsymbol{\mu})$ is a *lower bound* for $s^{\mathcal{N}}$, in fact: (i) $s_N(\boldsymbol{\mu}) = a(u_N(\boldsymbol{\mu}), u_N(\boldsymbol{\mu}); \boldsymbol{\mu})$ is a positive quantity, and (ii) the error in the output is the *square* of the error of the field variable (Rozza et al., 2008).

Offline-Online procedures: algebraic formulation. The algebraic formulation for the coercive problem will be explained. The crucial point that will be treated is the Online/Offline splitting procedure; this procedure will be equipped with an operation count to highlight the potential computational saving offered by the *RB* method.
In order to apply the standard variational procedure to obtain the algebraic formulation of the problem, we first expand $u_N(\boldsymbol{\mu})$:

$$u_N(\boldsymbol{\mu}) = \sum_{j=1}^{N} u_N^j(\boldsymbol{\mu}) \tag{59}$$

now, inserting the expansion (59) in the problem (53) and choosing $v = \zeta^i, \;\; 1 \leq i \leq N$ as our *test function*, we obtain the set of linear algebraic equations

$$\sum_{j=1}^{N} a(\zeta^j, \zeta^i; \boldsymbol{\mu})\, u_N^j(\boldsymbol{\mu}) = f(\zeta^i; \boldsymbol{\mu}), \quad 1 \leq i \leq N \tag{60}$$

for the reduced basis coefficients $u_N^j(\boldsymbol{\mu})$ $1 \leq i \leq N$.
The output can then be expressed as

$$s_N(\boldsymbol{\mu}) = \sum_{j=1}^{N} u_N^j(\boldsymbol{\mu})\, f(\zeta^j; \boldsymbol{\mu}) \tag{61}$$

We now express these operations in matrix form; we first introduce the array of *RB* basis coefficients $u_N(\boldsymbol{\mu})$ as

$$\underline{u}_N \equiv [u_{N_1} u_{N_2} \dots u_{N_N}] \tag{62}$$

It follows from (60) that $\underline{u}_N \in \mathbb{R}^N$ satisfies

$$\underline{\underline{A}}_N(\boldsymbol{\mu})\, \underline{u}_N(\boldsymbol{\mu}) = \underline{F}_N(\boldsymbol{\mu}) \tag{63}$$

where $\underline{\underline{A}}_N(\boldsymbol{\mu}) \in \mathbb{R}^{N \times N}$ is the "stiffness matrix", and $\underline{F}_N(\boldsymbol{\mu}) \in \mathbb{R}^N$ is the "load/source" array. This quantity are in particular given by:

$$\underline{\underline{A}}_{N_{i,j}}(\boldsymbol{\mu}) = a(\zeta^j, \zeta^i; \boldsymbol{\mu}) \quad 1 \leq i, j \leq N \tag{64}$$

and

$$\underline{F}_{N_i}(\boldsymbol{\mu}) = f(\zeta^i; \boldsymbol{\mu}) \quad 1 \leq i \leq N. \tag{65}$$

Finally, the output can now be expressed as

$$\underline{s}_N(\boldsymbol{\mu}) = \underline{F}_N^T\, \underline{u}_N \tag{66}$$

It follows from our assumption of linear independence of the snapshots that the stiffness matrix is symmetric and positive definite.

Offline-Online. It is now possible, starting from the algebraic problem, to introduce the *Offline/Online* procedure.
The reduced basis system (63) is clearly of small size, in fact it is an $N \times N$ linear system that requires $\mathcal{O}(N^3)$ operation to solve it, plus $\mathcal{O}(N)$ operation to obtain the output from the equation (66).
By appealing to our previous assumption of affine parameter dependence discussed in section 2.2, from (11) and (15), the *stiffness matrix* and *load/source vector* can be expressed, respectively, as

$$a(\zeta^m, \zeta^n; \boldsymbol{\mu}) = \sum_{q=1}^{Q_a} \theta_a^q(\boldsymbol{\mu})\, a(\zeta^m, \zeta^n) \quad 1 \le m, n \le N \tag{67}$$

and

$$f(\zeta^n; \boldsymbol{\mu}) = \sum_{q=1}^{Q_f} \theta_f^q(\boldsymbol{\mu})\, f(\zeta^n) \quad 1 \le n \le N. \tag{68}$$

The Offline-Online decomposition is now possible.

Offline: In the offline part we form:

1. the parameter independent matrices $\underline{\underline{\mathbb{A}}}_N^q \in \mathbb{R}^{N \times N}$

$$\underline{\underline{\mathbb{A}}}_{N_{m,n}}^q = a^q(\zeta^m, \zeta^n), \quad 1 \le m, n \le N, \;\; 1 \le q \le Q_a \tag{69}$$

2. the parameter independent vectors $\underline{\mathbb{F}}_N^q \in \mathbb{R}^N$

$$\underline{\mathbb{F}}_{N_n}^q = f^q(\zeta^n), \quad 1 \le n \le N, \;\; 1 \le q \le Q_f \tag{70}$$

This operations $\mathcal{N}$-dependent and hence very expensive are computed *once*.

Online: In the online stage we assemble, for any new $\boldsymbol{\mu} \in \mathcal{D}$:

1. the *RB* reduced stiffness matrix $\underline{\underline{A}}_N(\boldsymbol{\mu})$

$$\underline{\underline{A}}_N(\boldsymbol{\mu}) = \sum_{q=1}^{Qa} \theta_a^q(\boldsymbol{\mu})\, \underline{\underline{\mathbb{A}}}_N^q \tag{71}$$

2. the *RB* reduced load/source vector $\underline{F}_N(\boldsymbol{\mu})$

$$\underline{F}_N(\boldsymbol{\mu}) = \sum_{q=1}^{Q_f} \theta_f^q(\boldsymbol{\mu})\, \underline{\mathbb{F}}_N^q \tag{72}$$

the operation count is actually $\mathcal{N}$-independent and hence very inexpensive.

Link between FE and RB. Before a detailed discussion over the operation count, it is necessary to provide the link between the *FE* and the *RB* stiffness matrix and load/source vector; it is worth to remark that this operation will be completed once in the offline stage.
In particular it can be showed that the former are linked to the latter via the *snapshots* matrices $\underline{\underline{\mathbb{Z}}} \in \mathbb{R}^{\mathcal{N} \times N}$, $1 \le N \le N_{\max}$.
The stiffness matrix (64) that can be written as:

$$a(\zeta^m, \zeta^n; \boldsymbol{\mu}) = \sum_{j=1}^{\mathcal{N}} \sum_{i=1}^{\mathcal{N}} \zeta_j^m\, a(\phi^i, \phi^j; \boldsymbol{\mu})\, \zeta_i^n \quad 1 \le m, n \le N_{\max} \tag{73}$$

thanks to the definition of the *basis matrix* $\underline{\underline{\mathbb{Z}}}$ (52) and the *FE* development of the reduced basis functions ζ^n (47) we may rewrite the stiffness matrix (73) as

$$\underline{\underline{A}}_N(\boldsymbol{\mu}) = \underline{\underline{\mathbb{Z}}}^T \underline{\underline{A}}(\boldsymbol{\mu})\, \underline{\underline{\mathbb{Z}}}. \tag{74}$$

In the same way the reduced parametric independent stiffness matrices $\underline{\underline{A}}_N^q$ (71) are linked to the *FE* matrices:

$$\underline{\underline{\mathbb{A}}}_N^q = \underline{\underline{\mathbb{Z}}}^T \underline{\underline{\mathbb{A}}}^q\, \underline{\underline{\mathbb{Z}}}. \tag{75}$$

The load/source vectors (66) admit a similar treatment

$$\underline{F}_N(\boldsymbol{\mu}) = \underline{\underline{\mathbb{Z}}}^T \underline{F}(\boldsymbol{\mu}). \tag{76}$$

finally the parameter independent load/source vector 72 can be written as

$$\underline{\mathbb{F}}_N^q = \underline{\underline{\mathbb{Z}}}^T \underline{\mathbb{F}}^q(\boldsymbol{\mu}) \quad 1 \le q \le Q_f. \tag{77}$$

Operation count and storage. Thanks to the Offline/Online splitting procedure, we have achieved an Online $\mathcal{N}$-independent stage, hence very inexpensive. It is necessary to focus on the Offline and Online complexity to quantify the computational reduction provided by the *RB* method.
We make use of Table 1 to summarize the computational burden requested to perform: (i) Offline, the *RB* basis assembling, (ii) Online, a single input/output evaluation.

PART	ITEM	BURDEN	EQUATION
Offline	$\underline{\underline{\mathbb{Z}}}_N$	$N\,\mathcal{O}(\mathcal{N}^3)$	(52)
	$\underline{\underline{\mathbb{A}}}_N^q$	$Q_a\,N\,\underline{\underline{A}}$-matvec $+\, Q_a\,N^2\,X^{\mathcal{N}}$-inprod	(75)
	$\underline{\mathbb{F}}_N$	$Q_f\,N\,X^{\mathcal{N}}$-inprod	(77)
Online	$\underline{\underline{A}}_N$	$Q_a\,N^2$	(71)
	$\underline{F}_N$	$Q_f\,N$	(72)
	u_N	$\mathcal{O}(N^3)$	(60)
	s_N	N^2	(66)

Table 1: Offline/Online: coercive case

In this table we have denoted with "A-matvec" and "$X^{\mathcal{N}}$-inprod", the matrix-vector multiplication and the inner product between two vectors $\in X^{\mathcal{N}}$, respectively.
As regard the storage we need only to store $\underline{\underline{\mathbb{A}}}_{N_{\max}}^q$ $1 \le q \le Q_a$ and $\underline{\mathbb{F}}_{N_{\max}}^q$ $1 \le q \le Q_f$, then extract only the sub-matrices and sub-vectors of desired N thanks to the hierarchical base property, as explained in (37).

3.3 Sample/space assembling

We now discuss the procedure used to select the snapshots in order to assemble the reduced basis approximation spaces, after a few preliminaries. We then turn to the *Greedy sampling* strategy exploited in this chapter (Patera and Rozza, 2007). See also (Huynh et al., 2007; Rozza et al., 2008) for more options sampling

strategies.
We shall denote by Ξ a finite sample of points in $\mathcal{D}$. These "test" samples Ξ serve as surrogates for $\mathcal{D}$ in the calculation and presentation of errors over the parameter domain. Typically these samples are chosen by *Monte Carlo* methods with respect to a uniform or log $-$uniform density.
Concerning the dimension of the sample, we always ensure that Ξ is sufficiently large that the reported results are *insensitive* to further refinement of the parameter sample.

Definition 3.3. Given a function $y : \mathcal{D} \to \mathbb{R}$, we define the $L^\infty(\Xi)$ and $L^p(\Xi)$ norms respectively as:

$$\begin{aligned} ||y||_{L^\infty(\Xi)} &\equiv \max_{\boldsymbol{\mu}\in\Xi} |y(\boldsymbol{\mu})| \\ ||y||_{L^p(\Xi)} &\equiv \left(|\Xi|^{-1} \sum_{\boldsymbol{\mu}\in\Xi} |y(\boldsymbol{\mu})|^p \right)^{1/p} . \end{aligned} \tag{78}$$

Definition 3.4. Given a function $z : \mathcal{D} \to X^{\mathcal{N}}$ (or X^e), we define the $L^\infty(\Xi; X)$ and $L^p(\Xi; X)$ norms respectively as:

$$\begin{aligned} ||z||_{L^\infty(\Xi;X)} &\equiv \max_{\boldsymbol{\mu}\in\Xi} |z(\boldsymbol{\mu})|_X \\ ||z||_{L^p(\Xi;X)} &\equiv \left(|\Xi|^{-1} \sum_{\boldsymbol{\mu}\in\Xi} ||z(\boldsymbol{\mu})||_X^p \right)^{1/p} . \end{aligned} \tag{79}$$

Here $|\Xi|$ denotes the cardinality of (the finite number of elements in) the test sample Ξ. We now introduce the *Greedy Lagrange spaces*, that will be used to build our *RB* approximation.

Greedy Lagrange spaces. We have already introduced the concept of *Lagrange spaces* (see section 3.2), we now have to extend this idea to Greedy Lagrange spaces.
We remark that this strategy is not indispensable to build a basic model reduction, but it is a *prerogative* of the *Reduced Basis method*. In fact the *Greedy* sampling, we are going to discuss, can be efficiently exploited only combined to an Offline/Online splitting procedure.
The idea of this strategy is starting with a train sample Ξ_{train}, we select N parameters $\boldsymbol{\mu}_1, \ldots, \boldsymbol{\mu}_N$ and, as already seen in section 3.2, we form the reduced basis space X^N as:

$$X^N = \text{span}\left\{ \xi_n = u^{\mathcal{N}}(\boldsymbol{\mu_n}),\ 1 \le n \le N \right\}. \tag{80}$$

More precisely, for the *Greedy approach*, we need a also *sharp*, *rigorous* and *efficient bound* $\Delta_N^{en}(\boldsymbol{\mu})$ for the reduced basis error $||u^{\mathcal{N}}(\boldsymbol{\mu}) - u_N(\boldsymbol{\mu})||_X$, where u_N is our *RB* approximation associated with the space X_N (Rozza et al., 2008). The superscript ^{en} denotes that the bound is related to the *energy norm* of the error, other options are discussed in Patera and Rozza (2007).
To quantify the *sharpness* and *rigour* properties, we recall the *effectivity* of an error bound.

Definition 3.5. The *effectivity* of an error bound, denoted by η, is defined as follows

$$\eta_N^{en} = \frac{\Delta_N^{en}}{||u^{\mathcal{N}}(\boldsymbol{\mu}) - u_N(\boldsymbol{\mu})||_X} \tag{81}$$

we require that

$$1 \leq \eta_N^{en} \leq \eta_{\max,\mathrm{UB}}^{en} \quad \forall\, \boldsymbol{\mu} \in \mathcal{D},\ 1 \leq N \leq N_{\max} \tag{82}$$

where $\eta_{\max,\mathrm{UB}}^{en}$ is finite and N independent.

It is possible to show that the inequality (82) is always fullfilled in the *RB* method (Rozza et al., 2008). The *rigour* property is illustrated by the *left* inequality: the error bound $\Delta_N^{en}(\boldsymbol{\mu})$ is never smaller than the true error $||u^{\mathcal{N}}(\boldsymbol{\mu}) - u_N(\boldsymbol{\mu})||_X$. The *sharpness* property is illustrated by the *right* inequality: $\Delta_N^{en}(\boldsymbol{\mu})$ *has not to bee much bigger* than the true error. Last, *efficient* means that the evaluation of $\Delta_N^{en}(\boldsymbol{\mu})$ is $\mathcal{N}$ independent, thanks to the Offline/Online procedure that we will show in section 3.4. The last property is crucial in the *Greedy* procedure, in fact it permits us to exploit a *very large* train sample Ξ_{train}in order to select the best snapshots to be include in our *RB* approximation spaces.

Greedy algorithm. We define $\overline{N}_{\max}$, an upper bound for $N_{\max}$ and $\epsilon_{\mathrm{toll,min}}$ the desired minimum tolerance over the error bound.
Given Ξ_{train}, $S_1 = \{\boldsymbol{\mu}^1\}$ and $X^1 = \mathrm{span}\,\{u^{\mathcal{N}}(\boldsymbol{\mu}^1)\}$,

$$\begin{aligned}
&\texttt{for } N = 2 : \overline{N}_{\max} \\
&\quad \boldsymbol{\mu}^N = \arg \max_{\boldsymbol{\mu} \in \Xi_{\mathrm{train}}} \\
&\quad \epsilon_{N-1} = \Delta_N^{en}(\boldsymbol{\mu}^N) \\
&\quad \texttt{if } \epsilon_{N-1} \leq \epsilon_{\mathrm{toll,min}} \\
&\qquad N_{\max} = N - 1 \\
&\quad \texttt{end} \\
&\quad S_N = S_{N-1} \cup \boldsymbol{\mu}^N \\
&\quad X_N = X_{N-1} + \mathrm{span}\,\{u^{\mathcal{N}}(\boldsymbol{\mu}^N)\} \\
&\texttt{end}
\end{aligned} \tag{83}$$

In the *Greedy* algorithm the key point is to exploit an approximated (very cheap) error bound $\Delta_N^{en}(\boldsymbol{\mu}^N)$ instead of the true error (hence very expensive) $||u^{\mathcal{N}}(\boldsymbol{\mu}) - u_N(\boldsymbol{\mu})||$.
We remark that the *Greedy* algorithm *heuristically* minimizes the *RB* error bound in $L^\infty(\Xi_{\mathrm{train}}; X)$ norm (Patera and Rozza, 2007; Rozza et al., 2008): the algorithm evaluates the error bounds $\forall\, \boldsymbol{\mu} \in \Xi_{\mathrm{train}}$, then the next snapshot is selected such that it corresponds to the *maximum error bound*.

3.4 A-posteriori error bound

A-posteriori error bounds are crucial in the *RB* methodology. They are important for both *efficiency* and *reliability* of *RB* approximations.
As regards *efficiency*, error bounds play a role in *Offline* and *Online* stage. In the *Greedy* algorithm for example, the application of *error bounds* permits larger training sample at reduced *Offline* computational cost. Hence, we have a better accuracy of the reduced basis approximation which can be obtained with a smaller number N of basis functions, and hence we have a further reduction in the *Online* computational cost.
In other words, a posteriori error estimation permits us to control the error thus allowing us to *minimize* the computational effort (Patera and Rozza, 2007).

As regards *reliability*, our *Offline* sampling procedures could not be exhaustive without a Greedy approach. For a large number of parameters P, there would be a large portion of the parameter space $\mathcal{D}$ which would remain unexplored. So, the error of a large parts of the parameter domain $\mathcal{D}$ would be affected by uncertainty. The *a-posteriori* error bounds permit to *rigorously* bound the error for all new value of parameter $\boldsymbol{\mu}^* \in \mathcal{D}$. So we do not lose any confidence in the solution compared to the underlying *FE* solution while exploiting the rapid predictive power of the *RB* approximation.
As mentioned in section 3.3, the *a-posteriori* error bound must be rigorous (greater or equal to the true error) for all N and all parameters values in the parameter domain $\mathcal{D}$. Second, the bound must be reasonably *sharp*. An overly conservative error bound can yield inefficient approximations, typically N too large, or *suboptimal* engineering results, for example too much big safety margins.
For the coercive case, see Patera and Rozza (2007); Rozza et al. (2008), whereas for the non-coercive case see Rozza (2009a); Rovas (2003).

Preliminaries. We define the residual $r : \mathcal{D} \to \left(X^{\mathcal{N}}\right)'$ as

$$r(v;\boldsymbol{\mu}) = f(v;\boldsymbol{\mu}) - a(u_N^{\mathcal{N}}(\boldsymbol{\mu}, v;\boldsymbol{\mu})) \quad \forall\, v \in X^{\mathcal{N}} \tag{84}$$

where $\left(X^{\mathcal{N}}\right)'$ is the dual space of $X^{\mathcal{N}}$.
We also introduce the function $\hat{e} : \mathcal{D} \to X^{\mathcal{N}}$, the *Riesz* representation of $r(v;\boldsymbol{\mu})$, see (Quarteroni, 2013):

$$(\hat{e}(\boldsymbol{\mu}), v)_X = r\,(v;\boldsymbol{\mu}) \quad \forall\, v \in X^{\mathcal{N}}. \tag{85}$$

Finally, introducing the real error $e^{\mathcal{N}}(\boldsymbol{\mu})\,(\equiv e(\boldsymbol{\mu}))$

$$e(\boldsymbol{\mu}) = u^{\mathcal{N}}(\boldsymbol{\mu}) - u_N^{\mathcal{N}}. \tag{86}$$

Recalling that $u^{\mathcal{N}}(\boldsymbol{\mu})$ and $u_N(\boldsymbol{\mu})$ satisfies the equations (26) and (53), respectively, we get from (84), (85) that the error $e(\boldsymbol{\mu})$ satisfies the following relation

$$a(e(\boldsymbol{\mu}), v;\boldsymbol{\mu}) = r(v;\boldsymbol{\mu}) = (\hat{e}(\boldsymbol{\mu}), v) \quad \forall\, v \in X^{\mathcal{N}}. \tag{87}$$

We note that for our choice of inner product (25): $\hat{e}(\boldsymbol{\mu}) = e(\boldsymbol{\mu})$.
We then define the *dual norm* of $r(\,\cdot\,;\boldsymbol{\mu})$ associated to the dual space $\left(X^{\mathcal{N}}\right)'$:

$$||r(v;\boldsymbol{\mu})||_{X'} = \sup_{v \in X} \frac{r(v;\boldsymbol{\mu})}{||v||_X} = ||\hat{e}(\boldsymbol{\mu})||_X. \tag{88}$$

Note that the second equality follows from the *Riesz representation theorem*. This definition is crucial for the *Offline-Online* procedure.
Our aim is to find an approximated lower bound for $\alpha^{\mathcal{N}}(\boldsymbol{\mu})$ (5), that is a function $\alpha_{\mathrm{LB}}^{\mathcal{N}} : \mathcal{D} \to \mathbb{R}$ such that

1. $0 < \alpha_{\mathrm{LB}}^{\mathcal{N}}(\boldsymbol{\mu}) \leq \alpha^{\mathcal{N}}(\boldsymbol{\mu}) \quad \forall\, \boldsymbol{\mu} \in \mathcal{D}$;
2. the evaluation $\boldsymbol{\mu} \to \alpha_{\mathrm{LB}}^{\mathcal{N}}$ should be independent of $\mathcal{N}$.

We will discuss the procedure to evaluate this coercivity lower bound in 3.5.

Error bound estimators. Now we can define our *energy*, *output* and *relative output error bound* estimators, that are defined respectively as (Patera and Rozza,

2007; Rozza et al., 2008):

$$\Delta_N^{en}(\boldsymbol{\mu}) = \frac{||\hat{e}(\boldsymbol{\mu})||_X}{\left(\alpha_{\mathrm{LB}^{\mathcal{N}}}(\boldsymbol{\mu})\right)^{1/2}}, \tag{89a}$$

$$\Delta_N^{s}(\boldsymbol{\mu}) = \frac{||\hat{e}(\boldsymbol{\mu})||_X^2}{\alpha_{\mathrm{LB}^{\mathcal{N}}}(\boldsymbol{\mu})}, \tag{89b}$$

$$\Delta_N^{s,rel}(\boldsymbol{\mu}) = \frac{||\hat{e}(\boldsymbol{\mu})||_X^2}{\alpha_{\mathrm{LB}^{\mathcal{N}}}(\boldsymbol{\mu})\, s_N^{\mathcal{N}}(\boldsymbol{\mu})} = \frac{\Delta_N^{s}(\boldsymbol{\mu})}{s_N^{\mathcal{N}}(\boldsymbol{\mu})}. \tag{89c}$$

Effectivity estimators. As already discussed in Section 3.3, associated to each estimator theres is an *effectivity estimator* as a measure of the *quality* of the error bound estimators and are needed to certify that the *RB* method is *rigorous* and *sharp*. We introduce the following ones:

$$\eta_N^{en}(\boldsymbol{\mu}) = \frac{\Delta_N^{en}(\boldsymbol{\mu})}{|||e(\boldsymbol{\mu})|||_{\boldsymbol{\mu}}}, \tag{90a}$$

$$\eta_N^{s}(\boldsymbol{\mu}) = \frac{\Delta_N^{s}(\boldsymbol{\mu})}{s^{\mathcal{N}}(\boldsymbol{\mu}) - s_N^{\mathcal{N}}(\boldsymbol{\mu})}, \tag{90b}$$

$$\eta_N^{en,rel}(\boldsymbol{\mu}) = \frac{\Delta_N^{s,rel}(\boldsymbol{\mu})}{\left(s^{\mathcal{N}}(\boldsymbol{\mu}) - s_N^{\mathcal{N}}(\boldsymbol{\mu})\right)/s^{\mathcal{N}}(\boldsymbol{\mu})}. \tag{90c}$$

It is can be shown that the *effectivities* are a measure of the *rigor* and *sharpness* for an error bound.

Proposition 3.6. *The following results holds (see Rozza et al. (2008) for the proof):*

$$1 < \eta_N^{en}(\boldsymbol{\mu}) \leq \sqrt{\frac{\gamma^e(\boldsymbol{\mu})}{\alpha_{\mathrm{LB}}^{\mathcal{N}}(\boldsymbol{\mu})}}, \tag{91}$$

$$1 < \eta_N^{s}(\boldsymbol{\mu}) \leq \frac{\gamma^e(\boldsymbol{\mu})}{\alpha_{\mathrm{LB}}^{\mathcal{N}}(\boldsymbol{\mu})}, \tag{92}$$

and finally, with regard to $\eta_N^{en,rel}(\boldsymbol{\mu})$, it can be shown that:

$$\eta_N^{en,rel}(\boldsymbol{\mu}) = (\eta_N^{en}(\,\boldsymbol{\mu}))^2. \tag{93}$$

Offline-Online procedure. The main component of the error bound is the computation of the dual norm of the residual $||\hat{e}(\boldsymbol{\mu})||_X$. To develop the Offline-Online procedure, we introduce the residual expansion, $\forall\, v \in X$:

$$r(v;\boldsymbol{\mu}) = \sum_{q=1}^{Q_f} \theta_f^q(\boldsymbol{\mu})\, f^q(v) + \sum_{q=1}^{Q_a}\sum_{n=1}^{N} \theta_a^q(\boldsymbol{\mu})\, u_{N_n}(\boldsymbol{\mu})\, a^q\left(\xi_n, v\right). \tag{94}$$

This expansion directly follows from our affine assumption (11) and from the *RB* development $u_N(\boldsymbol{\mu}) = \sum_{n=1}^{N} u_{N_n}\, \xi_n$.
Moreover, we have from (87) that:

$$\left(\hat{e}(\boldsymbol{\mu}), v\right)_X = \sum_{q=1}^{Q_f} \theta_f^q(\boldsymbol{\mu})\, f^q(v) + \sum_{q=1}^{Q_a}\sum_{n=1}^{N} \theta_a^q(\boldsymbol{\mu})\, u_{N_n}(\boldsymbol{\mu})\, a^q\left(\xi_n, v\right). \tag{95}$$

Consequently, defining

$$(\mathcal{C}^q, v)_X = f^q(v) \qquad 1 \le q \le Q_f \tag{96a}$$

$$(\mathcal{L}^q_n, v)_X = -a^q(\xi_n, v) \qquad 1 \le q \le Q_a,\ 1 \le n \le N \tag{96b}$$

we can write

$$\hat{e}(\boldsymbol{\mu}) = \sum_{q=1}^{Q_f} \theta^q_f(\boldsymbol{\mu})\, \mathcal{C}^q + \sum_{q=1}^{Q_a} u_{N_n}(\boldsymbol{\mu})\, \theta^q_a(\boldsymbol{\mu})\, \mathcal{L}^q_n. \tag{97}$$

We remark that (96a) and (96b) are parameter-independent *Poisson-like* problems, hence $\mathcal{C}^q$ and $\mathcal{L}^q_n$ are computed *Offline*. We thus obtain

$$\begin{aligned}
||\hat{e}(\boldsymbol{\mu})||_X &= \left(\sum_{q=1}^{Q_f} \theta^q_f(\boldsymbol{\mu})\, \mathcal{C}^q + \sum_{q=1}^{Q_a} \sum_{n=1}^{N} \theta^q_a(\boldsymbol{\mu})\, u_{n_N}(\boldsymbol{\mu})\, \mathcal{L}^q_n, \right)_X \\
&= \sum_{q=1}^{Q_f} \sum_{q'=1}^{Q_f} \theta^q_f(\boldsymbol{\mu}) \theta^{q'}_f(\boldsymbol{\mu}) \left(\mathcal{C}^q, \mathcal{C}^{q'} \right)_X + \\
&\quad + \sum_{q=1}^{Q_a} \sum_{n=1}^{N} \theta^q_a(\boldsymbol{\mu})\, u_{N_n} \left\{ 2 \sum_{q'=1}^{Q_f} \theta^q_a(\boldsymbol{\mu}) \theta^{q'}_f(\boldsymbol{\mu}) \left(\mathcal{L}^q_n, \mathcal{C}^{q'} \right)_X + \right. \\
&\quad \left. + \sum_{q'=1}^{Q_a} \sum_{n'=1}^{N} \theta^{q'}_a \left(\mathcal{L}^q_n, \mathcal{L}^{q'}_{n'} \right)_X \right\}.
\end{aligned} \tag{98}$$

The Offline-Online procedure is clear. In the Offline stage, we first compute $\mathcal{C}^q$, $1 \le q \le Q_f$ and $\mathcal{L}^q_n$, $1 \le q \le Q_a$, $1 \le n \le N$, then we compute and store the quantities:

$$\left(\mathcal{C}^q, \mathcal{C}^{q'} \right)_X \qquad 1 \le q \le Q_f,\ 1 \le q' \le Q_f \tag{99}$$

$$(\mathcal{L}^q_n, \mathcal{C}^q)_X \qquad 1 \le q \le Q_a,\ 1 \le q' \le Q_f \tag{100}$$

$$(\mathcal{L}^q_n, \mathcal{L}^q)_X \qquad 1 \le q \le Q_a,\ 1 \le q \le Q_a \tag{101}$$

In the *Online* stage we evaluate the expression 98 which consists in a sum. The computational cost to perform this evaluation is:

$$n^2 Q_a^2 \ + \ 2nQ_aQ_f \ + \ nQ_f^2, \tag{102}$$

so it is $\mathcal{N}$ independent, hence very inexpensive.

3.5 Successive constraint method

We now discuss the successive constraint method (SCM). This tool enables the construction of lower (and upper) bounds for the *coercivity* (and *inf-sup* stability) constants (5), required in a posteriori error analysis of RB approximations: Without risk of a global comprehension loss, the reader can go to proposition 3.7. The method, based on an *Offline-Online* strategy, reduces the *Online* calculation to a small *Linear Programming problem*: the *objective* is a parametric expansion of the underlying *Rayleigh* quotients, the *constraints* reflect stability information at optimally selected parameter points. The *state of the art* method is presented in Huynh et al. (2007), see also Rozza et al. (2008).

Coercive case. We define

$$\mathcal{Y} \equiv \left\{ y = (y_1 \dots y_{Q_a}) \in \mathbb{R}^{Q_a} \mid \exists w_y \in X^{\mathcal{N}} \text{ s.t. } y_q = \frac{a^q(w_y, w_y)}{||w||_{X^{\mathcal{N}}}}, \, 1 \le q \le Q_a \right\}. \quad (103)$$

We further define the *objective function* $\mathscr{F} : \mathcal{D} \times \mathbb{R}^{Q_a} \to \mathbb{R}$ as

$$\mathscr{F}(y; \boldsymbol{\mu}) = \sum_{q=1}^{Q_a} \theta_a^q(\boldsymbol{\mu}) \, y_q. \quad (104)$$

We may then write our *coercivity* constant as

$$\alpha^{\mathcal{N}}(\boldsymbol{\mu}) = \min_{y \in \mathcal{Y}} \mathscr{F}(y; \boldsymbol{\mu}). \quad (105)$$

We next introduce a *constraint box* that is the set of all the feasible value for y, defined as

$$\begin{aligned} \mathcal{B} &= \prod_{q=1}^{Q_a} \left\{ \sigma_-^q, \, \sigma_+^q \right\} \\ &= \prod_{q=1}^{Q_a} \left\{ \inf_{w \in X^{\mathcal{N}}} \frac{a^q(w,w)}{||w||^2_{X^{\mathcal{N}}}}, \, \sup_{w \in X^{\mathcal{N}}} \frac{a^q(w,w)}{||w||^2_{X^{\mathcal{N}}}} \right\}. \end{aligned} \quad (106)$$

We also introduce the two parameter sets $\mathcal{S}$ and $\mathcal{P}$, that will be used to define the stability and positivity constraint, respectively:

$$\mathcal{S} = \{ s_1 \in \mathcal{D}, \dots, s_k \in \mathcal{D} \}, \quad (107)$$

$$\mathcal{P} = \{ p_1 \in \mathcal{D}, \dots, p_k \in \mathcal{D} \}. \quad (108)$$

Moreover, for any finite-dimensional *subset* of $\mathcal{D}$ ($= \mathcal{S}$ or $\mathcal{P}$), we denote with $\mathcal{S}^{\mathrm{M},\boldsymbol{\mu}}$ $\left(\text{or } \mathcal{P}^{\mathrm{M},\boldsymbol{\mu}}\right)$ the set of M points closest to[4] $\boldsymbol{\mu}$ in $\mathcal{S}$ (or $\mathcal{P}$).
If $\mathrm{M} > |\mathcal{S}|$, (or $> |\mathcal{P}|$)[5], then $\mathcal{S}^{\mathrm{M},\boldsymbol{\mu}} = |\mathcal{S}|$ $\left(\text{or } \mathcal{P}^{\mathrm{M},\boldsymbol{\mu}} = \mathcal{P}\right)$.

Lower and Upper bound. For given $\mathcal{S} \subset \mathcal{D}$, $\mathrm{M}_\alpha \in \mathbb{N}$ (stability constraints), $\mathrm{M}_+ \in \mathbb{N}$ (positivity constraints), we define the *lower bound* set as

$$\begin{aligned} \mathcal{Y}_{\mathrm{LB}}(\mathcal{S}; \boldsymbol{\mu}) \equiv \Bigg\{ & y \in \mathcal{B} \mid \sum_{q=1}^{Q_a} \theta_a^q(\boldsymbol{\mu}') y_q \ge \alpha^{\mathcal{N}}(\boldsymbol{\mu}'), \, \forall \boldsymbol{\mu}' \in \mathcal{S}^{\mathrm{M}_\alpha,\boldsymbol{\mu}}; \\ & \sum_{q=1}^{Q_a} \theta_a^q(\boldsymbol{\mu}') y_q \ge 0, \, \forall \boldsymbol{\mu}' \in \mathcal{P}^{\mathrm{M}_+,\boldsymbol{\mu}} \Bigg\}. \end{aligned} \quad (109)$$

Furthermore we define the *upper bound* set as

$$\mathcal{Y}_{\mathrm{UB}}(\mathcal{S}) \equiv \{ y^\star(\boldsymbol{\mu})(s_k), \, 1 \le k \le |\mathcal{S}| \} \quad (110)$$

for

$$y^\star(\boldsymbol{\mu}) \equiv \arg\min_{y \in \mathcal{Y}} \mathscr{F}(y; \boldsymbol{\mu}). \quad (111)$$

[4] In the *Euclidean norm*

[5] We recall that $|\cdot|$ denotes the *cardinality* of a finite set of elements

Finally we obtain the *coercivity lower* and *upper bound* as

$$\alpha_{\text{LB}}(\mathcal{S};\boldsymbol{\mu}) = \min_{y\in\mathcal{Y}_{\text{LB}}(y;\mathcal{S})} \mathscr{F}(y;\boldsymbol{\mu}), \tag{112}$$

$$\alpha_{\text{UB}}(\mathcal{S};\boldsymbol{\mu}) = \min_{y\in\mathcal{Y}_{\text{UB}}(\mathcal{S})} \mathscr{F}(y;\boldsymbol{\mu}). \tag{113}$$

It is possible to show that the *lower/upper bounds* provided above, *effectively bound* the coercivity constant, the subsequent result holds:

Proposition 3.7. *Given* $\mathcal{S}$, $\mathcal{P}$ *and* $\mathrm{M}_\alpha \in \mathbb{N}$, $\mathrm{M}_+ \in \mathbb{N}$

$$\alpha_{\text{LB}}(\mathcal{S};\boldsymbol{\mu}) \le \alpha^{\mathcal{N}}(\boldsymbol{\mu}) \le \alpha_{\text{UB}}(\mathcal{S};\boldsymbol{\mu}) \qquad \forall \boldsymbol{\mu}\in\mathcal{D} \tag{114}$$

The proof can be found in Huynh et al. (2007); Rozza et al. (2008).

We expect that if $\mathcal{S}$ is sufficiently large, then

1. $y^\star(\boldsymbol{\mu})$ will be sufficiently close to a member of $\mathcal{Y}_{\text{UB}}$ to provide a good *upper bound*;
2. the *stability* and *positivity* constraints in $\mathcal{Y}_{\text{LB}}$ will sufficiently restrict y to provide a good *lower bound*.

SCM algorithm. We now present the algorithm to exploit the evaluation of the *coercivity* constant.
The task of the *SCM* is – given a sample train $\Xi_{\text{SCM}} = \left\{\boldsymbol{\mu}^1_{\text{SCM}},\dots,\boldsymbol{\mu}^{n_{\text{SCM}}}_{\text{SCM}}\right\}$ of dimension $|\Xi_{\text{SCM}}| = n_{\text{SCM}}$ – to select Greedy parameters in Ξ_{SCM} and construct the sets $\mathcal{S}_k = \left\{s_1 = \boldsymbol{\mu}^1_{\text{SCM}} \cup \ldots \cup s_{K_{\max}} = \boldsymbol{\mu}^{K_{\max}}_{\text{SCM}}\right\}$. We now introduce the algorithm.
We define M_α, M_+, $\mathcal{P}$ and a tolerance $\epsilon_{\text{SCM}} \in \left]0,1\right[$, then we set $K_{\mathcal{S}} = 1$ and choose $\mathcal{S}_1 = \left\{s_1 = \boldsymbol{\mu}^1_{\text{SCM}}\right\}$ *arbitrarily*, then

$$\begin{aligned}
&\texttt{while} \max_{\boldsymbol{\mu}\in\Xi_{\text{SCM}}} \left[\frac{\alpha_{\text{UB}}(\mathcal{S};\boldsymbol{\mu}) - \alpha_{\text{LB}}(\mathcal{S};\boldsymbol{\mu})}{\alpha_{\text{UB}}(\mathcal{S};\boldsymbol{\mu})}\right] > \epsilon_{\text{SCM}} \\
&\qquad s_{K+1} = \arg\max_{\boldsymbol{\mu}\in\Xi_{\text{SCM}}} \left[\frac{\alpha_{\text{UB}}(\mathcal{S};\boldsymbol{\mu}) - \alpha_{\text{LB}}(\mathcal{S};\boldsymbol{\mu})}{\alpha_{\text{UB}}(\mathcal{S};\boldsymbol{\mu})}\right] \\
&\qquad \mathcal{S}_{\mathcal{K}+\infty} = \mathcal{S}_{\mathcal{K}} \cup s_{K+1} \\
&\qquad K = K+1 \\
&\texttt{end} \\
&K_{\max} = K
\end{aligned} \tag{115}$$

Normally we set $\epsilon_{\text{SCM}} \approx 0.75$ which is a crude lower bound but with a little effect on error bounds, (Huynh et al., 2007).

Offline-Online procedure. We note that to compute the arg max we must solve a *linear optimization problem* or *Linear Program* (*LP*), for the lower bound $\alpha_{\text{LB}}(\boldsymbol{\mu})$ (112).
In the coercive case, the lower bound *LP*'s contains:

- design variables
  1. Q_a variables, $y = \{y_1,\dots,y_{Q_a}\}$;
- constraints
  1. $2Q_a$ bounding boxes for $y \in \mathcal{B}$;
  2. M_α stability constraints;
  3. M_+ positivity constraints.

It is clear that the operation count for the *Online* stage $\boldsymbol{\mu} \to \alpha_{\text{LB}}(\boldsymbol{\mu})$ is *independent* of $\mathcal{N}$.
Nonetheless we first must determine our set $\mathcal{S}$ and obtain the $\alpha^{\mathcal{N}}(s_k)$, $1 \le k \le |\mathcal{S}|\,(\equiv K_{\mathcal{S}})$, by an Offline *Greedy SCM* algorithm.

Offline: In the *Offline* stage, we have to construct the set $\mathcal{B}$ (once) and then:

1. evaluate $\alpha^{\mathcal{N}}(s_k)$;
2. evaluate $y^{\star}(s_k)$;
3. form $\mathcal{Y}_{\text{LB}}$;
4. perform a lower bound LP's to evaluate $\alpha_{\text{LB}}(s_k)$.

The first three quantities of course depends on $\mathcal{N}$, nonetheless it is important to *remark* that there are no *cross terms* $\mathcal{O}\left(n_{\text{SCM}} \times \mathcal{N}\right)$.

Online: In the *Online* stage, given a new value $\boldsymbol{\mu}$ we have to perform a lower bound LP's (LP) to evaluate $\alpha_{\text{LB}}(\boldsymbol{\mu})$. This Online stage is hence independent on $\mathcal{N}$.
In the table 2 we summarize the computational cost to evaluate the *Offline/Online* stage of the SCM:

PART	ITEM	COMPLEXITY	EQUATION
Offline	$\mathcal{B}$	$2Q_a$-eigenproblems over $X^{\mathcal{N}}$	(106)
	$\alpha^{\mathcal{N}}(s_k)$	$K_{\max}$-eigenproblems over $X^{\mathcal{N}}$	(109)
	$y^{\star}(s_k)$	$K_{\max}\, Q_a$-inner product	(111)
	$\mathcal{Y}_{\text{LB}}$	$\mathcal{N}\, Q_a\, K_{\max}$	(109)
	$\alpha_{\text{LB}}(s_k)$	$n_{\text{SCM}}\, K_{\max}$ LP's of "size" $\mathcal{O}\left(2Q_a + \text{M}_\alpha + \text{M}_+\right)$	(112)
Online	$\alpha_{\text{LB}}(\boldsymbol{\mu})$	1 LP's of "size" $\mathcal{O}\left(2Q_a + \text{M}_\alpha + \text{M}_+\right)$	(72)

Table 2: Offline/Online: SCM

3.6 Choice of the truth approximation

It would be preferable to build the RB approach directly upon the exact solution, but this is not in general possible. As indicated earlier, the RB approximation shall be built upon and reduced basis error will be measured relative to a "truth" Galerkin FE approximation. Therefore it is necessary to choose *properly* the underlying discretization.

Choice of $\mathcal{N}$. In order to obtain a satisfying reduced basis model able to describe in an accurate way the exact behavior of the physical process, it is necessary to chose the discretization properly; that is in order to minimize the underlying error between *exact* solution and the *truth approximation*.
Let $u^{RB}(\boldsymbol{\mu})$ be the RB solution of the problem and $u^{\mathcal{N}}(\boldsymbol{\mu})$ the finite element solution, than the error is the sum of (at least) two terms:

$$||u^e(\boldsymbol{\mu}) - u^{RB}(\boldsymbol{\mu})|| = \underbrace{||u^e(\boldsymbol{\mu}) - u^{\mathcal{N}}(\boldsymbol{\mu})||}_{\text{neglected}} + \underbrace{||u^{\mathcal{N}}(\boldsymbol{\mu}) - u_N(\boldsymbol{\mu})||}_{\text{considered}}. \tag{116}$$

The minimization of the second addendum is a task delagated to the reduced basis method, on the contrary the minimization of the first is not related to the method. Because of this, it is necessary to provide a feasible "starting point". This can be achieved thanks to the choice of a discretization method able to describe correctly the problem.

We shall require that our family of truth subspaces $X^{\mathcal{N}}$ satisfies the approximation condition:

$$\max_{\boldsymbol{\mu}\in\mathcal{D}} \inf_{w\in X^{\mathcal{N}}} ||u(\boldsymbol{\mu}) - w||_{X^e} \to 0 \quad \text{as} \quad \mathcal{M} \to \infty. \tag{117}$$

The choice of a *finite element* approximation automatically fulfill this requirement because the method is *strongly consistent* (Quarteroni and Valli, 1997; Quarteroni, 2013); thus for sufficiently large $\mathcal{N}$, it is possible to approximate $u^e(\boldsymbol{\mu})$ and $s^e(\boldsymbol{\mu})$ arbitrarily closely.
In particular we define the difference $\epsilon^{\mathcal{N}}$ between the exact solution and the approximation as:

$$\epsilon^{\mathcal{N}} = \max_{\boldsymbol{\mu}\in\mathcal{D}} ||u(\boldsymbol{\mu}) - u^{\mathcal{N}}(\boldsymbol{\mu})||_{X^e} \overset{\mathcal{N}\to\infty}{\longrightarrow} 0. \tag{118}$$

In general, $\mathcal{N}$ must be chosen rather large to achieve a reasonable engineering accuracy $\epsilon^{\mathcal{N}}$.
In 3D problems the complexity is higher since there is greater variability of the solution field as the parameters changes. Therefore it is necessary to discretize the problem so that for any possible combination of the parameters the accuracy is kept under a safe tolerance. In fact it is worth to recall that the *RB Offline* representation has to be built over a *unique truth representation* for all $\boldsymbol{\mu} \in \mathcal{D}$; the truth approximation is *"frozen"* in the *RB* methodology. The choice of the optimum (or at least of a suitable) *truth* solution is *not trivial*, nevertheless it is possible to verify *a-posteriori* if the discretization is enough rich to seize all the geometrical and physical complexity of the problem.

4 Geometrical parametrization

In this section we will introduce how to handle a domain which is parameter dependent.
The *RB* method described in section 3 requires that Ω is parameter independent: if we wish to consider linear combinations of snapshots, these snapshots must be defined relative to a common spatial configuration (domain) .
Then to allow geometrical variations, we must express Ω, our parameter independent domain, as the pre-image of Ω_o, the original (actual, deformed) parameter dependent domain (Rozza et al., 2008).
The geometrical transformation will yield *variable* (parameter-dependent) *coefficients* in the reference-domain linear and bilinear forms that, under suitable hypotheses to be discussed below, will take at the end the requisite affine form (11).

4.1 Affine parametric precondition

We now introduce a domain decomposition:

$$\Omega_o(\boldsymbol{\mu}) = \bigcup_{k=1}^{K_{\text{dom}}} \Omega_o^k(\boldsymbol{\mu}) \tag{119}$$

where the $\Omega_o^k(\boldsymbol{\mu})$ are mutually non overlapping subdomains, that is for any $\boldsymbol{\mu} \in \mathcal{D}$

$$\Omega_o^k(\boldsymbol{\mu}) \cap \Omega_o^{k'}(\boldsymbol{\mu}) = 0 \quad 1 \le k, k' \le K_{\text{dom}},\ k \ne k'.$$

This coarse domain decomposition will be denoted *RB* discretization.
We now choose a parameter of reference $\boldsymbol{\mu}_{\text{ref}} \in \mathcal{D}$ and define our reference domain

as $\Omega_r \equiv \Omega(\boldsymbol{\mu}_{\rm ref})$.
We will never omit the pedix script beside the domain Ω we are dealing with, to avoid any confusion between the parameter dependent *original domain* $\Omega_o(\boldsymbol{\mu})$ (sometimes for brevity, just Ω_o) and the parameter independent reference domain Ω_r.
We will build our *FE* approximation on a very fine *FE* subtriangulation of the coarse *RB* decomposition.
This *FE* subtriangulation ensures that the *FE* approximation accurately treats the perhaps discontinuous coefficients (that could arise from property and geometry variation) associated with the different subdomains. The subtriangulation also plays an *important role* in the generation of the affine representation.
The choice of $\boldsymbol{\mu}_{\rm ref}$ has to be done in an optimal way to reduce both Offline and Online computational effort.
Tipically the reference domain shall be built choosing a $\boldsymbol{\mu}_{\rm ref}$ at the *"center"* of our parameter domain $\mathcal{D}$ in order to *minimize* the *distorsion* and consequently reduce the requisite $\mathcal{N}$.

We now state our *Affine Geometry Precondition*. We can treat any *original* domain $\Omega_o(\boldsymbol{\mu})$, that *admits* a *domain decomposition* (119), for which, $\forall\, \boldsymbol{\mu} \in \mathcal{D}$

$$\Omega_r = \mathcal{T}^{\text{aff},k}(\Omega o(\boldsymbol{\mu})^k; \boldsymbol{\mu}) \tag{120}$$

for *affine mappings* $\mathcal{T}^{\text{aff},k}(\,\cdot\,;\boldsymbol{\mu}) : \Omega_o(\boldsymbol{\mu}) \to \Omega_r,\ 1 \le k \le K_{\rm dom}$, that satisfy two requisites:

1. *individually bijective*;
2. *collectively continuos* (interface condition), that is, given two different subdomains denoted with k and k', $\forall\, \mathbf{x}_o \in \Omega_o^k(\boldsymbol{\mu}) \cap \Omega_o^{k'}$, holds the following condition
$$\mathcal{T}^{\text{aff},k}(\mathbf{x_o}; \boldsymbol{\mu}) = \mathcal{T}^{\text{aff},k'}(\mathbf{x_o}; \boldsymbol{\mu}). \tag{121}$$

We have depicted the idea of the affine transformation in Figure 6. Of course,

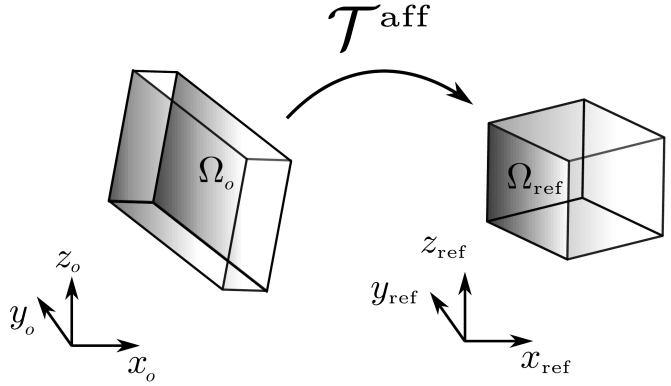

Figure 6: A 3D affine transformation

thanks to the requested bijective property, we can replace this definition with the forward version taking the inverse of $\mathcal{T}^{\text{aff}}$ committing any crime.
The *Affine Geometry Precondition* is a *necessary* condition for affine parameter dependence as defined in (11).
Note that we purposely define $K_{\rm dom}$ with respect to the *exact* problem, rather

than the *FE* approximation: K_{dom} is not depending on $\mathcal{N}$.
We now give a more explicit representation of the *affine transformation* $\mathcal{T}^{\text{aff}}$, to better understand how this geometry precondition will be exploited.
We state that, for $1 \leq k \leq K_{\text{dom}}$, for any $\boldsymbol{\mu} \in \mathcal{D}$ and for all $\mathbf{x}_o \in \Omega_o^k(\boldsymbol{\mu})$, the affine transformation is defined as follows:

$$\mathbf{x}_r = \mathcal{T}_i^{\text{aff},k}(\mathbf{x}_o; \boldsymbol{\mu}) = C_i^{\text{aff},k}(\boldsymbol{\mu}) + \sum_{j=1}^{d} G_{ij}^{\text{aff},k}(\boldsymbol{\mu})\, \mathbf{x}_o, \quad 1 \leq i \leq d \tag{122}$$

for given $C^{\text{aff},k}(\boldsymbol{\mu}) : \mathcal{D} \to \mathbb{R}^d$ and $G^{\text{aff},k}(\boldsymbol{\mu}) : \mathcal{D} \to \mathbb{R}^{d \times d}$, that are called the *affine mapping coefficients*; we recall that d is the spatial dimension of the problem, hence in our case $d = 3$.
The affine transformation is thus the superposition of a translation $C^{\text{aff}}(\boldsymbol{\mu})$, that do not modify the shape of the domain, and a deformation $G^{\text{aff}}(\boldsymbol{\mu})$ that can be a dilation/contraction or a shear. It is worth to remark that, in this work, the transformation *must* depends only upon the parameter $\boldsymbol{\mu}$.

A more general transformation, that involves a spatial coordinates dependence, is not considered in the framework of this thesis. This kind of transformation called *"nonaffine"* has been recently adopted in the context of the *RB* methodology (M. et al., 2004; Rozza, 2009a). The *non-affine* representation of the geometry arises from the so-called *free form deformation* techniques, which are very well suited, for example, for shape optimizations of complex geometries (Manzoni et al., 2012; Lassila and Rozza, 2010) and (Rozza and Manzoni, 2010).
The basic idea is that, thanks to an highly specialized technique, the so-called *empirical interpolation* (*EIM*), it is possible to approximate a *nonaffine* tranformation thanks to a *superposition* of different *affine* transformations.
Nonetheless this results has been established in a 2D context, the extension to the 3D case in still under investigation.

We can now define the associated *Jacobians*:

$$J^{\text{aff},k}(\boldsymbol{\mu}) = \left|\det\left(G^{\text{aff},k}(\boldsymbol{\mu})\right)\right|, \quad 1 \leq k \leq K_{\text{dom}}, \tag{123}$$

which are constants in space over each subdomain. We further define, for any $\boldsymbol{\mu} \in \mathcal{D}$

$$D^{\text{aff},k}(\boldsymbol{\mu}) = G^{\text{aff},k}(\boldsymbol{\mu}), \tag{124}$$

this matrix shall prove convenient in subsequent *derivative* transformations, as we will see in section 4.3.
We may interpret our *local mappings* in terms of a *global transformation*. In particular, for any $\boldsymbol{\mu} \in \mathcal{D}$, the local mapping (120) induces a global *bijective piecewise-affine* mapping $\mathcal{T}^{\text{aff}} : \Omega_o(\boldsymbol{\mu}) \to \Omega_r$, such that:

$$\mathcal{T}^{\text{aff}}(\mathbf{x}_o; \boldsymbol{\mu}) = \mathcal{T}^{\text{aff},k}(\mathbf{x}_o; \boldsymbol{\mu}), \qquad k = \min_{k' \in \{1,\ldots,K_{\text{dom}}\} \,|\, \mathbf{x} \in \Omega_o^{k'}(\boldsymbol{\mu})} \tag{125}$$

note the one-to-one property of this mapping (and, hence the arbitrariness of our *min* choice in (125)) is ensured by the interface condition (121).
In the following section the creation of an affine mappings will be discussed, subsequently the treatment of the parametric geometry dependence will be exploited thanks to an operative example.

4.2 Affine mappings construction

For simplicity we now consider a single subdomain, nonetheless the extension to the multi-subdomains case is readily obtainable as we will see.

As we consider a single subdomain in this section, we shall suppress the subdomain superscript for clarity of exposition. The procedure, in the 2D case, is explained in Rozza et al. (2008), in this work it has been extended to the more general 3D case.
In the 3D case ($d = 3$, see equation 122) the affine mapping coefficients are $C^{\text{aff}}(\boldsymbol{\mu}) \in \mathbb{R}^3$ and $G^{\text{aff}}(\boldsymbol{\mu}) \in \mathbb{R}^{3\times 3}$, that is we have $3 + 9 = 12$ unknows to find in order to entirely define the affine transformation.
Under our assumption that the mapping is invertible, we know that the Jacobian J^{aff} of (123) is *strictly positive* and that the *derivative transformation matrix* D^{aff} of (124) is well defined.

Then the mapping coefficient can be identified by the relationship between 4 *non-planar parametrized image points* $\in \Omega_o(\boldsymbol{\mu})$, denoted with $\underline{\mathbf{z}}_o(\boldsymbol{\mu})$ and the corresponding 4 pre-image points $\in \Omega_r$, denoted with $\underline{\mathbf{z}}_r$ [6]:

$$\left\{ \begin{array}{c} \underline{\mathbf{z}}_o^1(\boldsymbol{\mu}) \\ \underline{\mathbf{z}}_o^2(\boldsymbol{\mu}) \\ \underline{\mathbf{z}}_o^3(\boldsymbol{\mu}) \\ \underline{\mathbf{z}}_o^4(\boldsymbol{\mu}) \end{array} \right\} = \left\{ \begin{array}{c} \{z_{o_1}^1,\, z_{o_2}^1,\, z_{o_3}^1\} \\ \{z_{o_1}^2,\, z_{o_2}^2,\, z_{o_3}^2\} \\ \{z_{o_1}^3,\, z_{o_2}^3,\, z_{o_3}^3\} \\ \{z_{o_1}^4,\, z_{o_2}^4,\, z_{o_3}^4\} \end{array} \right\},$$

$$\left\{ \begin{array}{c} \underline{\mathbf{z}}_r^1 \\ \underline{\mathbf{z}}_r^2 \\ \underline{\mathbf{z}}_r^3 \\ \underline{\mathbf{z}}_r^4 \end{array} \right\} = \left\{ \begin{array}{c} \{z_{r_1}^1,\, z_{r_2}^1,\, z_{r_3}^1\} \\ \{z_{r_1}^2,\, z_{r_2}^2,\, z_{r_3}^2\} \\ \{z_{r_1}^3,\, z_{r_2}^3,\, z_{r_3}^3\} \\ \{z_{r_1}^4,\, z_{r_2}^4,\, z_{r_3}^4\} \end{array} \right\}.$$

In particular, for given $\boldsymbol{\mu} \in \mathcal{D}$, the application of (122) to the selected nodes yields to:

$$z_{r_i}^m = C_i^{\text{aff}} + \sum_{j=1}^{3} G_{ij}^m \, z_{o_j}^m, \quad 1 \le i \le 3, \quad 1 \le m \le 4, \tag{126}$$

The (126) provides a system made of 12 equations, by which to determine the 12 *mapping coefficients*. If we choose at least two coplanar points, than the system is singular.
To be more explicit, we provide a matricial representation of equation 126:

$$\underline{\underline{\mathbb{B}}}^{\text{aff}} \underline{\mathbf{c}}^{\text{aff}} = \underline{\mathbf{v}}^{\text{aff}}. \tag{127}$$

Where the matrix $\mathbb{B} \in \mathbb{R}^{12\times 12}$ summarizes the coefficients of the linear system, that depends upon the coordinates of the *"original"* points:

$$\underline{\underline{\mathbb{B}}}^{\text{aff}} = \begin{bmatrix} \begin{bmatrix} & \\ \underline{\underline{I}}^{3\times 3} & \\ & \end{bmatrix} & \begin{bmatrix} \underline{\mathbf{z}}_o^1 & \underline{0} & \underline{0} \\ \underline{0} & \underline{\mathbf{z}}_o^1 & \underline{0} \\ \underline{0} & \underline{0} & \underline{\mathbf{z}}_o^1 \end{bmatrix} \\ \begin{bmatrix} & \\ \underline{\underline{I}}^{3\times 3} & \\ & \end{bmatrix} & \begin{bmatrix} \underline{\mathbf{z}}_o^2 & \underline{0} & \underline{0} \\ \underline{0} & \underline{\mathbf{z}}_o^2 & \underline{0} \\ \underline{0} & \underline{0} & \underline{\mathbf{z}}_o^2 \end{bmatrix} \\ \begin{bmatrix} & \\ \underline{\underline{I}}^{3\times 3} & \\ & \end{bmatrix} & \begin{bmatrix} \underline{\mathbf{z}}_o^1 & \underline{0} & \underline{0} \\ \underline{0} & \underline{\mathbf{z}}_o^2 & \underline{0} \\ \underline{0} & \underline{0} & \underline{\mathbf{z}}_o^3 \end{bmatrix} \end{bmatrix} \tag{128}$$

[6] Here we denote with the superscript one of the 4 point considered, whereas the subscript indicates one of the 3 the components (x, y, z) of the spatial coordinates.

moreover $\underline{\mathbf{c}}^{\text{aff}} \in \mathbb{R}^{12\times 1}$ is the array of unknows (i.e. the *mapping coefficients*) sorted as shown in (129); finally $\underline{\mathbf{v}}^{\text{aff}} \in \mathbb{R}^{12\times 1}$ is the array of known terms, that depends upon the coordinates of the *reference* points:

$$\underline{\mathbf{c}}^{\text{aff}} = \left\{ \begin{array}{c} C_1^{\text{aff}} \\ C_2^{\text{aff}} \\ C_3^{\text{aff}} \\ G_{11}^{\text{aff}} \\ G_{12}^{\text{aff}} \\ G_{13}^{\text{aff}} \\ G_{21}^{\text{aff}} \\ G_{22}^{\text{aff}} \\ G_{23}^{\text{aff}} \\ G_{31}^{\text{aff}} \\ G_{32}^{\text{aff}} \\ G_{33}^{\text{aff}} \end{array} \right\}, \quad \underline{\mathbf{v}}^{\text{aff}} = \left\{ \begin{array}{c} \underline{\mathbf{z}}_r^1 \\ \underline{\mathbf{z}}_r^2 \\ \underline{\mathbf{z}}_r^3 \\ \underline{\mathbf{z}}_r^4 \end{array} \right\}. \tag{129}$$

The mapping coefficients can be easily found solving the linear system (127) as it follows:

$$\underline{\mathbf{c}}^{\text{aff}} = \underline{\underline{\mathbb{B}}}^{\text{aff}^{-1}} \underline{\mathbf{v}}^{\text{aff}}. \tag{130}$$

The solution of the system requires 12^3 operation, negligible if compared to the previously discussed basis assembling cost.

Single domain mapping. We now use an example to illustrare the procedure. We will use as test case the transformation depicted in Figure 7.

With regard to the figure 7, we choose as geometrical parameters $\boldsymbol{\mu} = \{\mu_2, \mu_3, \mu_1\} = \{2, 3, 4\}$, in addition to simplify we choose $\underline{d}_r = \underline{d}_o(\boldsymbol{\mu})$, hence we can use a local system attached to the first node ($\underline{\mathbf{z}}_*^1$).
Now, exploiting the procedure showed in section 4.2, we can build the system (127) by which we obtain the mapping coefficients.

$$\left\{ \begin{array}{c} C_1^{\text{aff}} \\ C_2^{\text{aff}} \\ C_3^{\text{aff}} \\ G_{11}^{\text{aff}} \\ G_{12}^{\text{aff}} \\ G_{13}^{\text{aff}} \\ G_{21}^{\text{aff}} \\ G_{22}^{\text{aff}} \\ G_{23}^{\text{aff}} \\ G_{31}^{\text{aff}} \\ G_{32}^{\text{aff}} \\ G_{33}^{\text{aff}} \end{array} \right\} = \left(\left[\begin{array}{cccccccccccc} 1 & 0 & 0 & 0 & 0 & 0 & 0 & 0 & 0 & 0 & 0 & 0 \\ 0 & 1 & 0 & 0 & 0 & 0 & 0 & 0 & 0 & 0 & 0 & 0 \\ 0 & 0 & 1 & 0 & 0 & 0 & 0 & 0 & 0 & 0 & 0 & 0 \\ 1 & 0 & 0 & \mu_1 & 0 & 0 & 0 & 0 & 0 & 0 & 0 & 0 \\ 0 & 1 & 0 & 0 & 0 & 0 & \mu_1 & 0 & 0 & 0 & 0 & 0 \\ 0 & 0 & 1 & 0 & 0 & 0 & 0 & 0 & 0 & \mu_1 & 0 & 0 \\ 1 & 0 & 0 & \mu_1 & 0 & \mu_3 & 0 & 0 & 0 & 0 & 0 & 0 \\ 0 & 1 & 0 & 0 & 0 & 0 & \mu_1 & 0 & \mu_3 & 0 & 0 & 0 \\ 0 & 0 & 1 & 0 & 0 & 0 & 0 & 0 & 0 & \mu_1 & 0 & \mu_3 \\ 1 & 0 & 0 & \mu_1 & \mu_2 & \mu_3 & 0 & 0 & 0 & 0 & 0 & 0 \\ 0 & 1 & 0 & 0 & 0 & 0 & \mu_1 & \mu_2 & \mu_3 & 0 & 0 & 0 \\ 0 & 0 & 1 & 0 & 0 & 0 & 0 & 0 & 0 & \mu_1 & \mu_2 & \mu_3 \end{array} \right] \right)^{-1} \left\{ \begin{array}{c} 0 \\ 0 \\ 0 \\ 1 \\ 0 \\ 0 \\ 1 \\ 0 \\ 1 \\ 1 \\ 1 \\ 1 \end{array} \right\}. \tag{131}$$

Then solving the system (131) we obtain:

$$\underline{C}^{\text{aff}}(\boldsymbol{\mu}) = \left\{ \begin{array}{c} 0 \\ 0 \\ 0 \end{array} \right\}, \quad \underline{\underline{G}}^{\text{aff}}(\boldsymbol{\mu}) = \left[\begin{array}{ccc} \frac{1}{\mu_1} & 0 & 0 \\ 0 & \frac{1}{\mu_2} & 0 \\ 0 & 0 & \frac{1}{\mu_3} \end{array} \right]. \tag{132}$$

The Jacobian of the transformation (123) is $J^{\text{aff}}(\boldsymbol{\mu}) = \frac{1}{\mu_1\mu_2\mu_3} = \frac{1}{12}$.
We remark that the Jacobian of a transformation can be seen as the ratio between

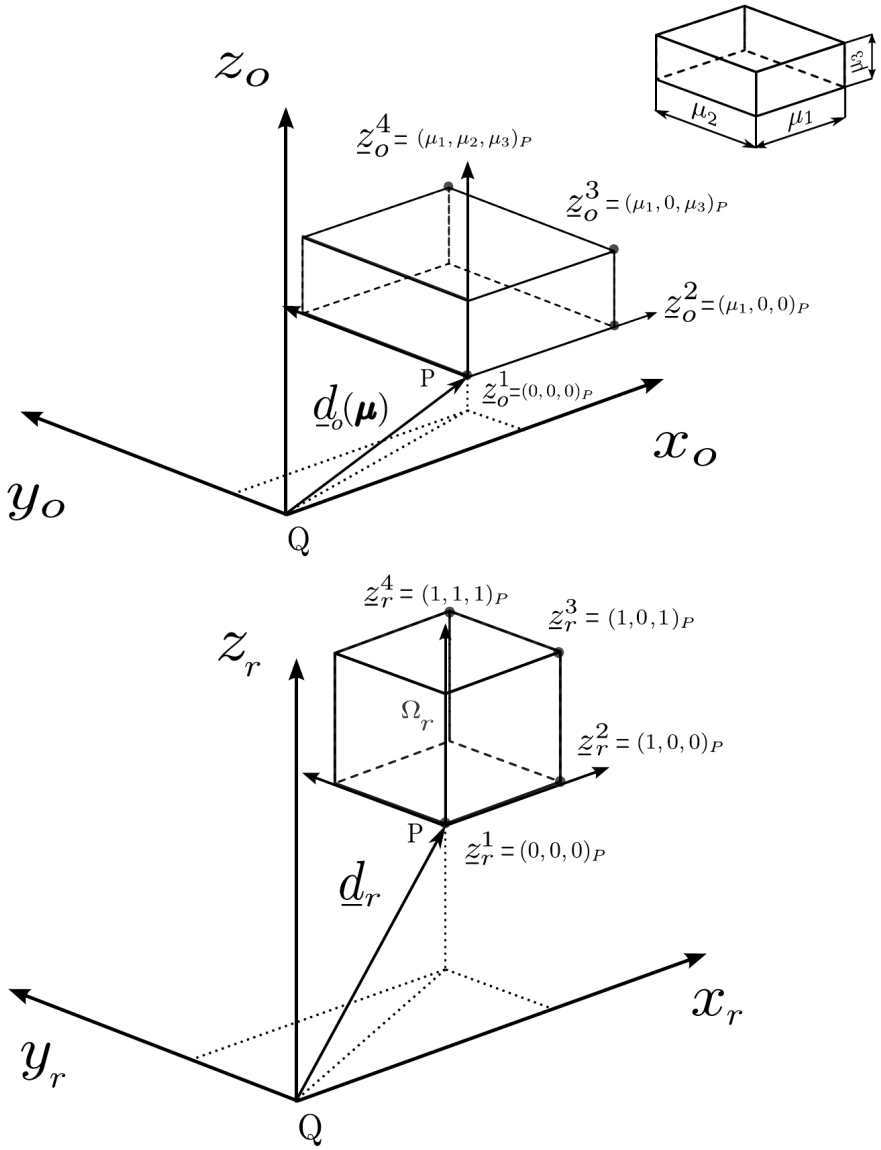

Figure 7: Affine transformation construction

the final and initial volumes on which the deformation takes place.
In order to verify the affine transformation we apply the transformation to each nodes of the *original domain* and, the *affine mapping* should trace back the corresponding nodes on the *reference domain*:

$$\begin{aligned}
&\boxed{\mathbf{z}^1}\ \underline{\underline{G}}^{\text{aff}} \left\{ \begin{array}{c} 0 \\ 0 \\ 0 \end{array} \right\} = \left\{ \begin{array}{c} 0 \\ 0 \\ 0 \end{array} \right\}, \qquad \boxed{\mathbf{z}^2}\ \underline{\underline{G}}^{\text{aff}} \left\{ \begin{array}{c} \mu_1 \\ 0 \\ 0 \end{array} \right\} = \left\{ \begin{array}{c} 1 \\ 0 \\ 0 \end{array} \right\}, \\
&\boxed{\mathbf{z}^3}\ \underline{\underline{G}}^{\text{aff}} \left\{ \begin{array}{c} \mu_1 \\ 0 \\ \mu_3 \end{array} \right\} = \left\{ \begin{array}{c} 1 \\ 0 \\ 1 \end{array} \right\}, \qquad \boxed{\mathbf{z}^4}\ \underline{\underline{G}}^{\text{aff}} \left\{ \begin{array}{c} \mu_1 \\ \mu_2 \\ \mu_3 \end{array} \right\} = \left\{ \begin{array}{c} 1 \\ 1 \\ 1 \end{array} \right\}.
\end{aligned} \tag{133}$$

We remark that in this simple test case the transformation is *"diagonal"* because we are deforming the domain by mean of a simple *dilation*. In the case of a shear deformation for example, we would have even the *extradiagonal* terms (Rozza et al., 2008).

Global affine mappings. Exploited the case of a single domain, we need to extend the procedure to a multi-subdomain case. We will make use of an example sketched in Figure 8. We have two adjacent subdomains denoted with Ω^1_* and

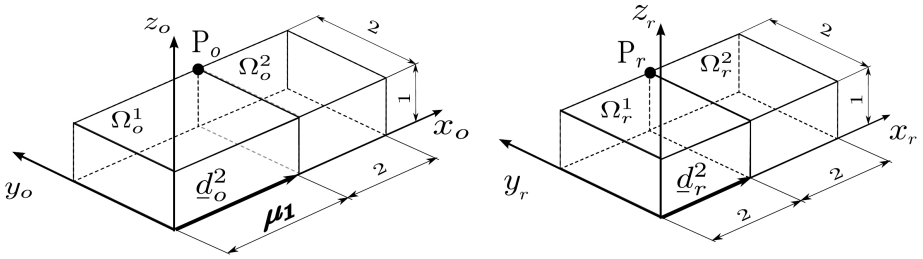

Figure 8: Global affine mappings

Ω^2_*. The first domain can be deformed along the x-axes thanks to the parameter denoted with μ_1, all the other dimensions are held fixed.
The procedure is quite similar, we just need in addition to satisfy the *global continuity condition* (121). A way to satisfy it, is to use a *unique system of reference* for the different subdomains.
In this way the procedure described in section 4.2 will *implicitly* provide the suitable translation $\underline{C}^{\text{aff}}(\boldsymbol{\mu})$ to satisfy the interface condition.
Using the procedure for the two domains we obtain the following results:

$$\begin{aligned}
&\underline{C}^{\text{aff}}_1(\boldsymbol{\mu}) = \left\{ \begin{array}{c} 0 \\ 0 \\ 0 \end{array} \right\}, \qquad \underline{\underline{G}}^{\text{aff}}_1(\boldsymbol{\mu}) = \left[\begin{array}{ccc} \frac{1}{\mu_1} & 0 & 0 \\ 0 & 1 & 0 \\ 0 & 0 & 1 \end{array} \right], \\
&\underline{C}^{\text{aff}}_2(\boldsymbol{\mu}) = \left\{ \begin{array}{c} 2-\mu_1 \\ 0 \\ 0 \end{array} \right\}, \qquad \underline{\underline{G}}^{\text{aff}}_2(\boldsymbol{\mu}) = \left[\begin{array}{ccc} 1 & 0 & 0 \\ 0 & 1 & 0 \\ 0 & 0 & 1 \end{array} \right].
\end{aligned} \tag{134}$$

We now take two *adjacent nodes* (denoted with P_o in the Figure 8) on the *original domains*; if the global mappings satisfies the *interface condition*, applying the two different *affine transformation* at the node, we will obtain again two *adjacent nodes*

(P_r) on the *reference domain*:

$$\mathcal{T}_1^{\text{aff}}(P_o(\boldsymbol{\mu}),\boldsymbol{\mu}) = \underline{C}_1^{\text{aff}} + \underline{\underline{G}}_1^{\text{aff}} \{\mu_1, 2, 1\}^T = \{2, 2, 1\} = P_r,$$

$$\mathcal{T}_2^{\text{aff}}(P_o(\boldsymbol{\mu}),\boldsymbol{\mu}) = \underline{C}_2^{\text{aff}} + \underline{\underline{G}}_2^{\text{aff}} \{\mu_1, 2, 1\}^T = \{2, 2, 1\} = P_r.$$

The node P_o is identically projected into P_r thanks to the two different *affine transformations*, hence the *continuity* of the *global mapping* is satisfied.

4.3 Linear and bilinear forms

We now focus on the transformations that we have to operate on the *weak forms* that arise from our system of partial differential equations, if our domain $\Omega_o(\boldsymbol{\mu})$ allows the *affine geometry precondition* described in the previous section. We will use a simple *scalar coercive* 3D problem to show how to exploit the *geometry parametric dependence* of the domain.
The procedure is discussed in the 2D case in Rozza et al. (2008); Rozza (2009a).

Formulation on the original domain. The problem is initially posed on the original domain $\Omega_o(\boldsymbol{\mu})$. We shall assume for simplicity that $X_0^e(\boldsymbol{\mu}) = H_0^1(\Omega_0(\boldsymbol{\mu}))$, which corresponds to homogeneous Dirichlet boundary conditions over the entire boundary $\partial\Omega_o(\boldsymbol{\mu})$. Given $\boldsymbol{\mu} \in \mathcal{D}$, find $u_o^e(\boldsymbol{\mu}) \in X_0^e(\boldsymbol{\mu})$ such that:

$$a_o(u_o^e(\boldsymbol{\mu}), v; \boldsymbol{\mu}) = f_o(v; \boldsymbol{\mu}), \quad \forall\, v \in X_0^e(\boldsymbol{\mu}) \tag{135}$$

then evaluate

$$s_o^e(\boldsymbol{\mu}) = f_o(u_o^e(\boldsymbol{\mu})). \tag{136}$$

We now place conditions on a_o and f_o such that, in conjunction with the *affine geometry precondition*, we are ensured an *affine expansion* of the bilinear form (11).
We require that $a_o(\cdot\,,\cdot\,;\boldsymbol{\mu}) : H_0^1(\Omega_o(\boldsymbol{\mu})) \times H_0^1(\Omega_o(\boldsymbol{\mu})) \to \mathbb{R}$ can be expressed as:

$$a_o(w, v; \boldsymbol{\mu}) =$$

$$= \sum_{k=1}^{K_{\text{dom}}} \int_{\Omega_o^k(\boldsymbol{\mu})} \left\{ \begin{array}{cccc} \dfrac{\partial w}{\partial x_{o_1}} & \dfrac{\partial w}{\partial x_{o_2}} & \dfrac{\partial w}{\partial x_{o_3}} & w \end{array} \right\} \mathcal{K}_{o_{ij}}^k(\boldsymbol{\mu}) \left\{ \begin{array}{c} \dfrac{\partial w}{\partial x_{o_1}} \\ \dfrac{\partial w}{\partial x_{o_2}} \\ \dfrac{\partial w}{\partial x_{o_3}} \\ w \end{array} \right\} d\Omega_o^k \tag{137}$$

where $\mathbf{x}_o = \{x_{o_1}, x_{o_2}, x_{o_3}\}$ denotes a point in $\Omega_o(\boldsymbol{\mu})$; and where for $1 \le k \le K_{\text{dom}}$, $\underline{\underline{\mathcal{K}}}_o^k : \mathcal{D} \to \mathbb{R}^{4\times 4}$ is a given *symmetric positive definite* matrix (which in turn *ensures coercivity* of our bilinear form):

$$\underline{\underline{\mathcal{K}}}_o^k = \left[\begin{array}{cc} \left[\begin{array}{c} \mathbb{R}^{3\times 3} \\ \mathbb{R}^{1\times 3} \end{array} \right] & \left[\begin{array}{c} \mathbb{R}^{3\times 1} \\ \mathbb{R}^{1\times 1} \end{array} \right] \end{array} \right] \tag{138}$$

the upper 3×3 principal submatrix of $\underline{\underline{\mathcal{K}}}_o^k$ represent the usual *diffusion/conductivity tensor*, the element $(4,4)$ represent the identity tensor (*mass matrix* or a *reaction term*), finally the elements $\underline{\underline{\mathcal{K}}}_{o_{1:3,3}}^k$ and $\underline{\underline{\mathcal{K}}}_{o_{3,1:3}}^k$, that we set to zero because we are

dealing with symmetric operators, represent the *first derivative* operators (i.e. *convective terms*).
Similarly we require that $f_o : H^1_o(\Omega_o(\boldsymbol{\mu})) \to \mathbb{R}$ can be expressed as

$$f_o(v;\boldsymbol{\mu}) = \sum_{k=1}^{K_{\rm dom}} \int_{\Omega^k_o(\boldsymbol{\mu})} \underline{\mathcal{F}}^k_o \, v \, d\Omega^k_o. \tag{139}$$

In this case we have assumed that the linear functional is only due to *volume force*, a similar treatment is possible in the case of *Dirichlet non-homogeneus* condition and/or *non-homogeneus Neumann* condition.

Formulation on reference domain. We now apply standard techniques to transform the problem over the original domain to an equivalent problem over the reference domain.
Given $\boldsymbol{\mu} \in \mathcal{D}$, find $u^e(\boldsymbol{\mu}) \in X^e \equiv H^1_0(\Omega)$ such that:

$$a(u^e, v; \boldsymbol{\mu}) = f(v;\boldsymbol{\mu}) \quad \forall\, v \in X^e \tag{140}$$

then evaluate

$$s^e(\boldsymbol{\mu}) = f(u^e(\boldsymbol{\mu})). \tag{141}$$

We may then identify the relations between the *output* and the *solution field*, in the original and in the reference domain:

$$\begin{aligned} s^e(\boldsymbol{\mu}) &= s^e_o(\boldsymbol{\mu}) \\ u^e(\boldsymbol{\mu}) &= u^e_o(\boldsymbol{\mu}) \circ \mathcal{T}^{\rm aff}(\,\cdot\,;\boldsymbol{\mu}). \end{aligned} \tag{142}$$

The transformed bilinear form a, can be expressed as:

$$a(w, v; \boldsymbol{\mu}) = \tag{143}$$

$$\int_{\Omega^k_r} \left\{ \begin{array}{cccc} \dfrac{\partial w}{\partial x_{r_1}} & \dfrac{\partial w}{\partial x_{r_2}} & \dfrac{\partial w}{\partial x_{r_3}} & w \end{array} \right\} \mathcal{K}^k_{ij}(\boldsymbol{\mu}) \left\{ \begin{array}{c} \dfrac{\partial w}{\partial x_{r_1}} \\ \dfrac{\partial w}{\partial x_{r_2}} \\ \dfrac{\partial w}{\partial x_{r_3}} \\ w \end{array} \right\} d\Omega^k_r \tag{144}$$

where $\mathbf{x}_r = \{x_{r_1}, x_{r_2}, x_{r_3}\}$ denotes a point in Ω_r and where $\mathcal{K}\|_r : \mathcal{D} \to \mathbb{R}^{4\times 4},\ 1 \le k \le K_{\rm dom}$ are symmetric positive definite matrices.
To obtain this matrices we first need to find the relation between the *derivative operator* written in the original domain and the corresponding operator written in the original domain. In particular, we have that

$$\frac{\partial\,\cdot}{\partial x_{o_i}} = \frac{\partial x_{r_j}}{\partial x_{o_i}} \frac{\partial\,\cdot}{\partial x_{r_j}} = G^{\rm aff}_{ij}(\boldsymbol{\mu}) \frac{\partial\,\cdot}{\partial x_{o_i}} = \underline{\underline{D}}^{\rm aff}(\boldsymbol{\mu})\, \frac{\partial\,\cdot}{\partial x_{o_i}}. \tag{145}$$

The definition (124) of the *derivatives operator* $\underline{\underline{D}}^{{\rm aff},k}$ is now clear; the matrices $\underline{\underline{G}}^{{\rm aff},k}$ automatically provide the relation between the derivatives operator in the original and in the reference domain.
Moreover, since we are acting a change of variable $\mathbf{x}_o \to \mathbf{x}_r$ in the integral (137), recalling the equation (123), we get

$$d\Omega_o(\boldsymbol{\mu}) = \det(\underline{\underline{G}}^{\rm aff}(\boldsymbol{\mu})^{-1}) d\Omega_r = \left(J^{{\rm aff},k}(\boldsymbol{\mu})\right)^{-1}. \tag{146}$$

It follows that, considering the equations (145)-(146), the relation between $\underline{\underline{\mathcal{K}}}_o^k(\boldsymbol{\mu})$ and $\underline{\underline{\mathcal{K}}}_r(\boldsymbol{\mu})$ can be written as

$$\underline{\underline{\mathcal{K}}}_r^k(\boldsymbol{\mu}) = \left(\underline{\underline{\mathcal{G}}}^k(\boldsymbol{\mu})\right)^T \underline{\underline{\mathcal{K}}}_o^k(\boldsymbol{\mu})\, \underline{\underline{\mathcal{G}}}^k(\boldsymbol{\mu})\, \left(J^{\text{aff},k}(\boldsymbol{\mu})\right)^{-1} \quad 1 \le k \le K_{\text{dom}} \tag{147}$$

where we have defined $\underline{\underline{\mathcal{G}}}^k(\boldsymbol{\mu}) : \mathcal{D} \to \mathbb{R}^{4\times 4}$, $1 \le k \le K_{\text{dom}}$ as

$$\underline{\underline{\mathcal{G}}}^k(\boldsymbol{\mu}) = \begin{bmatrix} \underline{\underline{\mathcal{D}}}^{\text{aff},k}(\boldsymbol{\mu}) & \underline{0}^{3\times 1} \\ \underline{0}^{1\times 3} & 1 \end{bmatrix}. \tag{148}$$

Similarly, the transformed linear form can be expressed as

$$f(v;\boldsymbol{\mu}) = \sum_{k=1}^{K_{\text{dom}}} \int_{\Omega_r^k} \mathcal{F}^k(\boldsymbol{\mu})\, v\, d\Omega_r^k. \tag{149}$$

Here $\mathcal{F}^k(\boldsymbol{\mu}) : \mathcal{D} \to \mathbb{R}$, $1 \le k \le K_{\text{dom}}$ is given by:

$$\mathcal{F}^k(\boldsymbol{\mu}) = \mathcal{F}_o^k\, \left(J^{\text{aff},k}(\boldsymbol{\mu})\right)^{-1} \quad 1 \le k \le K_{\text{dom}}. \tag{150}$$

We note that, in general, the $\underline{\underline{\mathcal{K}}}^k(\boldsymbol{\mu})$, $\mathcal{F}(\boldsymbol{\mu})$, will be different for each subdomain Ω^k, $1 \le k \le K_{\text{dom}}$. The differences can be due to *property variation* (e.g. a diffusivity of a particular subdomain) or to *geometry variation* (e.g. a characteristic dimension of the physical problem), or *both*.
We thus require, as already indicated earlier, that the *FE* approximation be built upon a *subtriangulation* of the *RB* discretization: discontinuities in *PDEs* coefficients are therefore restricted to element faces.
In this way, the boundary elements chosen for the *RB* triangulation will delimit a very well defined region of space (our *RB* subdomains), on which we assume that the parameters will be *constants in space*. This allows a simpler *identification/extraction* of the terms in the affine expansion (11), as we now discuss.

Affine form. We focus here on a, though f admits a similar treatment. We simply expand the transformed form on the reference domain, by considering in turn each subdomain Ω_r^k and *each entry* of the diffusivity/conductivity tensor $\mathcal{K}_{ij}$, $1 \le ij \le 4$, $1 \le k \le K_{\text{dom}}$.
Thus the affine form (144) can be written as follows:

$$\begin{aligned} a(w,v;\boldsymbol{\mu}) =& \mathcal{K}_{11}^1 \int_{\Omega_r^1} \frac{\partial w}{\partial x_{r_1}} \frac{\partial v}{\partial x_{r_1}}\, d\Omega_r^1 + \dots \\ &\dots + \underbrace{\mathcal{K}_{ij}^k}_{\theta_a^q(\boldsymbol{\mu})} \underbrace{\int_{\Omega_r^k} \frac{\partial w}{\partial x_{r_i}} \frac{\partial v}{\partial x_{r_j}}\, d\Omega_r^k}_{a^q(w,v)} + \dots \\ &\dots + \mathcal{K}_{44}^{K_{\text{dom}}} \int_{\Omega_r^{K_{\text{dom}}}} w\, v\, d\Omega_r^{K_{\text{dom}}}. \end{aligned} \tag{151}$$

We can then identify each component in the affine expansion: for each term in 151 the pre-factor of the integral represents $\theta_a^q(\boldsymbol{\mu})$, whereas the integral represents the parameter independent matrices $\underline{\underline{\mathbb{A}}}^q = a^q(w,v)$.
For a better understanding of what we have just obtained, we can have a look to the equation (69), in which we were building the *RB* system in the coercive case. The *parameter independent* matrices $\underline{\underline{\mathbb{A}}}^q$ can be now exploited even in the general case of *geometric parameter dependence*, thanks to the *geometric affine precondition*.

Affine expansion terms count. In the most general *scalar* case, the number of affine expansion terms can be (at most) $Q_a = 4 \times 4 \times K_{\text{dom}}$. Exploiting the symmetry of the bilinear form, hence of the tensor $\underline{\underline{\mathcal{K}}}^k$, only $Q_a = 10 \times K_{\text{dom}}$ terms are needed. In fact since $\mathcal{K}^k_{ij} = \mathcal{K}^k_{ji},\ i \neq j$, the pre-factor associated to these integrals can be assembled together.
We first consider the 6 differents entries of the simmetric tensor $\mathcal{K}$ of the first subdomain, then the second subdomain and so on. Hence, the $\theta^q_a(\boldsymbol{\mu})$ and the associated *parametric independent matrices* are given by Table 3.

q	$\theta^q_f(\boldsymbol{\mu})$	$\underline{\mathbb{F}}^q$
1	$\mathcal{K}_{11}$	$\int_{\Omega^1_r} \frac{\partial w}{\partial x_{r_1}} \frac{\partial v}{\partial x_{r_1}}\, d\Omega^1_r$
2	$\mathcal{K}^1_{12}$	$\int_{\Omega^1_r} \frac{\partial w}{\partial x_{r_1}} \frac{\partial v}{\partial x_{r_2}}\, d\Omega^1_r$
7	$\mathcal{K}^2_{11}$	$\int_{\Omega^2_r} \frac{\partial w}{\partial x_{r_1}} \frac{\partial v}{\partial x_{r_1}}\, d\Omega^2_r$
Q_a	$\mathcal{K}^{K_{\text{dom}}}_{11}$	$\int_{\Omega^{K_{\text{dom}}}_r} w\, v\, d\Omega^{K_{\text{dom}}}_r$

Table 3: $\theta^q(\boldsymbol{\mu})-$functions and parameter independent matrices

Dealing with the *vectorial* case, the number of affine expansion terms can be $Q_a = 9 \times 9 \times K_{\text{dom}}$. Therefore it is crucial, in order to reduce the *RB* computational cost that depends on Q_a (see Table 3), to minimize the number of terms of the affine expansion.

5 Thermal problem

In this section we will exploit the creation of our *RB* example *in the 3D case* dealing with a *scalar elliptic coercive* problem.
We deal with a steady conduction thermal problem, assuming that the thermal conductivity $\underline{\underline{K}}$ is represented by a positive definite matrix; then the unknown is the field of temperature, that we will denote with $u(\mathbf{x}; \boldsymbol{\mu}) \in \mathbb{R}$. This class of problem, although rather simple, is able to describe a wide range of continuum mechanics problems, see for example Arpaci (1966).
We mention, for instance, the study of the performance of an heat sink designed for the thermal management of high-density electronic components, the design of an insulated coverage of a building to reduce the energetic consumption, the control of the temperature within an engine shaft to prevent thermal stresses or deformation, etc...
Another notable application can be the non-destructive testing of mechanical components or the identification of an inclusion within a casting steel; in short, despite the simple mathematical fomrulation, this case is more than a mathematical abstraction.

5.1 Problem description

We now briefly introduce the Thermal Block problem, henceforth we will refer to this case with the "TB" label.

Physical problem. The problem of a *steady-conduction* is considered here in a cubic domain.
We want to evaluate the thermal field in a non-isotropic conductive block, with an heat flux q imposed on a face of the cube, with regard to a reference environmental temperature taken on the opposite face and assuming that the other faces are insulated. The cube has an anisotropic conductivity due to an inclusion of different materials within the piece.
Dealing for example with the material science, the inclusion can be (Walker, 1993):

1. a *deficiency* of material, a hole due to gas bubble present within the casting during solidification, or due to a fatigue crack;
2. an inhomogeneity of the material, due to an unbalancing of concentration of the alloyants.

Therefore, in order to seize the behavior of such a phenomena, the *RB* parametric approach is very well suited. The thermal problem, in the 2D frame, has been treated in Rozza et al. (2008); Patera and Rozza (2007) and Huynh et al. (2007).
The output of interest is the average temperature of the heated face.
Now we formulate the problem into the mathematical setting.

Analytical problem. The equation that describes the field of temperature is represented by the *Fourier equation* in which the time derivative will be neglected thanks to the hypothesis of a steady state problem (no transient effect considered) as well as the volume force that will be considered negligible.

5.2 Parameters

Due to the nature of the inclusion, its shape and dimension can vary arbitrarily, hence we introduce some geometric parameters in order to describe it. It is important to remark that, due the fact that the parametrized geometry should allow an *affine geometric precondition* (discussed in section 4), we restrict our attention to a parallelepiped inclusion.
In particular, with regard to the Figure 9, we have assumed that the cubic block can vary its *dimension* along the three axis by means of a set of parameters $\boldsymbol{\mu} = \{\mu_4, \mu_5, \mu_6\}$. In addition we have chosen other three parameters, denoted by $\boldsymbol{\mu} = \{\mu_1, \mu_2, \mu_3\}$ to parametrize the *position* of the inclusion. The solid is sketched as $3 \times 3 \times 3$ cubic blocks, the central block (subdomain Ω^{14} in our scheme) represents the inclusion.
Each block, due to the parametric geometry dependence of the inclusion and to the hypothesis required by an affine geometry (Section 4.1), is subjected to a geometrical parametric dependence. Each sub-block is considered *isotropic*. The conductivity constant for the central sub-block (inclusion) is another parameter, denoted by μ_7, whereas for the other sub-blocks the conductivity is the unity (reference). We now summarize the parameters and the parameter domain chosen to describe our *TB* problem as:

- the dimension and the position of the inclusion, that can be described by 6 parameters, that are 3 *translations* and 3 *dimensions*. The parameters $\mu_{1:6}$ are shown in Figure 9.
  The parameter domain for the geometrical quantities is:

$$\begin{aligned} \mathcal{D}_{\text{geom}} &= \left[\mu_1^{\min}, \mu_1^{\max}\right] \times \ldots \times \left[\mu_6^{\min}, \mu_6^{\max}\right] \\ &= [0.5,\, 1.45] \times \ldots \times [0.5,\, 1.45]\,, \end{aligned} \tag{152}$$

- the conductivity coefficient of the inclusion, denoted with μ_7.

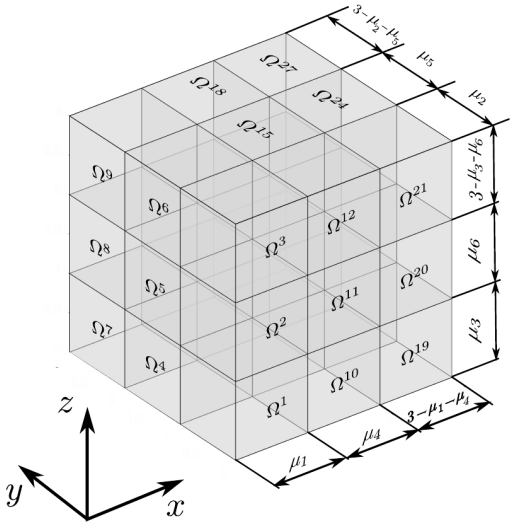

Figure 9: TB domain decomposition

The parameter domain for this physical quantity is:

$$\mathcal{D}_{\text{physics}} = \left[\mu_7^{\min}, \mu_7^{\max}\right] = [0.1,\, 10]\,. \tag{153}$$

The parameter domain is therefore given by $\boldsymbol{\mu} \in \mathcal{D} \in \mathbb{R}^{P=7}$, such that:

$$\begin{aligned}\mathcal{D} &= \mathcal{D}_{\text{geom}} \times \mathcal{D}_{\text{physics}} \\ &= [0.5,\, 1.45] \times \ldots \times [0.5,\, 1.45] \times [0.1,\, 10]\,.\end{aligned}$$

Boundary conditions. Concerning the boundary conditions (Figure 10), a non-homogeneus Neumann boundary condition is imposed on Γ_6 representing a *heat flux*, an homogeneus Dirichlet boundary condition is imposed on Γ_1 representing the imposition of a temperature (adimensional, i.e. environmental temperature), whereas on the other external faces of the cube $\Gamma_{2:5}$ homogeneus Neumann conditions has been chosen, representing insulation of the walls. Finally, on the internal faces we have assumed continuity of *temperature* and *fluxes*.

5.3 TB Problem formulation

Original domain. We introduce the analytical formulation of the governing *PDEs* on the *original domain*. The equation which describes the field of temperature, within the hypothesis described in section 5, is the following:

$$\begin{cases} -\nabla \cdot \left(\underline{\underline{K}}_o \nabla_o u\right) = 0 & \text{in } \Omega_o(\boldsymbol{\mu}) \\ u = 0 & \text{on } \Gamma_{o_1}(\boldsymbol{\mu}) \\ \dfrac{\partial u}{\partial \mathbf{n}} = q & \text{on } \Gamma_{o_6}(\boldsymbol{\mu}) \end{cases} \tag{154}$$

Multiplying the equation by a suitable *test function* v such that $v \in X^e \equiv \left\{v \in H_0^1(\Omega) |\; v|_{\Gamma^D} = 0\right\}$ and integrating over the domain Ω we obtain:

$$\int_{\Omega_o(\boldsymbol{\mu})} -\nabla_o \cdot \left(\underline{\underline{K}}_o \nabla_o u\right) v \, d\Omega_o = 0. \tag{155}$$

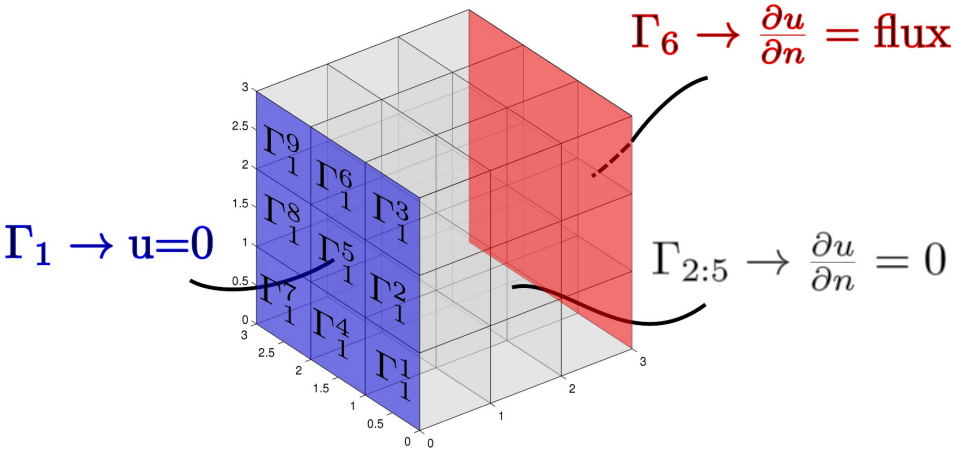

Figure 10: TB boundary conditions

The domain Ω_o is the *original domain* on which the *PDE* is defined. The whole domain $\Omega_o(\mu)$ is decomposed (section 4.1) in K_{dom} non-overlapping subdomains such that:

$$\Omega_o(\mu) = \bigcup_{k=1}^{K_{27}} \Omega_o^k(\mu),$$

in addition, recalling the *Green Theorem* for the laplacian, (Quarteroni, 2013):

$$\int_\Omega \Delta u \; v \; d\Omega = \int_\Omega \nabla u \cdot \nabla v \; d\Omega - \int_{\partial\Omega} \frac{\partial u}{\partial \mathbf{n}} \; v \; d\gamma$$

the equation (155) becomes

$$\sum_{k=1}^{27} \int_{\Omega_o^k} -\underline{\underline{K}}_o \, \nabla_o u \cdot \nabla_o v \; d\Omega_o^k + \sum_{k=1}^{27} \int_{\partial\Omega_o^k} \underline{\underline{K}}_o \frac{\partial u}{\partial \mathbf{n}} \; v \; \partial\Omega_o^k = 0.$$

Thanks to the functional space chosen, the boundary terms vanish on the face on which we have imposed a zero temperature (on $\Gamma_1 \rightarrow v = 0$). The boundary terms relatives to $\Gamma_{2:5}$ vanish because we have imposed an homogeneus Neumann condition (on $\Gamma_{2:5} \rightarrow \partial u / \partial \mathbf{n} = 0$).
The internal faces contributes disappear thanks to the continuity of temperature and fluxes. Then the only remaining boundary term is the one relative to the face Γ_6 on which we have imposed an heat flux q.
Therefore, the equation (156) can be simplified as:

$$\sum_{k=1}^{27} \int_{\Omega_o^k} \underline{\underline{K}}_o \, \nabla_o u \cdot \nabla_o v \; d\Omega_o^k = \int_{\Gamma_{o_6}} \underline{\underline{K}}_o \frac{\partial u}{\partial \mathbf{n}} \; v \; d\Gamma_{o_6}. \tag{156}$$

Replacing the Neumann boundary condition (154):

$$\underline{\underline{K}}_o \, \nabla_o u \cdot n = \underline{\underline{K}}_o \frac{\partial u}{\partial \mathbf{n}} = q$$

in the *weak formulation* (156), we finally obtain:

$$\sum_{k=1}^{27} \int_{\Omega_o^k} \underline{\underline{K}}_o \, \nabla_o u \cdot \nabla_o v \; d\Omega_o^k = \int_{\Gamma_{o_6}} q \, v \; d\Gamma_{o_6}. \tag{157}$$

Introducing the bilinear form

$$a(u, v; \boldsymbol{\mu}) = \sum_{k=1}^{27} \int_{\Omega_o^k} \underline{\underline{K}}_o \, \nabla_o u \cdot \nabla_o v \; d\Omega_o^k \tag{158}$$

and the linear functional

$$f(v; \boldsymbol{\mu}) = \int_{\Gamma_{o_6}} q \, v \; d\Gamma_{o_6}, \tag{159}$$

we can restate the problem (157) as: find $u \in X^e(\Omega_o(\boldsymbol{\mu}))$, such that

$$a(u, v; \boldsymbol{\mu}) = f(v; \boldsymbol{\mu}) \quad \forall v \in X^e(\Omega_o(\boldsymbol{\mu})). \tag{160}$$

The coercivity and the continuity of the bilinear form a and the continuity of the functional f can be proved. Then the *Lax-Milgram* theorem ensures the existence and uniqueness of the solution, see Quarteroni (2013).

Reference domain. In this section we apply standard techniques to transform the problem statement over the *original domain* to an equivalent problem fomrulated over *reference domain*.
We shall be ultimately able to write the problem in an *affine formulation* (11), to exploit the crucial Offline/Online computational splitting procedure. In order to obtain the problem formulation (160) on the reference domain, we need to evaluate the *affine transformation* for each subdomain $\Omega_o^k(\boldsymbol{\mu}) \in \Omega_o(\boldsymbol{\mu})$, tracing back the *derivatives operator* and all the *geometric parameter dependent quantities* to the *reference domain* by the recipe provided in section 4.3.
In order to build the *affine decomposition*, we must compute the affine mappings for each subdomain $\mathcal{T}^{\text{aff},k}(\,\cdot\,;\boldsymbol{\mu}) : \Omega_o(\boldsymbol{\mu}) \to \Omega_r,\ 1 \le k \le 27$, in order to evaluate:

1. the Jacobian $J^{\text{aff},k}(\boldsymbol{\mu}),\ 1 \le k \le 27$ (123)

$$J^{\text{aff},k}(\boldsymbol{\mu}) = \left| \det \left(\underline{\underline{G}}^{\text{aff},k}(\boldsymbol{\mu}) \right) \right|;$$

2. the derivatives operator $D^{\text{aff},k}(\boldsymbol{\mu})$ (equation 124)

$$\underline{\underline{D}}^{\text{aff},k}(\boldsymbol{\mu}) = \underline{\underline{G}}^{\text{aff},k}(\boldsymbol{\mu});$$

We will not present in detail the procedure to obtain the affine transformation for all the subdomains, we refer the reader to the section 4.2 for a detailed abstract explanation. In this section we just provide the results in Table 4.
We remark that the matrices $\underline{\underline{G}}^{\text{aff},k}(\boldsymbol{\mu}),\ 1 \le k \le 27$ are diagonal thanks to the particular choice of the geometric parameters. Once the affine mappings have been computed, we are able to rewrite the weak formulation 160 into the reference domain.

Bilinear forms. Recalling the bilinear form defined in (158), we recall the definition of the conductivity tensor $\underline{\underline{K}}_r$ given in (147) (section 4.3). Due to the isotropic nature of the material, for each subdomain $\Omega_r^k,\ 1 \le k \le 27$, we need to extract three different affine terms, corresponding to the three different entries of the conductivity tensor, hence we would have $27 \times 3 = 81$ terms in our affine

sub	G_{11}^{aff}	G_{22}^{aff}	G_{33}^{aff}	C_1^{aff}	C_2^{aff}	C_3^{aff}
Ω^1	$1/\mu_1$	$1/\mu_2$	$1/\mu_3$	0	0	0
Ω^2	$1/\mu_1$	$1/\mu_2$	$1/\mu_6$	0	0	$1-\mu_3$
Ω^3	$1/\mu_1$	$1/\mu_2$	$1/(3-\mu_6-\mu_3)$	0	0	$2-\mu_6-\mu_3$
Ω^4	$1/\mu_1$	$1/\mu_4$	$1/\mu_3$	0	$1-\mu_1$	0
Ω^5	$1/\mu_1$	$1/\mu_4$	$1/\mu_6$	0	$1-\mu_1$	$1-\mu_3$
Ω^6	$1/\mu_1$	$1/\mu_4$	$1/(3-\mu_6-\mu_3)$	0	$1-\mu_1$	$2-\mu_6-\mu_3$
Ω^7	$1/\mu_1$	$1/(3-\mu_5-\mu_2)$	$1/\mu_3$	0	$2-\mu_5-\mu_1$	0
Ω^8	$1/\mu_1$	$1/(3-\mu_5-\mu_2)$	$1/\mu_6$	0	$2-\mu_5-\mu_1$	$1-\mu_3$
Ω^9	$1/\mu_1$	$1/(3-\mu_5-\mu_2)$	$1/(3-\mu_6-\mu_3)$	0	$2-\mu_5-\mu_1$	$2-\mu_6-\mu_3$
Ω^{10}	$1/\mu_5$	$1/\mu_2$	$1/\mu_3$	$1-\mu_2$	0	0
Ω^{11}	$1/\mu_5$	$1/\mu_2$	$1/\mu_6$	$1-\mu_2$	0	$1-\mu_3$
Ω^{12}	$1/\mu_5$	$1/\mu_2$	$1/(3-\mu_6-\mu_3)$	$1-\mu_2$	0	$2-\mu_6-\mu_3$
Ω^{13}	$1/\mu_5$	$1/\mu_4$	$1/\mu_3$	$1-\mu_2$	$1-\mu_1$	0
Ω^{14}	$1/\mu_5$	$1/\mu_4$	$1/\mu_6$	$1-\mu_2$	$1-\mu_1$	$1-\mu_3$
Ω^{15}	$1/\mu_5$	$1/\mu_4$	$1/(3-\mu_6-\mu_3)$	$1-\mu_2$	$1-\mu_1$	$2-\mu_6-\mu_3$
Ω^{16}	$1/\mu_5$	$1/(3-\mu_5-\mu_2)$	$1/\mu_3$	$1-\mu_2$	$2-\mu_5-\mu_1$	0
Ω^{17}	$1/\mu_5$	$1/(3-\mu_5-\mu_2)$	$1/\mu_6$	$1-\mu_2$	$2-\mu_5-\mu_1$	$1-\mu_3$
Ω^{18}	$1/\mu_5$	$1/(3-\mu_5-\mu_2)$	$1/(3-\mu_6-\mu_3)$	$1-\mu_2$	$2-\mu_5-\mu_1$	$2-\mu_6-\mu_3$
Ω^{19}	$1/(3-\mu_4-\mu_1)$	$1/\mu_2$	$1/\mu_3$	$2-\mu_4-\mu_2$	0	0
Ω^{20}	$1/(3-\mu_4-\mu_1)$	$1/\mu_2$	$1/\mu_6$	$2-\mu_4-\mu_2$	0	$1-\mu_3$
Ω^{21}	$1/(3-\mu_4-\mu_1)$	$1/\mu_2$	$1/(3-\mu_6-\mu_3)$	$2-\mu_4-\mu_2$	0	$2-\mu_6-\mu_3$
Ω^{22}	$1/(3-\mu_4-\mu_1)$	$1/\mu_4$	$1/\mu_3$	$2-\mu_4-\mu_2$	$1-\mu_1$	0
Ω^{23}	$1/(3-\mu_4-\mu_1)$	$1/\mu_4$	$1/\mu_6$	$2-\mu_4-\mu_2$	$1-\mu_1$	$1-\mu_3$
Ω^{24}	$1/(3-\mu_4-\mu_1)$	$1/\mu_4$	$1/(3-\mu_6-\mu_3)$	$2-\mu_4-\mu_2$	$1-\mu_1$	$2-\mu_6-\mu_3$
Ω^{25}	$1/(3-\mu_4-\mu_1)$	$1/(3-\mu_5-\mu_2)$	$1/\mu_3$	$2-\mu_4-\mu_2$	$2-\mu_5-\mu_1$	0
Ω^{26}	$1/(3-\mu_4-\mu_1)$	$1/(3-\mu_5-\mu_2)$	$1/\mu_6$	$2-\mu_4-\mu_2$	$2-\mu_5-\mu_1$	$1-\mu_3$
Ω^{27}	$1/(3-\mu_4-\mu_1)$	$1/(3-\mu_5-\mu_2)$	$1/(3-\mu_6-\mu_3)$	$2-\mu_4-\mu_2$	$2-\mu_5-\mu_1$	$2-\mu_6-\mu_3$

Table 4: TB affine mappings

development. We obtain:

$$
\begin{aligned}
a(w,v;\boldsymbol{\mu}) &= \sum_{k=1}^{27} \int_{\Omega_r^k} \underline{\underline{K}}_r(\boldsymbol{\mu})\, \nabla u \cdot \nabla v \, d\Omega_r^k \\
&= \int_{\Omega_r^1} \frac{\mu_2\mu_3}{\mu_1} \frac{\partial u}{\partial x_{r_1}} \frac{\partial v}{\partial x_{r_1}} + \frac{\mu_1\mu_3}{\mu_2} \frac{\partial u}{\partial x_{r_2}} \frac{\partial v}{\partial x_{r_2}} + \frac{\mu_1\mu_2}{\mu_3} \frac{\partial u}{\partial x_{r_3}} \frac{\partial v}{\partial x_{r_3}} \, d\Omega_r^1 + \dots \\
&\dots + \int_{\Omega_r^3} \left(-\frac{\mu_2(\mu_3+\mu_6-3)}{\mu_1} \frac{\partial u}{\partial x_{r_1}} \frac{\partial v}{\partial x_{r_1}} + \right. \\
&\quad \left. -\frac{\mu_1(\mu_3+\mu_6-3)}{\mu_2} \frac{\partial u}{\partial x_{r_2}} \frac{\partial v}{\partial x_{r_2}} - \frac{\mu_1\mu_2}{\mu_3+\mu_6-3} \frac{\partial u}{\partial x_{r_3}} \frac{\partial v}{\partial x_{r_3}} \right) d\Omega_r^3 + \dots \\
&\dots + \theta_a^{81}(\boldsymbol{\mu}) \int_{\Omega_r^{27}} \frac{\partial u}{\partial x_{r_3}} \frac{\partial v}{\partial x_{r_3}} d\Omega_r^{27}
\end{aligned} \tag{161}
$$

Linear functional. In this case the parametric linear functional (159) arises from an inhomogeneous Neumann boundary condition. This case has not been treated in section 4.3. In order to cast the integral of equation (159) into the

reference domain, we proceed as follows:

$$f(v;\boldsymbol{\mu}) = \int_{\Gamma_{o_6}(\boldsymbol{\mu})} q\, v\, d\Gamma_{o_6}(\boldsymbol{\mu}) = \int_{\Gamma_{r_6}} q\, v \underbrace{\left|\left(G^{\text{aff},k}(\boldsymbol{\mu})\right)^{-1} \cdot \underline{e}^t\right| d\Gamma_{r_6}}_{d\Gamma_{o_6}}, \tag{162}$$

where $\underline{e}^t$ denotes the tangential unit vector and k indicates the indexes of the subdomains to which the face Γ_{r_6} belong. In particular, with regard the chosen subdomain enumeration (Figure 9), we see that Γ_{r_6} is given by

$$\Gamma_{r_6} = \bigcup_{k=1}^{6} \Gamma_{r_6}^k. \tag{163}$$

Therefore the linear functional can be rewritten in an affine development as:

$$\begin{aligned} f(v;\boldsymbol{\mu}) = &\int_{\Gamma^1_{r_6}} \mu_2\mu_3\, q\, v\, d\Gamma^1_{r_6} + \int_{\Gamma^2_{r_6}} \mu_1\mu_6\, q\, v\, d\Gamma^2_{r_6} + \dots \\ &\dots + \int_{\Gamma^6_{r_6}} -\mu_5\,(\mu_3+\mu_6-3)\; q\, v\, d\Gamma^6_{r_6} + \dots \\ &\dots + \theta^9_f(\boldsymbol{\mu}) \int_{\Gamma^9_{r_6}} q\, v\, d\Gamma^9_{r_6}. \end{aligned} \tag{164}$$

The affine decomposition is now clear and we have

$$a(u,v;\boldsymbol{\mu}) = \sum_{1}^{81} \theta^q_a(\boldsymbol{\mu}) a^q(u,v),$$

$$f(v;\boldsymbol{\mu}) = \sum_{1}^{9} \theta^q_f(\boldsymbol{\mu}) f^q(v),$$

where the *θ-functions* are the parameters dependent terms which appear in the bilinear form (161) and in the linear functional (164) expressed in the reference domain.
Since the geometric parameter dependence is quite involved, we will present only few results from our set of theta functions $\theta^q_a(\boldsymbol{\mu})$, $1 \le q \le 81$, $\theta^q_f(\boldsymbol{\mu})$, $1 \le q \le 9$ in Tables 5a and 5b. In the same tables we present also the definition of the $\boldsymbol{\mu}-$independent bilinear forms.

5.4 Results and visualization

We now present the results obtained by *RB* approximation for the *3D thermal block* example.
First we will give some informations about the *FE* approximation concerning the mesh, the basis function chosen.
Then we will focus on the results obtained with the *SCM* algorithm (section 3.5) for the error bounds calculations, then we will present the convergence of the *Greedy* procedure (section 3.3).
Finally we will present the output evaluation for particular combinations of the parameters, along with the *certified a-posteriori error bound*, to prove that the *RB* approximation is *reliable* and *efficient*.

q	$\theta_a^q(\boldsymbol{\mu})$	$\underline{\underline{\mathbb{A}}}^q$
1	$\frac{\mu_2\mu_3}{\mu_1}$	$\int_{\Omega_r^1} \frac{\partial u}{\partial x_{r_1}} \frac{\partial v}{\partial x_{r_1}} \, d\Omega_r^1$
2	$\frac{\mu_1\mu_3}{\mu_2}$	$\int_{\Omega_r^1} \frac{\partial u}{\partial x_{r_2}} \frac{\partial v}{\partial x_{r_2}} \, d\Omega_r^1$
5	$\frac{\mu_1\mu_3}{\mu_2}$	$\int_{\Omega_r^1} \frac{\partial u}{\partial x_{r_2}} \frac{\partial v}{\partial x_{r_2}} \, d\Omega_r^1$
9	$\frac{\mu_2\mu_6}{\mu_1}$	$\int_{\Omega_r^2} \frac{\partial u}{\partial x_{r_2}} \frac{\partial v}{\partial x_{r_2}} \, d\Omega_r^2$
14	$\frac{\mu 1\mu_6}{\mu_5}$	$\int_{\Omega_r^5} \frac{\partial u}{\partial x_{r_2}} \frac{\partial v}{\partial x_{r_2}} \, d\Omega_r^5$
27	$\frac{\mu_1(\mu_2+\mu_5-3)}{\mu_3+\mu_6-3}$	$\int_{\Omega_r^9} \frac{\partial u}{\partial x_{r_3}} \frac{\partial v}{\partial x_{r_3}} \, d\Omega_r^9$
40	$\frac{\mu_5\mu_6\mu_7}{\mu_4}$	$\int_{\Omega_r^{14}} \frac{\partial u}{\partial x_{r_1}} \frac{\partial v}{\partial x_{r_1}} \, d\Omega_r^{14}$
60	$-\frac{\mu_2(\mu_1+\mu_4-3)}{\mu_6}$	$\int_{\Omega_r^{20}} \frac{\partial u}{\partial x_{r_3}} \frac{\partial v}{\partial x_{r_3}} \, d\Omega_r^{20}$
70	$\frac{\mu_5(\mu_3+\mu_6-3)}{\mu_1+\mu_4-3}$	$\int_{\Omega_r^{24}} \frac{\partial u}{\partial x_{r_1}} \frac{\partial v}{\partial x_{r_1}} \, d\Omega_r^{24}$
78	$\frac{(\mu_2+\mu_5-3)(\mu_1+\mu_4-3)}{\mu 6}$	$\int_{\Omega_r^{26}} \frac{\partial u}{\partial x_{r_3}} \frac{\partial v}{\partial x_{r_3}} \, d\Omega_r^{26}$

(a) TB $\theta_a^q(\boldsymbol{\mu})$-functions

q	$\theta_f^q(\boldsymbol{\mu})$	$\underline{\mathbb{F}}^q$
1	$\mu_1\mu_3$	$\int_{\Gamma_{r_6}^1} q\, v \, d\Gamma_{r_6}^1$
2	$\mu_1\mu_3$	$\int_{\Gamma_{r_6}^2} q\, v \, d\Gamma_{r_6}^2$
3	$\mu_2\mu_6$	$\int_{\Gamma_{r_6}^3} q\, v \, d\Gamma_{r_6}^3$
6	$-\mu_5(\mu_3+\mu_6-3)$	$\int_{\Gamma_{r_6}^6} q\, v \, d\Gamma_{r_6}^6$
9	$(\mu_2+\mu_5-3)(\mu_3+\mu_6-3)$	$\int_{\Gamma_{r_6}^9} q\, v \, d\Gamma_{r_6}^9$

(b) TB $\theta_f^q(\boldsymbol{\mu})$-functions

Table 5: *TB* $\theta(\boldsymbol{\mu})$-functions

***FE* discretization on the reference domain.** We represent in Figure 11 the reference domain upon we assemble *FE* components.
In the figure 11 we also report the properties of the mesh and the basis functions chosen to discretize the *TB* problem.

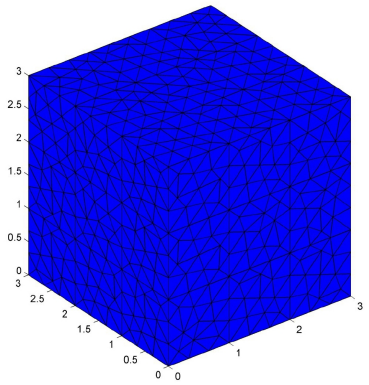

mesh vertices	1657
vertex	64
edges	432
triangle	3024
tetrahedral	7515
DOFs	1512
basis functions	$\mathbb{P}^1$

Figure 11: *TB* reference domain discretization

Matrices assembling. We now assemble the parameter independent matrices (Tables 5a and 5b) needed by the *RB* procedure.
In Figure 12 we depict a graphical view of the matrices assembling.
We consider the matrix $\underline{\underline{\mathbb{A}}}^{20}$, looking at Table 5a we note that the only subdomain that plays a role in the building of the parameter independent matrix is Ω_r^9, see Figure 12a. In Figure 12b we depict the matrix pattern.

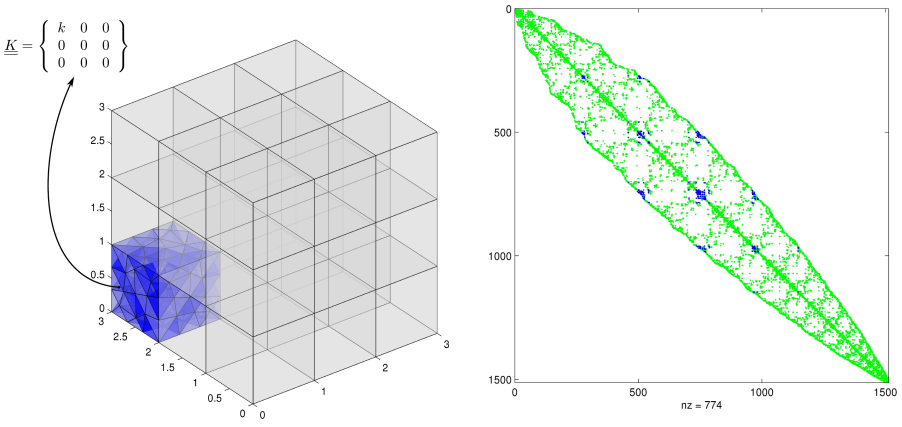

(a) subdomain Ω_r^7 (b) $\underline{\underline{\mathbb{A}}}^{20}$

Figure 12: In figure 12b we have depicted the contributes of the local $\underline{\underline{\mathbb{A}}}^{20}$ matrix (•) to the global stiffness matrix (•).

***SCM* algorithm.** For the *SCM* algorithm (section 3.5) we have took a sample train Ξ_{SCM} of size $n_{\text{SCM}} = 3000$, a tolerance $\epsilon_{\text{SCM}} = 0.7$, $\text{M}_\alpha = 16$, $\text{M}_+ = 0$ and $|\mathcal{P}| = 200$.
In Figure 13a we show the α_{LB} (–) and the α_{UB} (–) for each element of the

sample train Ξ_{SCM} of the first iteration $K = 1$, whereas in Figure 13b we depict the same quantities for the last iteration $K = K_{\max} = 4$ of the *SCM* algorithm. It is evident that the upper and lower bound for the parametric coercivity constant are converging to the exact value and restricting the possible gap between the lower and upper bound. Convergence for this problem is quite fast, see Gelsomino and Rozza (2011); Rozza et al. (2008).

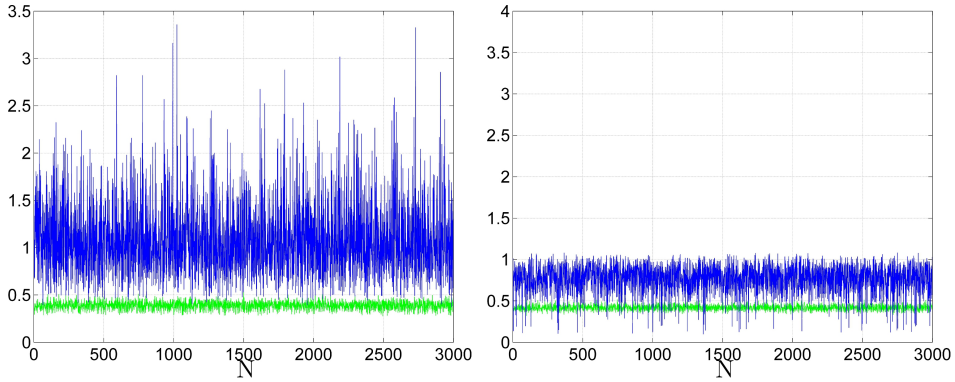

(a) *TB*: First iteration of the *SCM* (b) *TB*: Last iteration of the *SCM*

Figure 13: *TB SCM* algorithm

***Greedy* algorithm.** We present the results for the *Greedy* algorithm (section 3.3), during the *RB* aseembling procedure.
Here, we have chosen a sample train Ξ_{train} of size is $n_{\text{train}} = 3000$, the tolerance is $\epsilon_{\text{toll,min}} = 0.9 \cdot 10^{-3}$ and the maximum size of the *RB* space is taken $N_{\max} = 100$. We have chosen to minimize the absolute error bound in energy norm $\Delta_N^{en}(\boldsymbol{\mu})$ (section 3.4). In Figure 15a we have represented the error bound $\Delta_N^{en}(\boldsymbol{\mu})$ for $1 \leq N \leq N_{\max}$. We can see that the error is monotonically decreasing. Moreover, just few basis ≈ 40 (versus $\approx$1500 *FE DOFs*) are needed to obtain a maximum error bound $\leq 10^{-2}$ on the temperature field for all the samples in Ξ_{train}. We remark that this result holds despite a large variation of either physical (the conductivity) and geometrical (the dimension and the position of the central block) parameters. In Figure 15b we have depicted a subset of the parameters $\boldsymbol{\mu} = (\mu_2, \mu_5, \mu_6)$, automatically selected by the *Greedy algorithm* as representative snapshots. The error bounds help us to save also *Offline* computational cost since the evaluation of the error bounds during the *Greedy* procedure is very inexpensive. It is possible to see that the algorithm often select parameters near to the bounds (upper and lower) of the parameters domain. In fact the more the parameters are chosen distant from

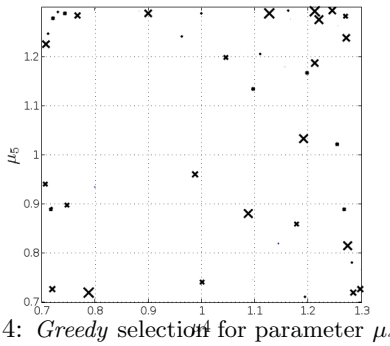

Figure 14: *Greedy* selection for parameter μ_4 and μ_5

the "center" of the set, the most the reference domain is deformed by means of the geometrical parameters. These phenomena will perforce increase the error bound, therefore the Greedy algorithm will preferably choose this outer parameters, being based on the *worst case scenario*.
This aspect can be better seen, looking at the Figure 14, we can see that the geometrical parameters chosen are always in the outer part of the domain, where it is evident a *clustering phenomena*. In this figure, the dimension of the markers are proportional to the maximum error bound at the K-th Greedy iteration.

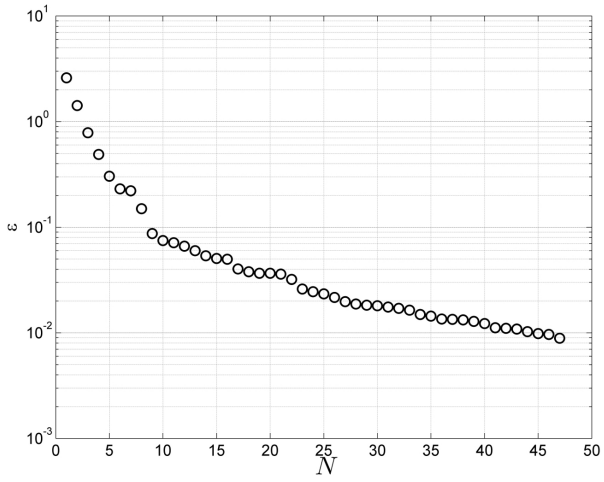

(a) Error bound $\Delta_N^{en}(\boldsymbol{\mu})$

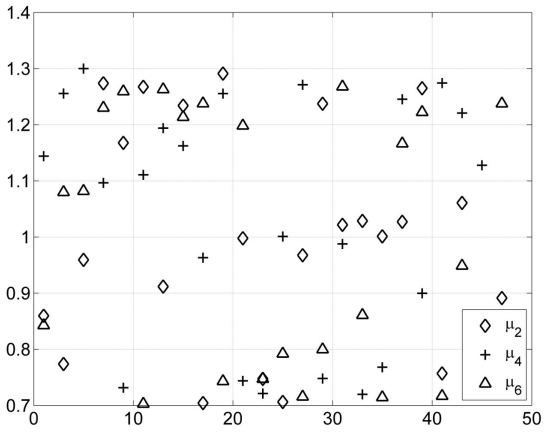

(b) Parameters distribution

Figure 15: *TB* Greedy results

Output. Since the output is the average of the temperature on the face Γ_6 of the domain, then we are dealing with a compliant case (see section 2.3). In fact we have that:

$$s_N(\boldsymbol{\mu}) = f(u_N; \boldsymbol{\mu}). \tag{165}$$

Since we have 7 parameters, we decided to fix some parameters and add relationship between others to obtain a graphical visualization of the output.

In particular we have chosen to vary the parameters μ_5 and μ_4, i.e. the x and y dimension of the inclusion. In addition we have introduced the following relationships:

$$\begin{aligned}\mu_1 &= \frac{3-\mu_4}{2};\\ \mu_2 &= \frac{3-\mu_5}{2};\\ \mu_3 &= 1;\\ \mu_6 &= 1;\\ \mu_7 &= 1.\end{aligned}$$

In Figure 16a we depict the tenmperature output obtained with the *RB* method, in Figure 16b we depict the *error bound* $\Delta_N^s(\boldsymbol{\mu})$ on the output between the *FE* and the *RB* method.
We can see that the output estimated error is under $8 \cdot 10^{-5}$, hence the error on the output is effectively bounded by the square of the error on the solution field (we recall that in the Greedy we have set $\Delta_N^{\text{en}}(\boldsymbol{\mu}) \leq \epsilon_{\text{toll,min}} = 0.9 \cdot 10^{-3},\ \forall \boldsymbol{\mu} \in \Xi_{\text{train}}$). We remark that this result follows from our assumption of compliance, enabling the so called *square effect* (57).
In Figure 16c we have depicted the ratio between the computational time needed to evaluate the output in the *FE* (denoted with $t_{\text{FE}}^s(\boldsymbol{\mu})$) and in the *RB* case ($t_{\text{RB}}^s(\boldsymbol{\mu})$) for a large test sample. We can see that the *RB* method provides a computational time saving of *two order of magnitude* with respect to the ordinary *FE* method.

Visualization. We now report the visualization of some representative *RB* solutions. On the upper figures, we show the solution for different value of the parameters $\boldsymbol{\mu}$. On the lower figures, we represent the pointwise error between the *RB* approximations and the *FE* solution.
In the first example, Figure 17, we show the solution on the reference domain. In the second example, Figure 18, we show the solution field after selecting a generic combination of parameters in the parameter domain $\mathcal{D}$. In the first case, thanks to the absence of geometrical distortion, we obtain a *smaller error bound* on the solution.

6 Summary and conclusions

We have presented the *RB* method for *coercive scalar* problems. First, we have introduced the fundamentals of the *RB* method for *parametrized coercive elliptic PDEs*: (i) the affine decomposition to enable an Offline/Online splitting procedure, (ii) the *a-posteriori error estimates* to efficiently create the *RB* Greedy space (Offline) and inexpensive and rigorous error bounds for the *RB* solution and output (Online). In order to obtain an affine representation of the parametrized linear and bilinear forms we exploited an *affine geometry precondition*. We presented the applications of the *RB* method to a *steady thermal conductivity problem* in heat transfer.
We obtained a good and rapid convergence of either the *SCM* and the Greedy algorithm. Hence we experimentally proved that the *RB* method is very well suited to efficiently approximate also 3D problems with a rather involved parameter dependence, either physical and geometrical.
The Offline stage is quite expensive in the 3D context, nonetheless the very inexpensive and rigorous Online stage renders invaluable the worth of the *RB* method

in many engineering field of interests: optimization, control, sensitivity analysis and real-time context.
In fact by the *RB* method we obtained (Online) a computational saving of at least two order of magnitude with respect to the *FE* approximation in the thermal application, corroborating other results (Gelsomino and Rozza, 2011) dealing with 3D coercive problems.

Different branches of the research field related to the *RB* method are dealing nowadays with a plenty of different problems and different contexts: the study of potential flows (Rozza, 2011), thermal problems, (Rozza et al., 2009b,a), hemodynamics and biomedical devices optimization (Manzoni et al., 2012), the study of nonlinear equations such as the Navier-Stokes problem, (Deparis and Rozza, 2009), the development of *RB* approximation in parabolic (Nguyen et al., 2010) and hyperbolic equations (Nguyen et al., 2009). Unfortunately, the affine parametrization of a geometry, is not enough *flexible* for some purposes, e.g. the shape-optimization of a vessel in a hemodynamic context or the design of an *air intake* in an aerodynamic context. Hence in the few last years, new techniques based on the so-called *free form deformation* has been re-invented in cooperation with the *RB* method (Manzoni et al., 2012; Lassila and Rozza, 2010; Rozza and Manzoni, 2010) in the shape optimization field.
A possible and remarkable upgrade of this work would be to enrich the 3D geometrical parametrization with *free-shape* techniques to improve the power of reduced order methods in the engineering context.

Bibliography

B.O. Almroth, P. Stern, and F.A. Brogan. Automatic choice of global shape functions in structural analysis. *AIAA Journal*, 16(7):525–528, 1978.

V.S. Arpaci. *Conduction Heat Transfer*. Addison-Wesley, 1966.

J.A. Atwell and B.B. King. Proper Orthogonal Decomposition for Reduced Basis Feedback Controllers for Parabolic Equations. *Mathematical and computer modeling*, 33(1-3):1–19, 1999.

T. Bui-Thanh, K. Willcox, and O. Ghattas. Model Reduction for Large-Scale Systems with High-Dimensional Parametric Input Space. *Proceedings of the 48th AIAA/ASME/ASCE/AHS/ASC structures, structural dynamics and material conference*, 30(6):3270–3288, 2008.

S. Deparis and G. Rozza. Reduced Basis Method for Multi-Parameter dependent Steady Navier-Stokes Equations: Applications to Natural Convection in a cavity. *Journal of Computational Physics*, 228:4359–4378, 2009.

R. Fox and H. Miura. An approximate analysis technique for design calculations. *AIAA Journal*, 9(1):177–179, 1971.

F. Gelsomino and G. Rozza. Comparison and combination of reduced order modeling techniques in 3d parametrized heat transfer problems. *Mathematical and Computer Modelling of Dynamical Systems*, 17(4):373–391, 2011.

M.A. Grepl, Y. Maday, N.C. Nguyen, and A.T. Patera. Efficient Reduced Basis Treatment of Nonaffine and Nonlinear Partial Differential Equations. *European Series in Applied and Industrial Mathematics: Mathematical Modelling and Numerical Analysis*, 41(3):575–605, 2007.

B. Haasdonk and M. Ohlberger. Reduced Basis method for Finite Volume Approximations of Parametrized Linear Evolution Equations. *Mathematical Modelling and Numerical Analysis*, 42(2):277–302, 2008.

D.B.P. Huynh, G. Rozza, S. Sen, and A.T. Patera. A Successive Constraint Linear Optimization Method for Lower Bounds of Parametric Coercivity and Inf−Sup

Stability Constants. *Comptes Rendus de l'Academie des Sciences*, 345(8):473–478, 2007.

K. Ito and S.S. Ravindran. Reduced Basis method for Optimal Control of Unsteady Viscous Flows. *International Journal of Computational Fluid Dynamics*, 15: 97–113, 2001.

K. Ito and S.S. Ravindran. A Reduced Order Method For Control Problems Governed by PDEs. volume 126 of *International Series of Numerical Mathematics*, pages 153–168. Birkhauser, Boston, 1998.

M. Jabbar and A. Azeman. Fast optimization of Electromagnetic-Problems: the Reduced Basis Finite Element Approach. *IEEE Transactions on Magnetics*, 40 (4):2161–2163, 2004.

K. Kunisch and S. Volkwein. Galerkin Proper Orthogonal Decomposition Methods for a General Equation in Fluid Dynamics. *SIAM Journal on Numerical Analysis*, 40(2):492–515, 2003.

T. Lassila and G. Rozza. Parametric Free-Form Shape Design with PDE Models and Reduced Basis Method. *Computer Methods in Applied Mechanics and Engineering*, 199:1583–1592, 2010.

Barrault M., Maday Y., Nguyen N.C., and Patera A.T. An Empirical Interpolation Method: Application to Efficient Reduced Basis discretization of Partial Differential Equations. *Comptes Rendus Mathematiques*, 339(9):667–672, 2004.

A. Manzoni, A. Quarteroni, and G. Rozza. Shape Optimization in Cardiovascular Geometries using Reduced Basis Method and Free-Form Deformations. *International Journal for Numerical Methods in Fluids*, 70(5):646–670, 2012.

C.D. Meyer. *Matrix analysis and applied linear algebra*. SIAM, Philadelphia, Colorado State University, 1st edition, 2000.

D.A. Nagy. Modal representation of geometrically nonlinear behaviour by the finite element method. *Computers & Structures*, 10(4):683–688, 1979.

N.C. Nguyen, K. Veroy, and A.T. Patera. *Certified Real-Time Solution of Parametrized Partial Differential Equations*. Yip S(ed) Handbook of materials modeling. Springer, Berlin, 2005.

N.C. Nguyen, G. Rozza, and A.T. Patera. Reduced Basis Approximation and A-Posteriori Error Estimation for Time Dependent Viscous Burgers Equation. *Calcolo*, 46(3):157–187, 2009.

N.C. Nguyen, G. Rozza, D.B.P. Huynh, and A.T. Patera. Reduced Basis Approximation and A-Posteriori Error Estimation for Parametrized Parabolic PDEs; Application to Real-Time Bayesian Parameter Estimation. In *Computational Methods for Large Scale Inverse Problems and Uncertainty Quantification*, pages 151–173. John Wiley & Sons, UK, 2010.

A.K. Noor. On making large nonlinear problems small. *Computer Methods in Applied Mechanics and Engineering*, 34(2):955–985, 1982.

A.K. Noor. Recent advances in reduction methods for nonlinear problems. *Computers & Structures*, 13(1-3):31–44, 1978.

A.K. Noor and J.M. Peters. Reduced Basis Technique for Nonlinear Analysis of structures. *Computers & Structures*, 18(4):455–462, 1980.

A.T. Patera and E.M. Ronquist. On the error behavior of the Reduced Basis Technique for Nonlinear Finite Element Approximations and A-Posteriori Error estimation for a Boltzmann model. *Computer Methods in Applied Mechanics and Engineering*, 196:2925–2942, 2007.

A.T. Patera and G. Rozza. *Reduced Basis Approximation and A-Posteriori Error Estimation for Parametrized Partial Differential Equations*. MIT Pappalardo Graduate Monographs in Mechanical Engineering. ©MIT, Massachusetts Institute of Technology, Cambridge, MA, USA, 2007.

J.S. Peterson. The Reduced Basis method for incompressible viscous flow calculations. *SIAM Journal on Scientific Computing*, 10(4):777–786, 1989.

T.A. Porsching. Estimation of the Error in the Reduced Basis Method Solution of Nonlinear Equations. *Mathematics of Computation*, 45(172):487–496, 1985.

T.A. Porsching and M.L. Lee. The Reduced Basis method for Initial Value Problems. *SIAM Journal on Numerical Analysis*, 24(6):1277–1287, 1987.

C. Prud'homme, D. Rovas, K. Veroy, Y. Maday, A. Patera, and G. Turinici. Reliable real-time solution of parametrized partial differential equations: Reduced Basis output bounds methods. *Journal of Fluid Engineering*, 124(1):70–80, 2002a.

C. Prud'homme, D.V. Rovas, K. Veroy, and A.T. Patera. A mathematical and Computational Framework for Reliable Real-Time Solution of Parametrized Partial Differential Equations. *Mathematical Modeling and Numerical Analysis*, 36(5):747–771, 2002b.

A. Quarteroni. *Numerical Models for Differential Problems*, volume 8 of *MS&A*. Springer, 2013.

A. Quarteroni and A. Valli. *Numerical Approximation of Partial Differential Equations*. Springer series on Computational Mathematics. Springer, 1997.

A. Quarteroni, R. Sacco, and F. Saleri. *Numerical Mathematics*. Texts in Applied Mathematics. Springer, New York, 2000.

S.S. Ravindran. Adaptive reduced order controllers for a thermal flow system using Proper Orthogonal Decomposition. *SIAM Journal on Scientific Computing*, 23 (3):1924–1942, 2002.

D. Rovas. *Reduced-Basis Output Bound Methods for Parametrized Partial Differential Equations*. PhD thesis, Massachusetts Institute of Technology, Cambridge, MA, USA, 2003.

G. Rozza. Reduced basis approximation and error bounds for potential flows in parametrized geometries. *Communications in Computational Physics*, 9(1): 1–48, 2011.

G. Rozza. Reduced Basis for Stokes equations in domains with non-affine parametric dependence. *Computing and Visualization in Science*, 12(1):23–35, 2009a.

G. Rozza. An Introduction to Reduced Basis Method for Parametrized PDEs. In *In Applied and Industrial Mathematics in Italy, Vol. III, Series on Advances in Mathematics for Applied Sciences*, pages 508–519. Societá Italiana di Matematica Applicata e Industriale, 2009b.

G. Rozza and A. Manzoni. Model Order Reduction by Geometrical Parametrization for Shape Optimization in Computational Fluid Dynamics. In *Proceedings of ECCOMAS CFD Conference, J.Pereira and A. Sequeira Editors*, Lisbon, Portugal, June, 2010.

G. Rozza and K. Veroy. On the Stability of the Reduced Basis method for Stokes Equations in parametrized domains. *Computer Methods in Applied Mechanics and Engineering*, 196:1244–1260, 2006.

G. Rozza, D.B.P. Huynh, and A.T. Patera. Reduced Basis approximation and A-Posteriori Error Estimation for Affinely Parametrized Elliptic Coercive Partial Differential Equations. *Archives of Computational Methods in Engineering*, 15: 229–275, 2008.

G. Rozza, D.B.P. Huynh, N.C. Nguyen, and A.T. Patera. Real-Time Reliable Simulation of Heat Transfer Phenomena. In *Heat Transfer Summer Conference Proceedings, HT-2009-88212*, S. Francisco, CA, US, July 2009a. American Society of Mechanical Engineers.

G. Rozza, N.C. Nguyen, A.T. Patera, and S. Deparis. Reduced Basis Methods and A-Posteriori Error Estimators for Heat Transfer Problems. In *Heat Transfer Summer Conference Proceedings, HT-2009-88211*, S. Francisco, CA, US, July 2009b. American Society of Mechanical Engineers.

P. Walker. *Chambers Dictionary of Materials Science and Technology*. Chambers Publishing, 1st edition, 1993.

K. Willcox and J. Peraire. Balanced Model Reduction via the Proper Orthogonal Decomposition. *AIAA Journal*, 40(11):2323–2330, 2002.

K. Yosida. *Functional Analysis*. New York: Springer-Verlag, 1971.

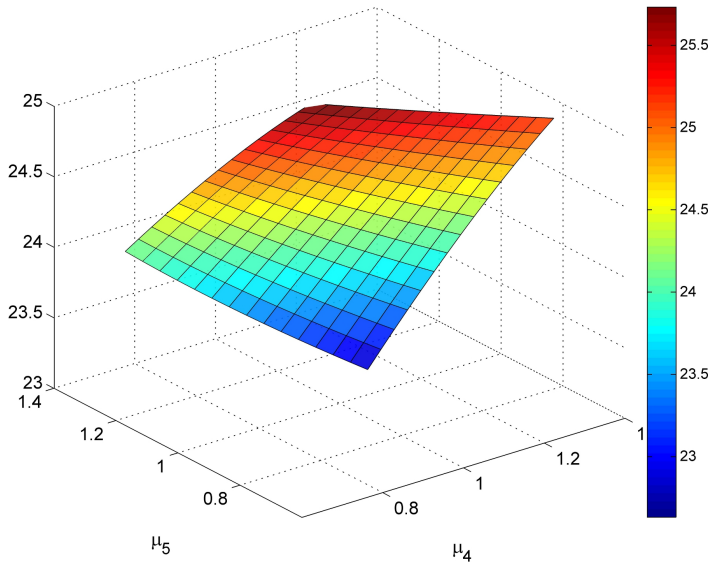

(a) *TB* output $s(\boldsymbol{\mu})$

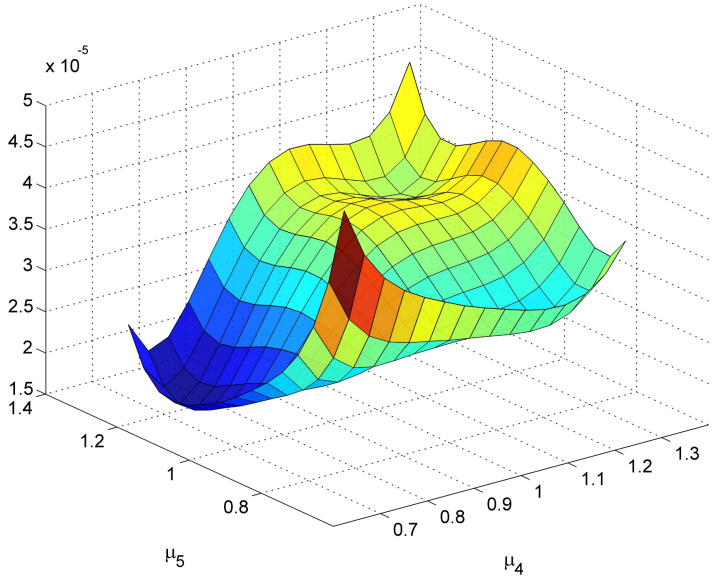

(b) *TB* error bound $\Delta_N^s(\boldsymbol{\mu})$

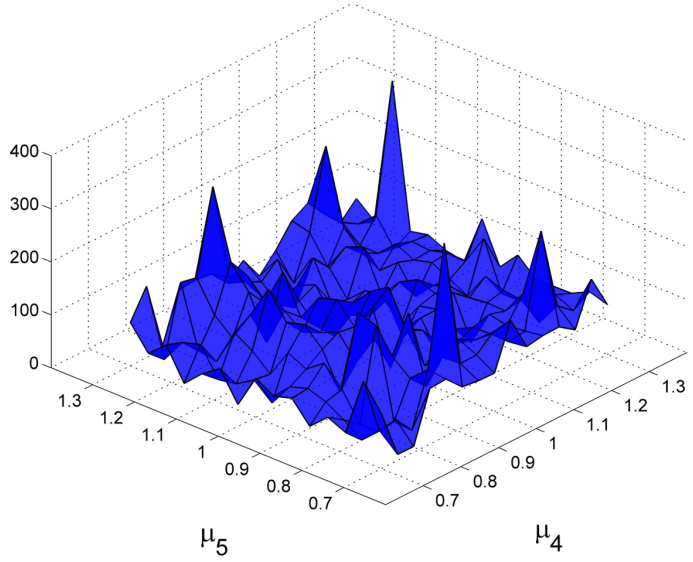

(c) $\frac{t_{\mathrm{FE}}^s(\boldsymbol{\mu})}{t_{\mathrm{RB}}^s(\boldsymbol{\mu})}$

Figure 16: *TB* output results

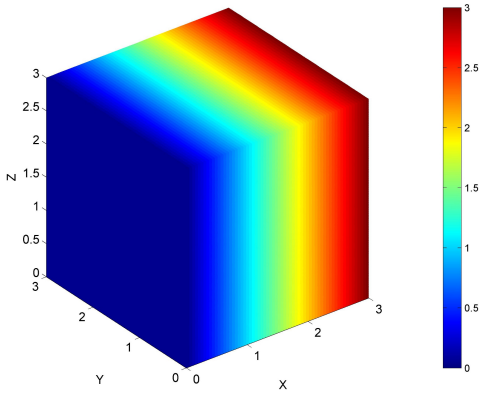

(a) Solution field: $\Delta_N^{\text{en}}(\boldsymbol{\mu}) \leq 2.3 \cdot 10^{-3}$

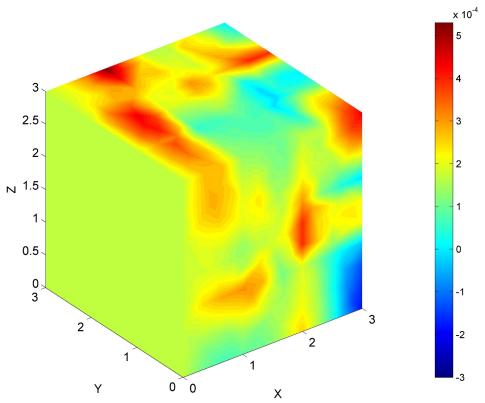

(b) Pointwise error: $u_N(\boldsymbol{\mu}) - u^{\mathcal{N}}(\boldsymbol{\mu})$

Figure 17: Example of representative solution for the *TB* problem and pointwise error for $\boldsymbol{\mu} = \{1, 1, 1, 1, 1, 1, 1\}$

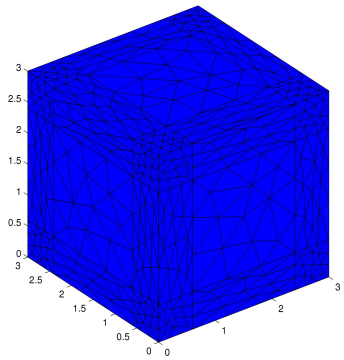

(a) Deformed domain

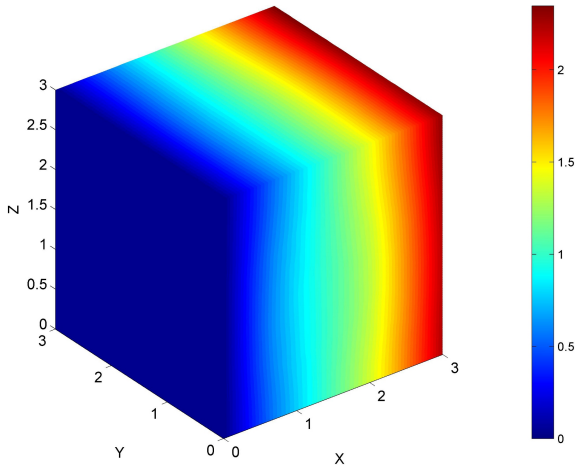

(b) Error bound: $\Delta_N^{\text{en}}(\boldsymbol{\mu}) \leq 6.3 \cdot 10^{-3}$

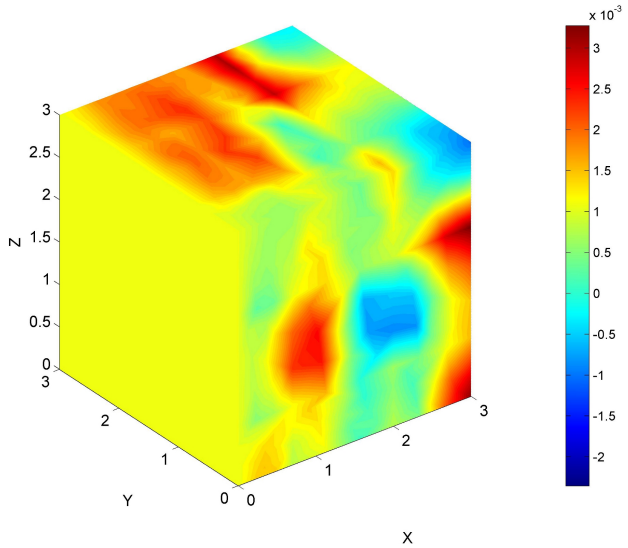

(c) Pointwise error: $u_N(\boldsymbol{\mu}) - u^{\mathcal{N}}(\boldsymbol{\mu})$

Figure 18: Example of representative solution and pointwise error for $\boldsymbol{\mu} = \{0.7, 0.7, 0.7, 1.3, 1.3, 1.3, 0.05\}$